THE DEVELOPMENT OF A SYNTHESIS APPROACH FOR OPTIMAL DESIGN OF SEAWATER REVERSE OSMOSIS DESALINATION NETWORKS

A Thesis

by

SABLA ALNOURI

Submitted to the Office of Graduate Studies of
Texas A&M University
in partial fulfillment of the requirements for the degree of

MASTER OF SCIENCE

August 2012

Major Subject: Chemical Engineering

The Development of a Synthesis Approach for Optimal Design of Seawater Reverse Osmosis Desalination Networks

THE DEVELOPMENT OF A SYNTHESIS APPROACH FOR OPTIMAL DESIGN OF SEAWATER REVERSE OSMOSIS DESALINATION NETWORKS

A Thesis

by

SABLA ALNOURI

Submitted to the Office of Graduate Studies of
Texas A&M University
in partial fulfillment of the requirements for the degree of

MASTER OF SCIENCE

Approved by:

Co-Chairs of Committee,	Patrick Linke
	Mahmoud El-Halwagi
Committee Member,	Eyad Masad
Head of Department,	Charles Glover

August 2012

Major Subject: Chemical Engineering

ABSTRACT

The Development of a Synthesis Approach for Optimal Design of Seawater Reverse Osmosis Desalination Networks. (August 2012)

Sabla Alnouri, B.S., Texas A&M University at Qatar

Co-Chairs of Advisory Committee: Dr. Patrick Linke
Dr. Mahmoud El-Halwagi

This work introduces a systematic seawater reverse osmosis (SWRO) membrane network synthesis approach, based on the coordinated use of process superstructure representations and global optimization. The approach makes use of superstructure formulations that are capable of extracting a globally optimal design as a performance target, by taking into consideration desired process conditions and constraints that are typically associated with reverse osmosis systems. Thermodynamic insights are employed to develop lean network representations so that any underperforming solutions can be eliminated a priori. This essentially results in considerable improvement of the overall search speed, compared to previously reported attempts. In addition, the approach enables the extraction of structurally different design alternatives. In doing so, distinct membrane network design classes were established by partitioning the search space, based on network size and connectivity. As a result, corresponding lean superstructures were then systematically generated, which capture all structural and operational variants within each design class. The overall purpose is thus to enable the extraction of multiple distinct optimal designs, through global optimization. This mainly

helps provide design engineers with a better understanding of the design space and trade-offs between performance and complexity.

The approach is illustrated by means of a numerical example, and the results obtained were compared to previously related work. As anticipated, the proposed approach consistently delivered the globally optimal solutions, as well as alternative efficient design candidates attributed to different design classes, with reduced CPU times.

This work further capitalizes on the developed representation, by accounting for detailed water quality information, within the SWRO desalination network optimization problem. The superstructures were modified to incorporate models that capture the performance of common membrane elements, as predicted by commercially available simulator tools, e.g. ROSA (Dow) and IMSDesign (Hydranautics). These models allow tracing of individual components throughout the system. Design decisions that are supported by superstructure optimization include network size and connectivity, flow rates, pressures, and post treatment requirements. Moreover, a detailed economic assessment capturing all the significant capital and operating costs associated in SWRO processes, including intake, pre and post treatment has also been accounted for. These modifications were then illustrated using a case study involving four seawater qualities, with salinities ranging from 35 to 45 ppt. The results highlight the dependency of optimal designs on the feed water quality involved, as well as on specified permeate requirements.

DEDICATION

To my parents

ACKNOWLEDGEMENTS

I am truly indebted to all those who have assisted me in the preparation and completion of this course of study. All the hard work, determination and persistence that culminated in creating this thesis would never have been successful without all the support, patience and guidance that I have received.

First and foremost, I would like to extend my deepest gratitude to my supervisor, Dr. Linke, who has never spared any effort to direct and help me throughout this course of research, by providing me with all the scientific back-up I was in need of. Not only was I given the opportunity to work on this interesting subject matter, Dr. Linke has undoubtedly helped me develop my own individuality, by allowing me to work with much independence. For your continuous guidance Dr. Linke, I thank you. I would also like to thank the remaining members of my committee, Dr. El-Halwagi and Dr. Masad, for their unending encouragement, assistance and support, as well as for all their input, and valuable discussions. Moreover, I would like to thank all my friends and fellow colleagues who have stood by me, cheered me up on rough days, and offered me all the help and consultation. Likewise, thank you to all CHEN faculty and staff for making my time at Texas A&M University a great experience. Last but not least, I would like thank my family for allowing me to be as ambitious as I wanted. Had it not been for my parents, their continuous prayers, and their deep faith in me, I would never have been able to successfully accomplish any of my studies.

NOMENCLATURE

I	Set of components in the feedwater stream $I=\{i\|i=1,N_c\}$
J	Set of RO membrane units/ set of corresponding mixing nodes preceding each membrane unit/set of permeate and reject splitting nodes associated with each membrane unit $J=\{j\|j=1,Nro\}$
i	Subscript referring to chemical component
j	Subscript referring to RO unit/ corresponding mixing nodes preceding each unit/ permeate and reject splitting nodes associated
$FEED$	Superscript denoting feed node
RO	Superscript denoting RO inlet mixing node
P	Superscript denoting RO unit permeate splitting node
B	Superscript denoting RO unit reject splitting node
PP	Superscript denoting outlet permeate mixing node
BB	Superscript denoting outlet reject mixing node
y	Binary variable representing the existence of a connection
z	Binary variable representing the existence of a pump/turbine
$f_{j'}^{FRO}$	Split fraction of feed from inlet splitting node to mixing node *j'*
f^{FEED}	Split fraction of feed from inlet splitting node to outlet permeate stream mixer
$f_{j,j'}^{P}$	Split fraction of permeate from permeate splitting node *j* to mixing node *j'*
$f_{j,j'}^{B}$	Split fraction of reject from reject splitting node *j* to mixing node *j'*
f_j^{PP}	Split fraction of permeate from permeate splitting node *j* to outlet permeate stream mixer
f_j^{BB}	Split fraction of reject from reject splitting node *j* to outlet reject stream mixer

F^{FEED}	Total inlet feedwater flowrate into the network
X_i^{FEED}	Composition of component i in inlet feedwater stream
X^{FEED}	Total composition of dissolved solids in the inlet feedwater stream
F^{PROD}	Total permeate flowrate
X_i^{PROD}	Composition of component i in the final permeate stream
X^{PROD}	Total composition of dissolved solids in the final permeate stream
F^{BRINE}	Total brine flowrate
X_i^{BRINE}	Composition of component i in the final reject stream
X^{BRINE}	Total composition of dissolved solids in the final reject stream
P^{FEED}	Feedwater pressure into the network
P^{PROD}	Final permeate pressure
P^{BRINE}	Final reject pressure
$PW_{j'}^{FRO}$	Power consumption/recovery for stream from inlet splitting node to mixing node *j'*
$PW_{j,j'}^{P}$	Power consumption/recovery for stream from permeate splitting node *j* to mixing node *j'*
$PW_{j,j'}^{B}$	Power consumption/recovery for stream from reject splitting node *j* to mixing node *j'*
PW_j^{PP}	Power consumption/recovery for stream from permeate splitting node *j* to outlet permeate stream mixer
PW_j^{BB}	Power consumption/recovery for stream from reject splitting node *j* to outlet reject stream mixer
F_j^F	Total feed flowrate into RO unit j
F_j^P	Total permeate flowrate leaving RO unit j
F_j^B	Total brine (retenate) flowrate leaving RO unit j
$X_{i,j}^F$	Composition of component i in feed stream into RO unit j
X_j^F	Total composition of dissolved solids in feed stream into RO unit j
$X_{i,j}^P$	Composition of component i in permeate stream leaving RO unit j
X_j^P	Total composition of dissolved solids in the permeate stream leaving

	RO unit j
$X_{i,j}^{B}$	Composition of component i in brine (retenate) stream leaving RO unit j
X_{j}^{B}	Total composition of dissolved solids in the concentrate stream leaving RO unit j
P_{j}^{F}	Feed pressure into RO unit j
P_{j}^{P}	Pressure of permeate stream leaving RO unit j
P_{j}^{B}	Pressure of brine (retenate) stream leaving RO unit j
NM_{j}	Number of modules in RO unit j
PI	Initial pressure of stream
PF	Final pressure of stream
R_{j}	Permeate recovery in RO unit j
$\Delta\pi_{j}$	Average osmotic pressure difference on the high pressure side in RO unit j
$\Delta\pi_{i,j}$	Average osmotic pressure difference of component i on the high pressure side in RO unit j
H	Hydraulic Head
$\bar{A}(\bar{\pi})_{j}$	Membrane Permeability
TCF_{j}	Temperature correction factor for membrane permeability in RO unit j
FF_{j}	Membrane fouling factor in RO unit j
$\Delta P_{fc,j}$	Average concentrate side system pressure drop in RO unit j
$\left(\frac{C_{fc}}{C_{f}}\right)_{j}$	Log mean concentrate-side to feed concentration ratio in RO unit j
TAC	Total Annualized Cost
TAI	Total Capital Investment
DCC	Direct Capital Cost
SC	Soft Cost
CC	Capital Cost

TOC	Total Operating & Maintenance Cost
VOC	Variable Operating & Maintenance Cost
FOC	Fixed Operating & Maintenance Cost
OC	Operating & Maintenance Cost
$PW^{RO,Pumps}$	Total energy requirements in RO network pumps
$PW^{RO,ERDs}$	Total energy recovered in RO network ERDs
$F^{PROD,MIN}$	Minimum permeate flow required in the network
$X^{PROD,MAX}$	Maximum allowable concentration of of dissolved solids in the permeate stream after post-treatment
A	pure water permeability
$\mathrm{K_i}$	transport parameter of solute i
γ	parameter define by membrane modeling equations
η	parameter define by membrane modeling equations
μ	viscosity
r_i	inner radius of hollow fiber
r_o	outer radius of hollow fiber
l	fiber length
l_s	fiber seal length
c_{ro}	cost coefficient of an RO module
a_{pu}	operating cost coefficient of a pump unit
a_{tu}	operating cost coefficient of an energy recovery turbine unit
b_{pu}	fixed cost coefficient of a pump unit
β_{pu}	fractional constant corresponding to a pump unit fixed cost
b_{tu}	fixed cost coefficient of a turbine unit
β_{tu}	fractional constant corresponding to a turbine unit fixed cost
T	Temperature
NS	Number of skids
LF	Lang Factor
D	Depreciation

PWC	Power Cost
η^{turb}	Turbine Efficiency
SG	Specific Gravity
NM_j^{MIN}	Minimum allowable number of modules in RO unit j
NM_j^{MAX}	Maximum allowable number of modules in RO unit j
SM_j	Membrane area per module in RO unit j
$\gamma_{i,j}$	Salt rejection of component i in RO unit j
ΔP_j	Pressure drop in RO unit j
$P_j^{F,MAX}$	Maximum allowable feed pressure in RO unit j
ΔP^{SPEC}	specified maximum lower end pressure difference (associated with ERD placement)

TABLE OF CONTENTS

LIST OF FIGURES

LIST OF TABLES

1. INTRODUCTION

The global desalination capacity is growing rapidly, particularly in areas with limited natural fresh water reserves and increasing populations. As a result of improvements in membrane technology, sea water reverse osmosis based desalination processes have seen major efficiency gains over the past decades, and more often than not constitutes the preferred technology choice. Besides the development of an efficient pretreatment system, the process design activity for such systems involves the development of optimal membrane network configurations. Process systems approaches involving superstructure formulations and optimization [1] are well suited to address such network design problems. Such methods have been highlighted as key technologies to enable improved process efficiencies that would be required for a sustainable development of the chemical process industries [2].

Superstructure-based approaches enrich the design process through their capability to identify optimal process configurations from large numbers of alternatives. This requires the ability to perform global searches quickly, and to capture the set of feasible alternatives with the potential to offer high performance. Current approaches require significant computational times when screening through RO networks represented by simple membrane unit models involving only two constituents: water and "salt" (TDS).

This thesis follows the style of *Journal of Membrane Science*.

Thus, further extensions of superstructure approaches will mostly benefit from advances on two main aspects. First, richer models are needed in terms of their ability to capture individual constituents such as Boron or ions participating in scaling. For instance, the presence of turbidity, as well as high concentration levels of hardness ions in general, such as calcium and magnesium, tends to degrade a SWRO plant performance. Moreover, the water recovery rate within the network is always limited by the scaling tendency of the concentrate streams. Even though these constituents are believed to have a significant impact on design decisions, their consideration will result in larger and more complex optimization models, posing additional burden on the already computationally very demanding superstructure optimization effort. Second, more compact representations are needed together with and a more structured synthesis strategy to make the combinatorial search more efficient so that richer process models can be afforded whilst ensuring acceptable computational times for determining high performing design options and yielding clarity and breadth of results.

This first section exclusively focuses on the second aspect, by introducing a leaner membrane network synthesis representation together with an optimization scheme, and a synthesis strategy that will enable the systematic and quick identification of optimal membrane networks. In other words, for given feed water conditions and product specifications, the approach enables the extraction of structurally distinct design alternatives, in addition to the globally optimal reverse osmosis process network solution identified as a design performance target. Even though many previous approaches capture rich sets of process configurations, the general inability to handle detailed water

quality information as part of the process synthesis and optimization problem usually presents inconsistency in terms of the richness of the solutions obtained.

The second section capitalizes on the benefits of a more compact representation and search strategy, by applying additional computational elements that involve embedding multiple water quality features into the overall network optimization problem. As mentioned before, detailed water quality information is often essential when assessing important operational and product constraints, rather than simply assuming two pseudo components, i.e. “water” and “total dissolved salts”. This would eventually assist in properly addressing the design impact of important phenomena, such as membrane scaling tendencies of sparingly soluble compounds. Such problematic constituents, if not removed place limits on the plant’s product water recovery due membrane degradation problems. Thus, better insight into much needed additional problem features could generously be explored via the proposed synthesis strategy.

2. LITERATURE REVIEW*

A number of works have proposed network optimization approaches for membrane networks, and more specifically, reverse osmosis networks (RONs) [3-16]. El Halwagi [5] was the first to introduce the idea of reverse osmosis network synthesis, which involves the development of a rich superstructure representation embedding all possible configurations of processing units by accounting for all units within the system (membranes, pumps and ERDs) as well as full stream connectivity, represented by the State Space approach. The problem is formulated as a mixed-integer nonlinear program (MINLP) and solved for local optimality. The formulation considers two components, i.e. water and salt through a lumped "total dissolved solids" (TDS) component. The solution provides the optimal arrangement, types and sizes of the RO units, optimum stream distributions, operating conditions as well as pumps, and energy-recovery turbines to be employed in the network [5]. The approach is illustrated with a simple seawater desalination design example based on Evangelista [6], which has subsequently become a popular case study to illustrate membrane network optimization approach. The optimal solution reported features a two unit RO design. Voros et al. [4, 7] propose a modified State Space representation and formulate the membrane desalination networks as a non-linear program. The same case study example based on Evangelista [6] was used for comparison, and several optimal two- RO unit structures have been reported. The formulation considers two components, i.e. water and salt (TDS). Maskan

*Reprinted with permission from " A Systematic Approach to Optimal Membrane Network Synthesis for Seawater Desalination" by Sabla Y. Alnouri, Patrick Linke, 2012. Journal of Membrane Science, In Press, Copyright [2012] by Elsevier.

et al. [8] formulate one and two unit reverse osmosis networks as non-linear programs. Zhu et al. [9] present a State Space based formulation for the optimal design and scheduling of flexible RONs. Their proposed design procedure resulted in a two-unit (stage) tapered flow scheme, for which the optimum maintenance schedule was determined. They considered two components, i.e. water and salt (TDS). Lu et al. [10] modify the State Space formulation by El-Halwagi [5] and propose a MINLP formulation with structural variables only involved in the selection of membrane types whilst also accounting for two components and performing local optimization. Vince et al. [11] propose the optimization of one and two-unit RONs for a feedwater consisting of 'salt' and 'water' using a multi-objective optimization approach, using a more detailed objective formulation which considers technical and environmental performance indicators. Their methodology allows for the identification of a set of optimal solutions representing trade-offs between conflicting objectives. All of these works involve the use of local rather than global optimization techniques. Moreover, emerging representations avoid the use of binary variables to determine the existence of stream connections, gaining computational speed but eliminating the benefits integer variables offer for decisions on network connectivity.

More recently, approaches have been proposed that adopt global optimization techniques. Other previous work introduces binary variables to better capture decisions on network connectivity. For instance, Marcovecchio et al. [12] propose a global optimization algorithm to determine optimal operating conditions for various conventional RON designs given a feedwater consisting of salt (TDS) and 'water'. Two

formulations capture decisions on stream connections in the State Space representation using binary variables. Marriott et al. [13] propose to globally search the membrane network superstructure optimization problem using Genetic Algorithms, but not specifically optimize SWRO systems. Guria et al. [14] apply Genetic Algorithms to optimize Reverse Osmosis process. However, superstructure optimization is not considered. Saif et al. [15] apply deterministic global optimization techniques to solve the SWRO membrane superstructure optimization problem. They demonstrate how the application of deterministic global optimization enables the identification of improved solutions. On the downside, significantly longer computational times. in the order of ten minutes have been reported. In another paper, Saif et al. [16] demonstrate superstructure optimization using iterative MILP, for finding local optimal solutions while applying a superstructure reduction strategy prior to the optimization.

To date, all available superstructure-based approaches employ simple membrane models that consider only two components, i.e. water and salt in the form of TDS, rather than accounting for individual ions with a multi component approach. In summary, the field of optimal membrane network synthesis has been the subject of research efforts for the past two decades. Significant computational times have been reported for the global optimization of small superstructures, most of which featuring only two membrane units. Moreover, no attempts have been made towards accounting for seawater compositions through more than only the two “components”, water and the lumped component TDS.

3. BACKGROUND*

Seawater Reverse Osmosis (SWRO) plant process feed water at high pressure in membrane units to produce a desalinated water stream as well as a concentrate or brine stream. SWRO plant designs can be arranged in a number of alternative configurations, ranging from simple single unit systems to more complex systems that incorporate multiple stages/passes. The design of an SWRO system strongly depends upon the feedwater characteristics and the product water specification. The membrane units in the process must operate are within the range of recommended operating conditions to minimize the membrane fouling and scaling and prevent any mechanical damage. Regardless of the membrane design, high feed pressure is always required to overcome osmotic pressure differences. Membrane elements can withstand feed water pressures up to 80-85 bars [15, 16]. The pressure drop in SWRO systems usually amounts to 0.3–2 bar from feed inlet to concentrate outlet [15, 16] depending on the number of membrane units, the feed flow velocity and the temperature. Since the energy costs to drive the high pressure feed pumps constitute a major part of operating costs, energy recovery devices (ERDs) are employed on the high pressure brine stream to significantly decrease in the specific energy demand of the system. ERDs enable energy savings up to 40% [17].

Before we turn to membrane network design we clarify the terminologies associated with membrane networks that will be used throughout the manuscript (Figures 1 and 2):

---

* Reprinted with permission from " A Systematic Approach to Optimal Membrane Network Synthesis for Seawater Desalination" by Sabla Y. Alnouri, Patrick Linke, 2012. Journal of Membrane Science, In Press, Copyright [2012] by Elsevier.

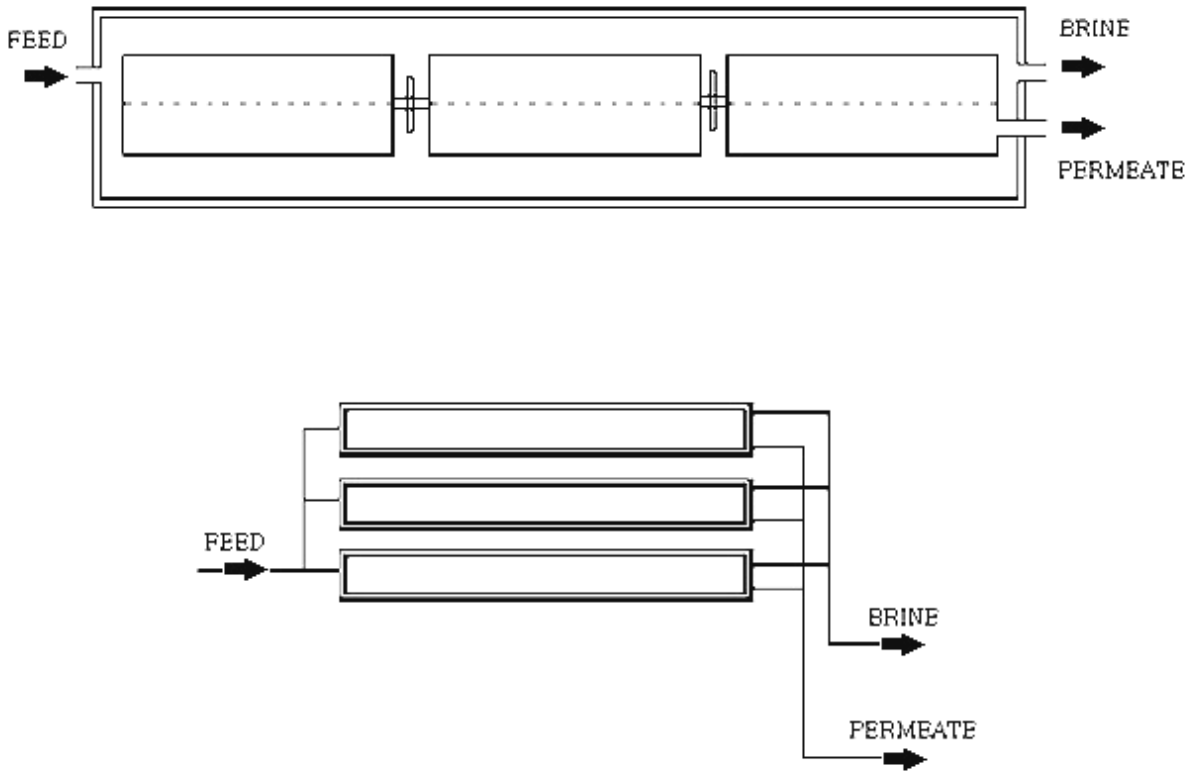

Figure 1. Membrane element/module/ illustrated

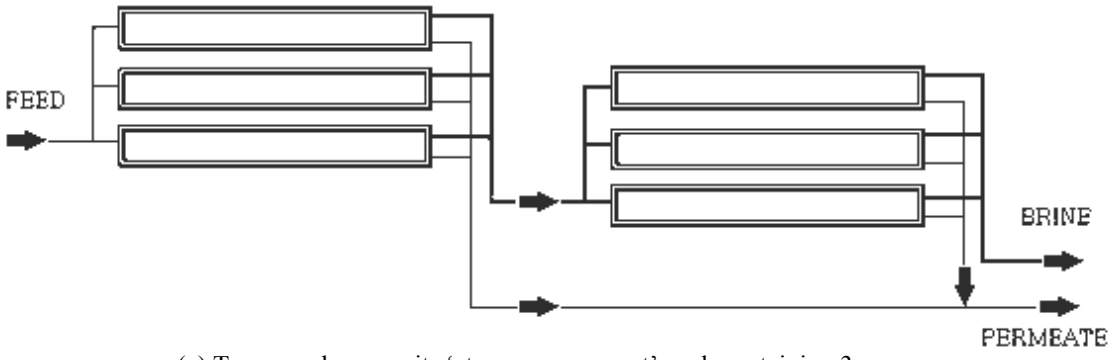

(a) Two membrane units 'stage arrangement' each containing 3 membrane Modules

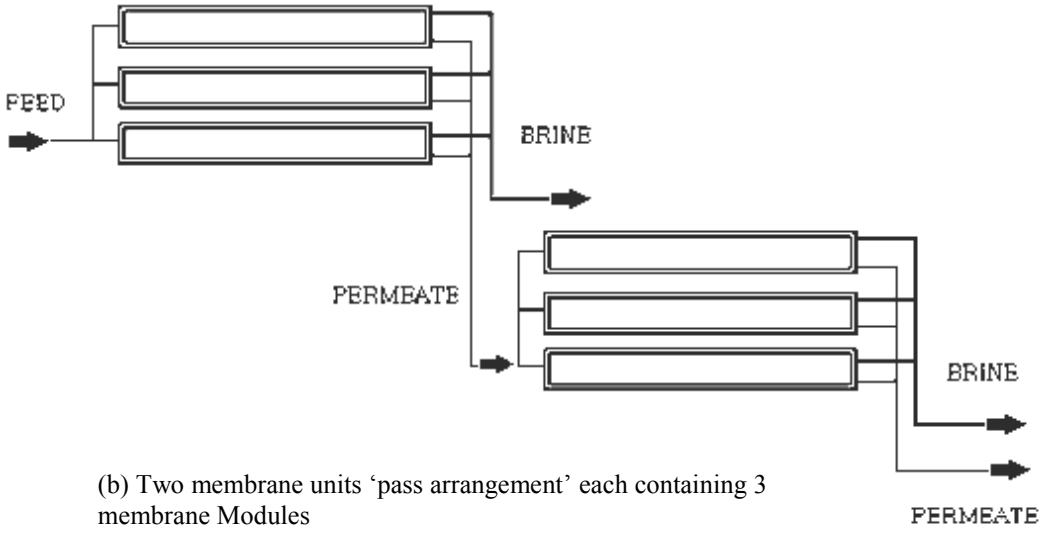

(b) Two membrane units 'pass arrangement' each containing 3 membrane Modules

Figure 2. Different unit arrangements illustrated

- A membrane 'element' is the smallest building block of a SWRO system and is characterized by two performance parameters: permeate flux and the permeate quality.

- A membrane ‘module’ is a system of membrane ‘elements’ connected in series. The number of membrane elements per module can reach up to 8 elements [18]. Permeate streams coming from all elements exit in a collective permeate port, which may be located either at the feed end or the concentrate end of the module.
- A membrane ‘unit’ is a system of ‘modules’ in a parallel arrangement. Feed, product and concentrate streams in each module within a single unit are connected to respective ports.
- An arrangement of two membrane units can be classified as either ‘stage’ or ‘pass’:
    - A ‘stage’ refers to the scenario in which the reject stream of the first membrane unit becomes the feed stream into the second.
    - A ‘pass’ refers to the scenario in which the permeate stream of the first membrane unit becomes the feed stream into the second.
- A membrane ‘network’ is a system of one or more membrane ‘units’ through which the feedwater is processed into desalinated water and brine streams.

Membrane network synthesis employs ‘superstructures’ of membrane networks that are characterized by multiple membrane units and full stream connectivity. The synthesis problem is typically formulated as a mixed-integer nonlinear program (MINLP) and solved to extract the best performing design embedded in the superstructure according to a performance measure, typically the total annualized cost. The superstructures embed all feasible unit arrangements and connectivity options to

capture the various possible design alternatives [4-16]. Figure 3 illustrates a superstructure for a SWRO network, consisting of three membrane units and full stream connectivity.

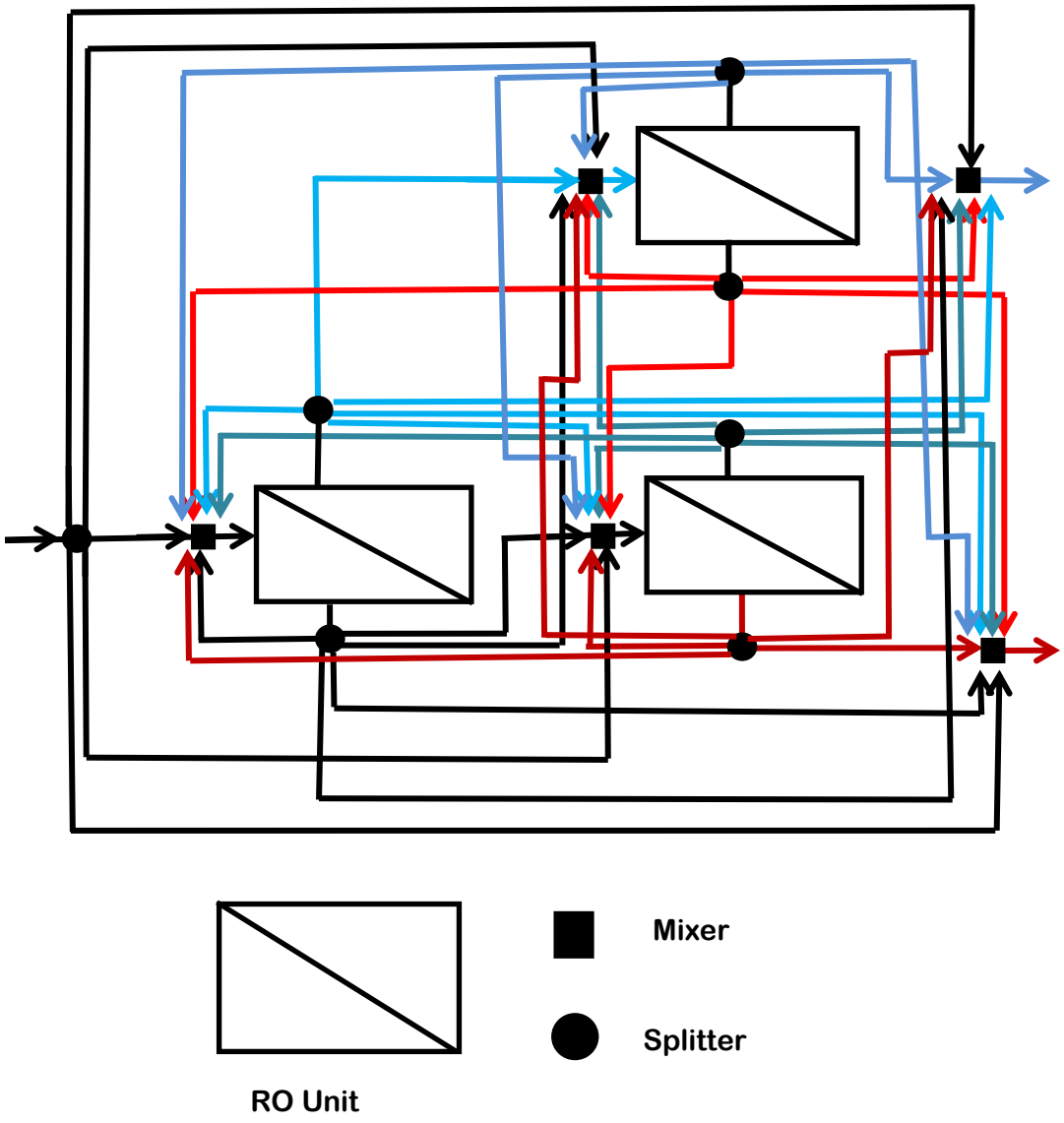

Figure 3. Comprehensive 3-unit superstructure arrangement example (red color corresponds to brine streams in units j≥2, blue color corresponds to permeate streams in units j≥1)

The superstructure illustration above has a total of five mixing and seven splitting points. Each membrane units associated with a single mixing node preceding its feed stream, and two splitting nodes on either side of the membrane output streams. Moreover, two mixing points are incorporated into the superstructure from which the two product streams of the network are obtained (one reject and one permeate outlet). In addition, a single splitting node is associated with the network's seawater feed stream to enable feed water distribution amongst the mixers within the superstructure. The complete three unit network arrangement allows for all possible stream distribution options between splitters and mixers. A very large number of possible design alternatives are incorporated in these networks. Unsurprisingly, the structural optimization of the superstructure network to extract a single optimal solution requires substantial computational time. For instance Saif et al. [15,16] recently reported a computational time of over ten minutes to solve a small two-unit network for global optimality. Larger structures and/or the incorporation of membrane models that better capture the complex membrane nature within the problem [e.g. 19-27] would substantially increase the computational burden and may not be robustly solved.

The existing superstructure network approaches lead to single solutions extracted from the superstructures. This will provide information about the performance limit of the system whilst the resulting optimal designs may be complex. A design engineer would benefit from additional information about the relative performance of different network configurations so as to be able to select a network of acceptable complexity and performance in the context of the performance limits of the system. In other words, a

simpler design may be preferred if its performance does not fall short of that of a more complex design by a wide margin. In order for our proposed approach to deliver the necessary insight to the design engineer, we would benefit from the ability to extract the performance limits as well as additional design information following a multi-level synthesis approach [28] that would support the design engineer in selecting a configuration.

4. A SYSTEMATIC APPROACH TO OPTIMAL MEMBRANE NETWORK SYNTHESIS FOR SEAWATER DESALINATION*

4.1 Overall Synthesis Approach

The overall synthesis approach is to develop the design performance target and a number of design alternatives to support decision-making by the design engineer. This is achieved using two optimization steps, each employing different superstructure network representations.

- Step 1 – Targeting: The performance target of the system is determined through global optimization of full superstructures to extract the best performing design and its performance. The target will serve as a performance benchmark against which design alternatives can be assessed.
- Step 2 – Development of Alternative Designs: Reduced superstructures resembling fundamentally distinct design classes are globally optimized to identify design alternatives of increasing complexity. Comparison of design performances against the target provides insight to the design engineer as to the potential performance advantages complex designs offer over simpler designs.

The following section explains the generation of the superstructures employed in Steps 1 and 2. The developments of these superstructures aim at eliminating design features that would lead to low performance, thus enabling leaner representations and faster searches.

4.2 Superstructure Representations

The proposed two step synthesis approach involves optimizations of multiple superstructures. First, a superstructure with rich connectivity is searched to extract the performance limit of the system. Then, multiple superstructures are searched to identify optimal solutions within different possible design classes.

A superstructure representation for SWRO desalination systems is generally comprised of a number of elements:

- A network feed stream that needs to be desalinated
- Two product streams. The desalinated water product and the concentrate (brine) product.
- Synthesis units. A synthesis unit (membrane unit) separates a feed stream into two product streams: a permeate and a retentate product.
- Splitters. A splitter divides a stream into multiple streams. Splitters are associated with the process feed water stream, and with all synthesis unit product streams.

- Mixers. A mixer receives one or more feed streams and produces one mixed exit stream. Mixers are associated with each synthesis unit feed and with each network product stream.
- Connecting streams. These streams connect splitters and mixers.

Given the relatively sharp separation of TDS by SWRO membrane units, which typically exceeds 95% rejection for most constituents, the network splitters are associated with either concentrates (network feed and retentates from synthesis units) or permeates (permeates from synthesis units). It can be noted that various stream connectivity options are possible, depending on the sources (unit splitters – both reject and permeate, feed splitter) and sinks (unit mixer, reject mixer, permeate mixer) involved. Next, we discuss the basics behind SWRO networks, which would always involve a combination of the following*:* arrangement of synthesis units and connectivity between network splitters and mixers.

4.2.1 ***Basic Arrangement of Synthesis Units***

The simplest arrangement of a membrane desalination process is a single-unit system with one only membrane unit. The incorporation of additional membrane units into the system might offer improved process performance over a single unit design. Additional membrane units can be introduced as passes and/or stages. The appropriate number of stages/passes in a particular design depends upon the desired permeate recovery, permeate quality, the feed water quality and temperature and the process

economics. SWRO systems requiring high permeate recoveries and high product water quality specifications that need to be met would usually incorporate multiple membrane units as stages and/or passes.

Figure 4 illustrates the alternatives for the placement of synthesis units in a SWRO membrane networks. There are four possible ‘unit arrangement categories’ in terms of how synthesis units are staged within SWRO networks. In order to be able to distinguish these categories, each is assigned a distinct binary combinatorial BINj, in the following manner: single staging -00-, an extra stage added to the system -01-, an extra pass added to the system -10- and an extra stage & pass added simultaneously -11- . The last unit arrangement category option is only feasible when two synthesis units are being added into the system simultaneously. The unit arrangement categories define an underlying basic network structure in terms of stages and passes.

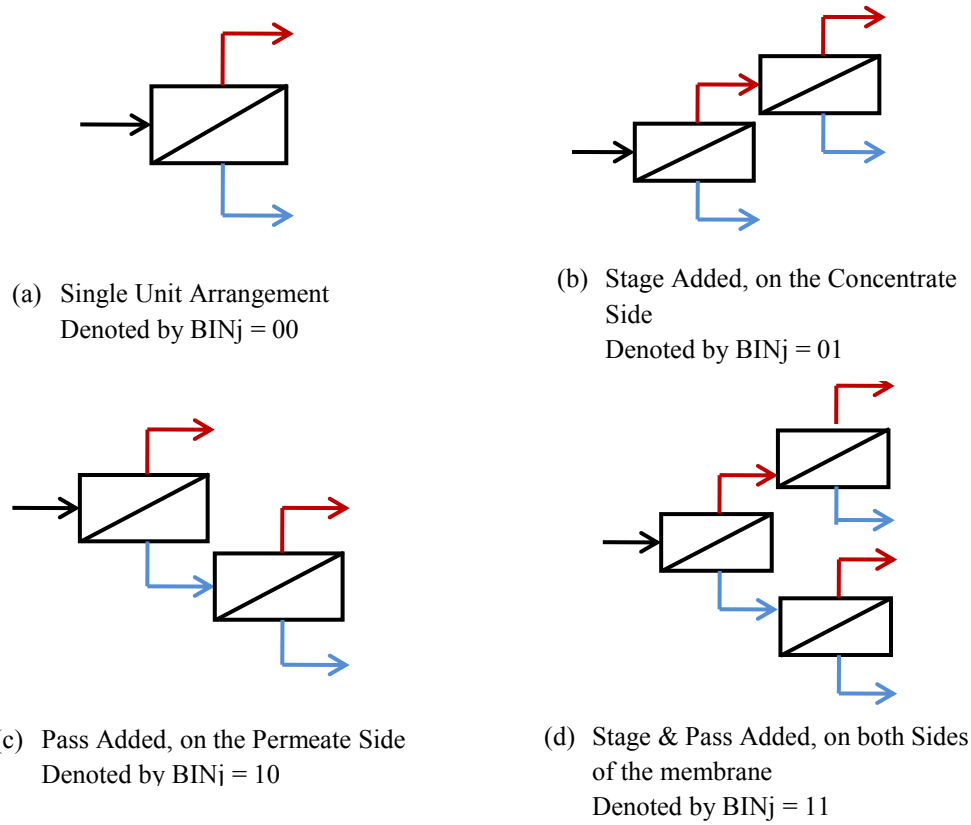

Figure 4. Demonstrative illustration involving arrangement of treatment units (red color corresponds to brine streams, blue color corresponds to permeate streams)

4.2.2 ***Connectivity***

The basic arrangement of synthesis units dictates an underlying connectivity from the feed water through the synthesis units to the permeate and brine products. Such connections are referred to as 'enforced connections' associated with the basic arrangements. In addition to the enforced connections, additional or alternative connections can be present in a network of a given basic arrangement. These connections are referred to as 'optional connections'.

In order to achieve a lean but rich network synthesis representation, the optional connections to be explored within the basic design arrangements should be limited to those that are deemed viable in that they will not by default introduce inefficiencies or redundancies. In general, network structural connectivity corresponds to the various combinations of sources connected to sinks, with splitters within the network acting as sources and mixers as sinks. Any design by default would include a feed splitter, as well as two outlet mixers for each resulting product stream (brine and desalinated water). Moreover, each Synthesis unit introduced into the system is associated with a mixer preceding its feed stream, as well as two separate splitters on either sides of the membrane (concentrate and permeate). Viable connectivity categories within a membrane desalination network are also summarized in Table 1 in terms of their status as enforced or variable, and are listed for the different basic arrangements.

Table 1. Connectivity manipulation, different connectivity groups and association with unit distinct design categories

Connectivity Categories (Sources-to-Sinks)	**Connectivity Binary Variables Defined within Each Category**	**Associated with the following Design Arrangements**
Feed-to-Outlet	y^{FEED}= binary variable representing the existence of a connection from the inlet splitting node to the outlet permeate stream mixer	$All\ (optional)$
Feed-to-Unit	$y_{j'}^{FRO}$ = binary variable representing the existence of a connection from the inlet splitting node to membrane mixing node *j'*	$BIN_j = 00$ $(enforced\ \forall(j' = j), j' \in J)$ $BIN_j = 01$ $(optional\ \forall(j' = j), j' \in J)$ $(BIN_j = 11) \wedge (BIN_{j-1} = 11)$ $(optional\ \forall(j' = j-1), j' \in J)$
Unit-to-Outlet	y_j^{PP}=binary variable representing the existence of a connection from membrane permeate splitting node *j* to outlet permeate stream mixer	$BIN_j = 00$ $(enforced\ \forall(j' = j), j' \in J)$ $BIN_j = 01$ $(enforced\ \forall(j' = j), j' \in J)$ $BIN_j = 10$ $(optional\ \forall(j' < N_{ro}), j' \in J)$ $(enforced\ \forall(j' = N_{ro}), j' \in J)$ $(BIN_j = 11) \wedge (BIN_{j-1} = 11)$ $(optional\ \forall(j' < N_{ro} - 1), j' \in J)$ $(enforced\ \forall(j' = N_{ro}), j' \in J)$ $(enforced\ \forall(j' = N_{ro} - 1), j' \in J)$
	y_j^{BB}=binary variable representing the existence of a connection from membrane reject splitting node *j* to outlet reject stream mixer	$BIN_j = 00$ $(enforced\ \forall(j' = j), j' \in J)$ $BIN_j = 01$ $(optional\ \forall(j' < N_{ro}), j' \in J)$ $(enforced\ \forall(j' = N_{ro}), j' \in J)$ $BIN_j = 10$ $(enforced\ \forall(j' = j), j' \in J)$ $(BIN_j = 11) \wedge (BIN_{j-1} = 11)$ $optional\ \forall(j' < N_{ro} - 1), j' \in J)$ $(enforced\ \forall(j' = N_{ro}), j' \in J)$ $(enforced\ \forall(j' = N_{ro} - 1), j' \in J)$
Unit-to-Unit	$y_{j,j'}^{P}$ = binary variable representing the existence of a connection from membrane permeate splitting node *j* to membrane mixing node *j'*	$BIN_j = 11 \wedge BIN_{j-1} = 11$ $(optional \forall(j' = j-1), j' \in J)$
	$y_{j,j'}^{B}$ = binary variable representing the existence of a connection from membrane reject from splitting node *j* to membrane mixing node *j'*	$BIN_j = 01 \wedge (BIN_{j-1} = 10$ $(optional\ \forall(j' = 0 \ldots j-1), j' \in J$ $BIN_j = 10$ $(optional\ \forall(j' = 0 \ldots j-1), j' \in J$ $BIN_j = 11 \wedge BIN_{j-1} = 11$ $(optional\ \forall(j' \neq j), j' \in J)$
	$y_{j-1,j'}^{P}$ = binary variable representing the existence of a connection from membrane permeate splitting node *j* preceding membrane mixing node *j'* to mixing node *j'*	$BIN_j = 10$ $(enforced\ \forall(j' = j), j' \in J)$ $BIN_j = 11$ $(enforced\ \forall(j' = j), j' \in J)$
	$y_{j-1,j'}^{B}$ = binary variable representing the existence of a connection from membrane reject splitting node *j* preceding mixing node *j'* to membrane mixing node *j'*	$BIN_j = 01$ $(enforced\ \forall(j' = j), j' \in J)$ $BIN_j = 11$ $(enforced\ \forall(j' = j), j' \in J)$

A leaner connectivity is therefore achieved by eliminating inefficient connections from the synthesis representation. The lean superstructures do not include connections that fall into one of the following categories:

- *Category 1:* Feed-to-network concentrate bypass: eliminated in order to avoid the inefficiency of wasting pretreated feed water.

- *Category 2:* Concentrated brine recycling to the same treatment unit and/or preceding units within the network: the option of recycling brine stream associated with concentrations higher than that of feed streams into any treatment unit (being it the same and/or preceding units in the network) was eliminated, since this connection would correspond to mixing a high salinity stream with a lower salinity feed stream into a treatment unit. Such connections result in treatment units having to desalinate feed streams of higher salinity, which would in turn correspond to higher energy and membrane area requirements within the network. Only connections involving relatively low salinity brine recycles (ie brine streams produced by a pass arrangement) were allowed, since mixing a treatment unit feedstreams with lower salinity streams help reduce the salinity of the feed into the treatment units.

- *Category 3:* Permeate recycling back to the same unit/ preceding units within the network: these connections involve the introduction of permeates into treatment unit mixers that in turn produce concentrates, and thus are thermodynamically unfavorable since the separation achieved in the first place would be reversed.

- *Category 4:* Connections which involve any form of mixing between brine and permeate streams: these connections are also classified as thermodynamically inefficient options, since the energy intensive separation is reversed as well (eg. a brine stream introduced into the outlet permeate mixer, a permeate stream introduced into the outlet reject mixer).

The different connectivity categories are illustrated in Figure 5, and the notations utilized for each connection category, along with a simple description, were already specified in Table 1.

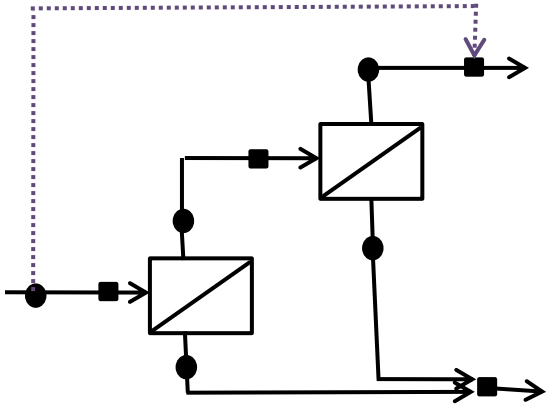

(a) Eliminated connections (Category 1): Feed -to- Network Concentrate Bypass

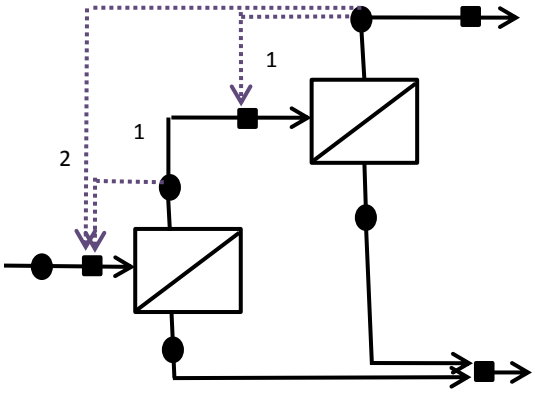

(b) Eliminated connections (Category 2): Brine Recycle *(1)* to the same treatment unit, *(2)* to preceding treatment units

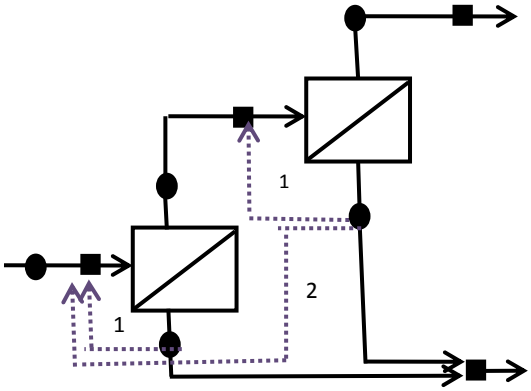

(c) Eliminated connections (Category 3): Permeate Recycle *(1)* to the same treatment unit, *(2)* to preceding treatment units

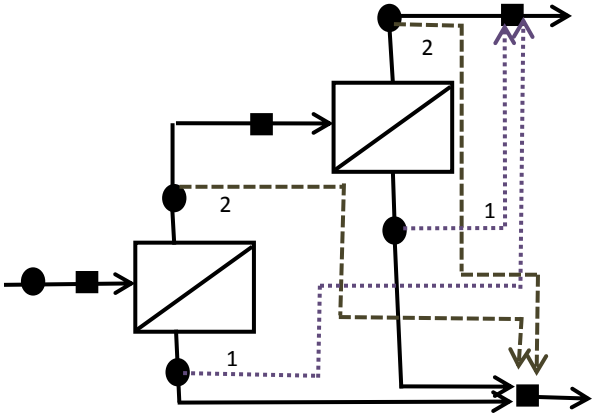

(d) Eliminated connections (Category 4): Brine and permeate stream mixing *(1)* permeate into the network concentrate mixer, *(2)* brine into the network permeate stream mixer

Figure 5. Eliminated connectivity categories illustrated

In order to be able to explore the existence of stream connections in network optimization, each distinct connection category is associated with a binary variable, the

description of which has been provided in Table 1. The association of binary variables with streams is illustrated in Figure 6.

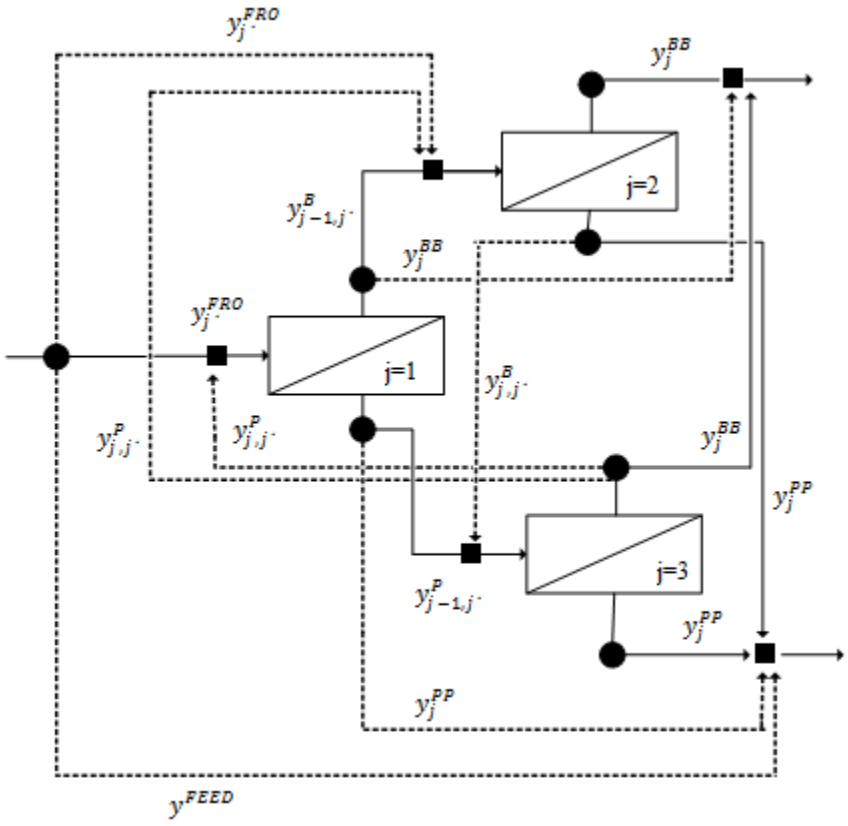

Figure 6. Binary connectivity annotation, demonstrative example

As a result, the existence of connections can be easily established based on the various unit arrangement categories, which in turn depend on the basic arrangement of the treatment units within the network. Thus, incorporating binary annotations for the distinct connectivity groups would easily coordinate their presence, by associating each with the four different unit arrangements discussed earlier. Further classification of

connections into ‘enforced’ and ‘optional’ allow certain connections to be emphasized and treated differently within the different basic arrangements, and this would establish a set of definitions to create distinctive individual ‘design classes’.

4.3 Targeting Superstructure (Step 1)

The comprehensive superstructure illustrated in Figure 3 is generated through a full connectivity between all mixtures and splitters of a network. This is to ensure that all possible design alternatives are included in the network. However, the richness of the network not only guarantees that the optimal configuration is included in the superstructure of a given size but also results in large numbers of design alternatives that need to be searched, which increase drastically with the number of synthesis units present in the superstructure. Figure 7 shows a single lean superstructure of three synthesis units that includes only those connections considered viable as it has been summarized in Table 1.

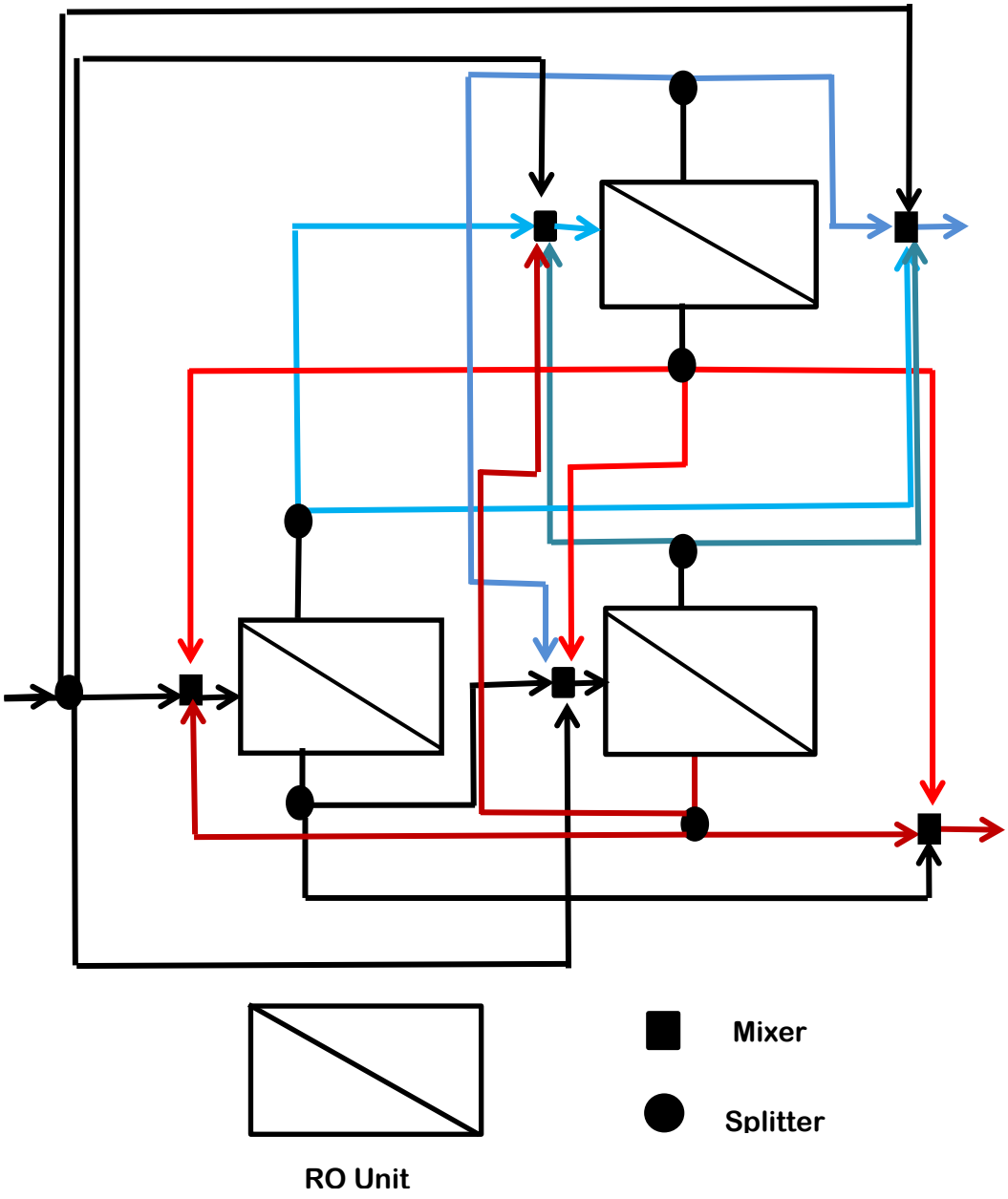

Figure 7. Lean 3-unit superstructure arrangement (red color corresponds to brine streams in units j≥2, blue color corresponds to permeate streams in units j≥1)

The lean superstructure combines all the basic unit arrangement categories that have been discussed earlier, together with all enforced and optional connections associated within each category. Stream connections are correlated with unit arrangements. For instance, if a design involves a stage arrangement, concentrate recycling to preceding units within the network is not allowed. On the other hand, if the design involves a pass arrangement, brine recycling (from the pass) back to preceding units within the network is allowed. The generation of the lean superstructure for targeting combines all different arrangement scenarios of stages/passes with all relevant interconnections (both enforced and optional) between mixers and splitters, that are given by Table 1. The resulting lean superstructure features significantly fewer streams as compared to the comprehensive superstructure of Figure 3. This translates into a significantly reduced number of design alternatives that need to be searched from the superstructure in order to obtain the performance target for the system in Step 1 of the synthesis approach.

4.4 Design Classes and Superstructures (Step 2)

Design classes feature distinct basic arrangements to ensure that structurally distinct designs are developed in Step 2 of the synthesis approach. This means that each design class has a distinct combination of unit arrangement categories. Within each design class, lean superstructures are generated to capture design variations within the basic arrangement of synthesis units so that the best design within the design class can be extracted through network optimisation. The basic arrangement of the design class is

ensured through the enforced connections whilst structural variations within the basic arrangement are possible for each design class in the form of optional connections. The construction of a lean superstructure for a given design class simply involves the integration of unit design categories with connectivity groups associated, both optional and enforced, according to Table 1. Figure 8 shows the different possible distinct design classes for designs ranging from one to three synthesis units.

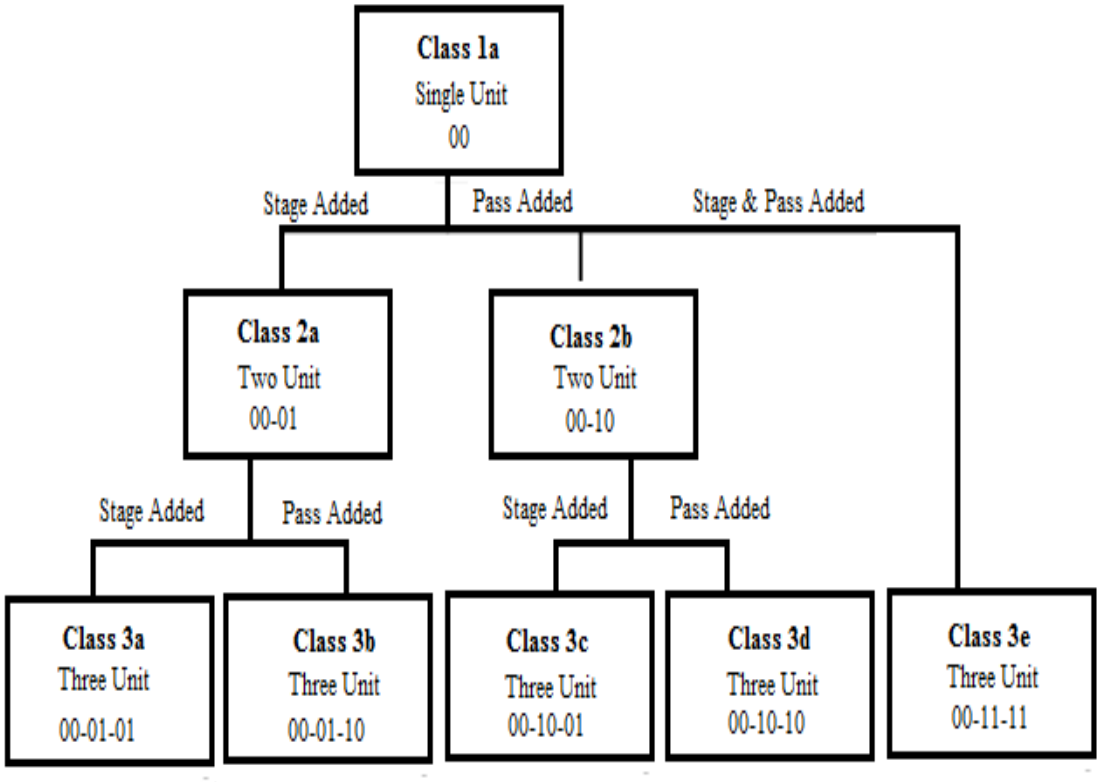

Figure 8. Simple-to-complex network design hierarchy, up to 3 units illustrated with respective binary unit-arrangement combinatorials

The number of design classes increases with the number of synthesis units present in the network. There is only one design class of a single unit network (class 1a), there are two design classes of a two unit networks (classes 2a and 2b), and five design classes of a three unit networks (classes 3a, 3b, 3c, 3d and 3e). At each node, a lean superstructure is generated that incorporates all enforced connections within the respective design class, as well as optional connections that could enhance all respective designs, that pertain to the identified design class. The corresponding lean superstructures are then solved, each separately, so as to determine the optimal system performance for a given design class. The design classes are explored in order of increasing numbers of synthesis units, starting from class 1a, to establish the benefits gained from adopting larger, more complex networks and minimize search time. Figure 9 shows the possible 'design classes' up to a total of three units in the network, according to the basic unit arrangement categories, and thus includes only enforced connections amongst all synthesis units involved.

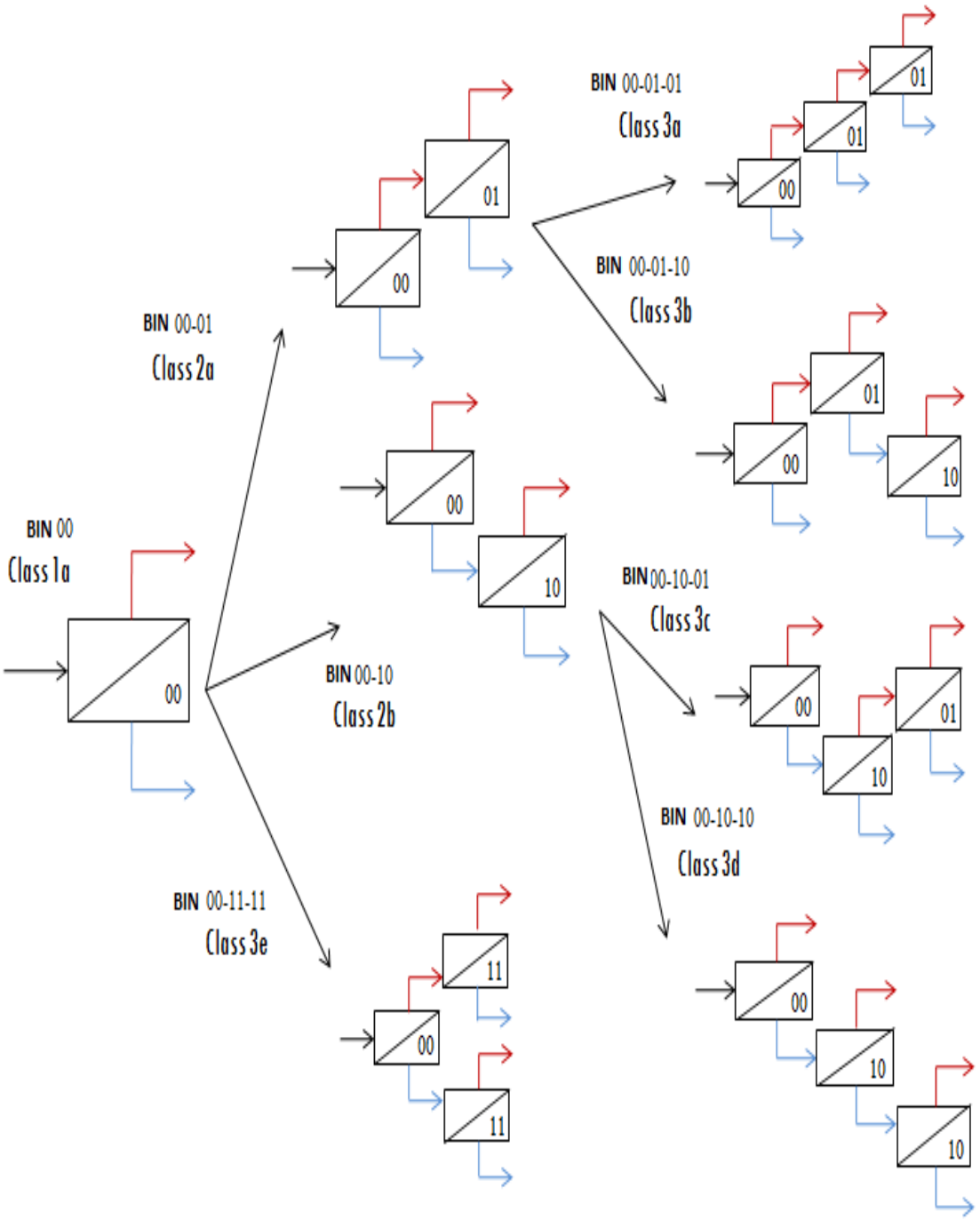

Figure 9. Design classes demonstrated according to unit arrangement categories, up to 3 units illustrated (red color corresponds to brine streams, blue color corresponds to Permeate streams)

Figure 10, illustrates the lean superstructures for the design classes, having introduced optional viable connections, in addition to enforced connections associated with each design class.

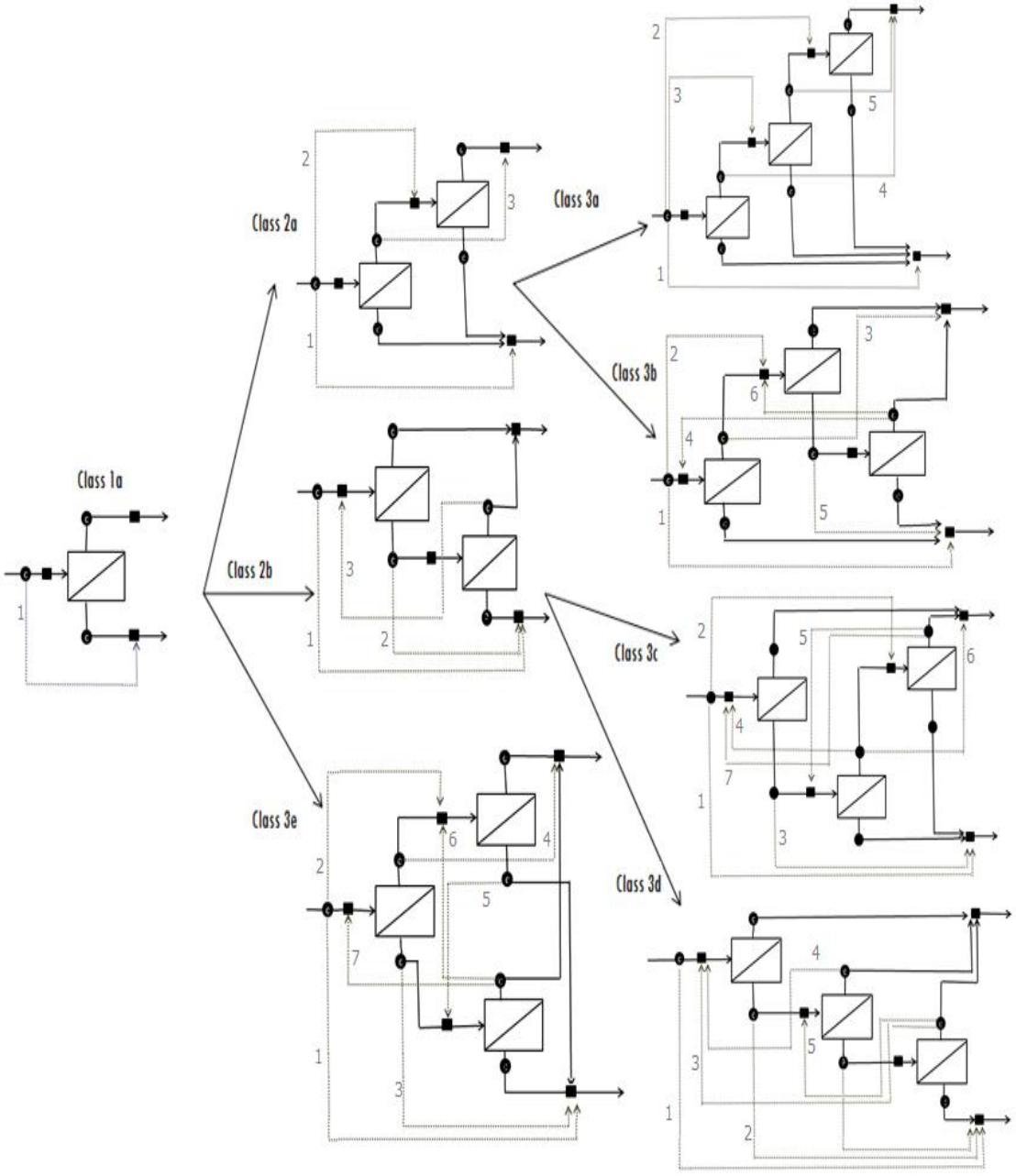

Figure 10. Design class superstructures demonstrated, having incorporated optional structural connectivity associated with each, up to 3 units illustrated

Design classes enable a well-defined search for optimal structural solutions, given certain performance criteria that need to be met, by means of thorough searches within a defined search domain. Both Figures 9 and 10 illustrate a hierarchical layout of multiple superstructures, starting with the simplest design and moving on to more complex ones, according to different design routes. Depending on the type of feed water to be treated, an appropriate route can be selected for evaluation accordingly. Moreover, any irrelevant design routes can be eliminated from the very beginning if no feasible solution exists, thus leading to a significant reduction in the number of choices that need to be evaluated later on.

The introduction of design classes allows optimal design alternatives with distinct underlying stage-pass connectivity to be explored. This is achieved by optimization of one reduced superstructure for each design class. The optimal solutions for all feasible design classes can be compared to the target global solution from the lean superstructure, and a performance comparison can thus be established. The information about the best possible performance of design alternatives with different underlying connectivity can support decision making by the design engineer.

4.5 Pressure Manipulation Options

The placement of pressure changing equipment within the network depends upon the individual stream origins and destinations within the design. There exist three types of pressure manipulation options:

1. Placement of a pump device which increase a stream pressure,
2. Placement of an energy recovery device to reduce a stream pressure, and
3. No placement of an energy recovery device if pressure differences from source to sink are insignificant.

The binary variables associated with the presence of a pressure manipulation device on a stream within the network and their settings based on pressure differences between sources and sinks are summarized in Table 2.

Table 2. Pressure manipulation options, corresponding to distinct connectivity groups

Connectivity Categories (Sources-to-Sinks)	**Binary Variables Defined corresponding to distinct Connectivity Categories**	**Presence based on the following Assessment Conditions**
Feed-to-Unit	$z_{j'}^{FRO}$ = binary variable representing the existence of a pump/turbine from the inlet splitting node to membrane mixing node *j'*	$if\ (PW_{j'}^{FRO} > 0) \vee\ (PW_{j'}^{FRO} < 0)\ \forall j' \in J$
Units-to-Outlet	z_j^{PP}=binary variable representing the existence of a pump/turbine from membrane permeate splitting node *j* to outlet permeate stream mixer	$if\ (PW_j^{PP} > 0) \vee (PW_j^{PP} < 0)\ \forall j' \in J$
	z_j^{BB}=binary variable representing the existence of a pump/turbine from membrane reject splitting node *j* to outlet reject stream mixer	$if\ (PW_j^{BB} > 0) \vee (PW_j^{BB} < 0)\ \forall j' \in J$
Unit-to-Unit	$z_{j,j'}^{P}$ = binary variable representing the existence of a pump/turbine from membrane permeate splitting node *j* to membrane mixing node *j'*	$if\ (PW_{j,j'}^{P} > 0) \vee (\ PW_{j,j'}^{P} < 0)$
	$z_{j,j'}^{B}$ = binary variable representing the existence of a pump/turbine from membrane reject from splitting node *j* to membrane mixing node *j'*	$if\ (PW_{j,j'}^{B} > 0) \vee (\ PW_{j,j'}^{B} < 0)$

Our representation of pressure manipulation options is different to recent work by Saif et al [15,16] who make use of pump and turbine collective unit operation boxes. In our work, the pump or energy recovery device options are based on the streams

available within the network rather than utilizing collective unit operation boxes for pressurization/depressurization. This allows more pressure change options to be considered in the network at the expense of requiring slightly more binary variables to be explored as compared to the representation by Saif et al. [15,16].

Table 3 shows the numbers of binary variables associated with the lean superstructure arrangements in Steps 1 and 2 as well as the comprehensive superstructure formulation.

Table 3. Summary of binary variables associated with each case described

	# of Binary Variables Explored		
Description	Superstructure size: 1 unit	Superstructure size: 2 units	Superstructure size: 3 units
Comprehensive Superstructure	18	40[a] (30)[b]	70
Combined Lean Superstructure	3	18	36
Class 1	3	-	-
Class 2a	-	8	-
Class 2b	-	8	-
Class 3a	-	-	13
Class 3b	-	-	15
Class 3c	-	-	17
Class 3d	-	-	17
Class 3e	-	-	15

[a] *Considering the representation of pressure manipulation options followed in this work*
[b] *Considering the representation of pressure manipulation options as in Saif et al. [15]*

The comprehensive superstructure formulation would require significantly more binary variables to be explored as compared to the leaner superstructure employed in

targeting. The lean superstructure formulations associated with design classes explored in Step 2 feature requires even less binary variables.

4.6 Network Optimization

For a given feed water stream with clearly defined compositions under specified feed temperature conditions, the synthesis goal is to determine the optimum membrane network configuration from the lean superstructure that achieves maximum performance with respect to an economic criterion whilst achieving the minimum required product water flow of a purity at or below specification. This section presents the mathematical formulation of the network superstructure optimization problem and describes its implementation.

The default objective considered in network optimization is to minimize the total annualized cost of the network (TC)

$$Minimize \;\; TC \tag{1}$$

In general it is possible to formulate any function of variables employed in the problem formulation as the objective function. A typical specific network cost function that is commonly employed in SWRO membrane network synthesis is presented in the example section.

For any feasible solution, a number of equality constraints must apply for mixers, splitters and RO units within the system so as to satisfy material conservation requirements. There exist three different types of splitting nodes: a feed splitting node, as

well as both a high pressure (reject) and a low pressure (permeate) splitting node associated with each unit j present in the network. The following constraints on split fraction apply at the feed splitting node:

$$\sum_{j'=1}^{Nro} f_{j'}^{FRO} y_{j'}^{FRO} + f^{FEED} y^{FEED} = 1 \quad (2)$$
$$y_{j'}^{FRO} \in \{0,1\} \ \forall j' \in J$$
$$y^{FEED} \in \{0,1\}$$

The constraints on split fractions for the permeate and the concentrate splitting nodes of membrane unit j take into consideration all split fractions of the steams into the splitter, multiplied by their respective binary variable, and are given below:

$$\sum_{j'=1}^{Nro} f_{j,j'}^{P} y_{j,j'}^{P} + f_j^{PP} y_j^{PP} = 1 \quad \text{j}\in\text{J} \quad (3)$$
$$y_{j,j'}^{P}, \ y_j^{PP}, \in \{0,1\} \ \forall j, j' \in J$$

$$\sum_{j'=1}^{Nro} f_{j,j'}^{B} y_{j,j'}^{B} + f_j^{BB} y_j^{BB} = 1 \quad \text{j}\in\text{J} \quad (4)$$
$$y_{j,j'}^{P}, \ y_j^{BB} \in \{0,1\} \ \forall j, j' \in J$$

Similarly, three different types of mixing nodes exist: an outlet permeate mixing node, an outlet reject mixing node, and a mixing node associated with feed into membrane units. Equations 5-10 describe total and component balances mixing at these mixing nodes.

$$F^{PROD} = F^{FEED} f^{FEED} y^{FEED} + \sum_{j=1}^{Nro} f_j^{PP} y_j^{PP} F_j^{P} \quad \text{j}\in\text{J} \quad (5)$$
$$F^{PROD} X_i^{PROD} = F^{FEED} f^{FEED} y^{FEED} X_i^{FEED} + \sum_{j=1}^{Nro} f_j^{PP} F_j^{P} y_j^{PP} X_{i,j}^{P} \quad \text{i}\in\text{I}, \ \text{j}\in\text{J} \quad (6)$$
$$y_j^{PP} \in \{0,1\} \ \forall j \in J$$
$$y^{FEED} \in \{0,1\}$$

$$F^{BRINE} = \sum_{j=1}^{Nro} f_j^{BB} y_j^{BB} F_j^{B} \quad \text{j}\in\text{J} \quad (7)$$
$$F^{BRINE} X_i^{BRINE} = \sum_{j=1}^{Nro} f_j^{BB} y_j^{BB} F_j^{B} X_{i,j}^{B} \quad \text{i}\in\text{I}, \ \text{j}\in\text{J} \quad (8)$$

$$y_j^{BB} \in \{0,1\} \ \forall j \in J$$

$$F_j^F = F^{FEED} f_{j'}^{FRO} y_j^{FRO} + \sum_{j=1}^{Nro} F_j^F f_{j,j'}^P y_{j,j'}^P + \sum_{j=1}^{Nro} F_j^F f_{j,j}^B y_{j,j'}^B \qquad \text{j,j'}\in\text{J} \qquad (9)$$

$$F_j^F X_{i,j}^F = F^{FEED} f_{j'}^{FRO} X_i^{FEED} y_j^{FRO} + \sum_{j=1}^{Nro} F_j^F f_{j,j'}^P X_{i,j,j}^P y_{j,j'}^P + \sum_{j=1}^{Nro} F_j^F f_{j,j'}^B X_{i,j,j}^B y_{j,j'}^B$$

$$\text{i}\in\text{I} \quad \text{j,j'}\in\text{J} \ y_{j'}^{FRO}, \ y_{j,j'}^B, \ y_{j,j'}^P \in \{0,1\} \ \forall j, j' \in J \qquad (10)$$

The total and component mass balances across a membrane unit conserves both the feed stream flow as well as the salt content into a certain membrane unit with brine and permeate streams exiting the unit, and are given by the following equations:

$$F_j^F = F_j^B + F_j^P \qquad \text{j}\in\text{J} \qquad (11)$$

$$F_j^P = R_j \times F_j^F \qquad \text{j}\in\text{J} \qquad (12)$$

$$F_j^F \times X_{i,j}^F = F_j^B \times X_{i,j}^B + F_j^P \times X_{i,j}^P \qquad \text{i}\in\text{I and j}\in\text{J} \qquad (13)$$

The total and component material balances across the entire treatment system conserve the total flow and salt content of the feed stream into the network with brine and permeate streams exiting the network, and are given by the following equations:

$$F^{FEED} = F^{BRINE} + F^{PROD} \qquad (14)$$

$$F^{FEED} X_i^{FEED} = F^{BRINE} X_i^{BRINE} + F^{PROD} X_i^{PROD} \qquad (15)$$

In addition to the equality constraints associated with the mass balances, a number of inequality constraints define the maximum permissible contamination limit on the final permeate concentration, the minimum permissible on the permeate flowrate, an upper inlet feed pressure limit and a specified range of modules within RO units respectively in order to maintain desirable RO operating conditions.

$$X_i^{PROD} \leq X_i^{PROD,MAX} \ \text{i}\in\text{I} \qquad (16)$$

$$F^{PROD} \geq F^{PROD,MIN} \qquad (17)$$

$$P_j^F \leq P_j^{F,MAX} \qquad \text{j}\in\text{J} \qquad (18)$$

$$NM_j^{MIN} \leq NM_j \leq NM_j^{MAX} \ \text{j}\in\text{J} \qquad (19)$$

The number of modules for each treatment unit within the network (NM_j) is calculated through membrane model equations, and is a function of flow, and differences between applied and osmotic pressures. A membrane model commonly employed in SWRO membrane network synthesis is presented in the example section. Equations 20-31 describe the handling of pressure within the network across all mixers, splitters and membrane units.

$$P_j^P = P^{PROD} \qquad j \in J \qquad (20)$$
$$P_j^B = P_j^F - \Delta P_j \qquad j \in J \qquad (21)$$
$$PI_{j'}^{FRO} = P^{FEED} \qquad j' \in J \qquad (22)$$
$$PI_j^{PP} = P_j^P \qquad j \in J \qquad (23)$$
$$PI_{j,j'}^P = P_j^P \qquad j,j' \in J \qquad (24)$$
$$PI_j^{BB} = P_j^B \qquad j \in J \qquad (25)$$
$$PI_{j,j'}^B = P_j^B \qquad j,j' \in J \qquad (26)$$
$$PF_{j'}^{FRO} = P_j^F \qquad j,j' \in J \qquad (27)$$
$$PF_{j,j'}^P = P_j^F \qquad j,j' \in J \qquad (28)$$
$$PF_{j,j'}^B = P_j^F \qquad j,j' \in J \qquad (29)$$
$$PF_j^{BB} = P^{BRINE} \qquad j \in J \qquad (30)$$
$$PF_j^{PP} = P^{PROD} \qquad j \in J \qquad (31)$$

All streams with positive pressure differences are associated with pumps. All streams with significant negative pressure differences are associated with energy recovery devices, whereas streams with insignificant negative pressure differences, less than a specified pressure value (P^{SPEC}), are not associated with an energy recovery device. The energy requirements are determined as:

$$PW_{j'}^{FRO} = \begin{Bmatrix} F_{j'}^{FRO}\left(PF_{j'}^{FRO} - PI_{j'}^{FRO}\right) \; if\left(PF_{j'}^{FRO} - PI_{j'}^{FRO} > 0\right) \forall j' \in J \\ 0 \; if\left(PF_{j'}^{FRO} - PI_{j'}^{FRO} = 0\right) \forall j' \in J \\ F_{j'}^{FRO}\left(PF_{j'}^{FRO} - PI_{j'}^{FRO}\right) \; if \; \left(PF_{j'}^{FRO} - PI_{j'}^{FRO}\right) < 0 \wedge \left|PF_{j'}^{FRO} - PI_{j'}^{FRO}\right| > \Delta P^{SPEC} \forall j' \in J \\ 0 \; if \; \left(PF_{j'}^{FRO} - PI_{j'}^{FRO}\right) < 0 \wedge \left|PF_{j'}^{FRO} - PI_{j'}^{FRO}\right| < \Delta P^{SPEC} \; \forall j' \in J \end{Bmatrix} \qquad (32)$$

$$PW_{j,j'}^{P} = \begin{Bmatrix} F_{j,j}^{P}\left(PF_{j,j'}^{P} - PI_{j,j'}^{P}\right)\ if\left(PF_{j,j'}^{P} - PI_{j,j'}^{P} > 0\right)\forall j' \in J \\ 0\ if\left(PF_{j,j'}^{P} - PI_{j,j'}^{P} = 0\right)\forall j' \in J \\ F_{j,j}^{P}\left(PF_{j,j'}^{P} - PI_{j,j'}^{P}\right)\ if\ \left(PF_{j,j'}^{P} - PI_{j,j'}^{P}\right) < 0 \wedge \left|PF_{j,j'}^{P} - PI_{j,j'}^{P}\right| > \Delta P^{SPEC}\forall j' \in J \\ 0\ if\ \left(PF_{j,j'}^{P} - PI_{j,j'}^{P}\right) < 0 \wedge \left|PF_{j,j'}^{P} - PI_{j,j'}^{P}\right| < \Delta P^{SPEC}\ \forall j' \in J \end{Bmatrix} \quad (33)$$

$$PW_{j,j'}^{B} = \begin{Bmatrix} F_{j,j}^{B}\left(PF_{j,j'}^{B} - PI_{j,j'}^{B}\right)\ if\left(PF_{j,j'}^{B} - PI_{j,j'}^{B} > 0\right)\forall j' \in J \\ 0\ if\left(PF_{j,j'}^{B} - PI_{j,j'}^{B} = 0\right)\forall j' \in J \\ F_{j,j}^{B}\left(PF_{j,j'}^{B} - PI_{j,j'}^{B}\right)\ if\ \left(PF_{j,j'}^{B} - PI_{j,j'}^{B}\right) < 0 \wedge \left|PF_{j,j'}^{B} - PI_{j,j'}^{B}\right| > \Delta P^{SPEC}\forall j' \in J \\ 0\ if\ \left(PF_{j,j'}^{B} - PI_{j,j'}^{B}\right) < 0 \wedge \left|PF_{j,j'}^{B} - PI_{j,j'}^{B}\right| < \Delta P^{SPEC}\ \forall j' \in J \end{Bmatrix} \quad (34)$$

$$PW_{j}^{PP} = \begin{Bmatrix} F_{j}^{PP}\left(PF_{j}^{PP} - PI_{j}^{PP}\right)\ if\left(PF_{j}^{PP} - PI_{j}^{PP} > 0\right)\forall j' \in J \\ 0\ if\left(PF_{j,j'}^{B} - PI_{j,j'}^{B} = 0\right)\forall j' \in J \\ F_{j}^{PP}\left(PF_{j}^{PP} - PI_{j}^{PP}\right)\ if\ \left(PF_{j}^{PP} - PI_{j}^{PP}\right) < 0 \wedge \left|PF_{j}^{PP} - PI_{j}^{PP}\right| > \Delta P^{SPEC}\forall j' \in J \\ 0\ if\ \left(PF_{j}^{PP} - PI_{j}^{PP}\right) < 0 \wedge \left|PF_{j}^{PP} - PI_{j}^{PP}\right| < \Delta P^{SPEC}\ \forall j' \in J \end{Bmatrix} \quad (35)$$

$$PW_{j}^{BB} = \begin{Bmatrix} F_{j}^{BB}\left(PF_{j}^{BB} - PI_{j}^{BB}\right)\ if\left(PF_{j}^{BB} - PI_{j}^{BB} > 0\right)\forall j' \in J \\ 0\ if\left(PF_{j}^{BB} - PI_{j}^{BB} = 0\right)\forall j' \in J \\ F_{j}^{BB}\left(PF_{j}^{BB} - PI_{j}^{BB}\right)\ if\ \left(PF_{j}^{BB} - PI_{j}^{BB}\right) < 0 \wedge \left|PF_{j}^{BB} - PI_{j}^{BB}\right| > \Delta P^{SPEC}\forall j' \in J \\ 0\ if\ \left(PF_{j}^{BB} - PI_{j}^{BB}\right) < 0 \wedge \left|PF_{j}^{BB} - PI_{j}^{BB}\right| < \Delta P^{SPEC}\ \forall j' \in J \end{Bmatrix} \quad (36)$$

The binary variables associated with stream connections are handled as summarized in Table 1. Enforced connections always ensure the structural integrity of the lean superstructure used for targeting in Stage 1 and all lean superstructures for the design classes associated with Step 2.

The optimization problem constitutes a mixed integer nonlinear program (MINLP), in which the aim is to minimize the total cost (Equation 1), subject to process equality constraints of Equations (2)-(13); (20)-(31) and inequality constraints of

Equations (16)-(19); (32)-(36), and for which the handling and manipulation of binary terms have been given in Tables 1 and 2.

The lean superstructure optimization problems are solved using the "*what'sBest"* Mixed-Integer Global Solver for Microsoft Excel by LINDO Systems Inc. [29]. In contract to optimization environments such as GAMS or LINGO, an Excel spread sheet acts as an interface to the global solver package. This ensures ease of use of the implemented methodology. The superstructure optimization schemes have been implemented using Microsoft Excel 2010 and "what's best 9.0.5.0", and run on a desktop PC (Intel® Core ™ i7-2620M, 2.7 GHz, 8.00 GB RAM, 64-bit Operating System).

4.7 Illustrative Example (Case Study 1)

The proposed approach is illustrated with a commonly studied sea water desalination example using hollow fiber reverse osmosis modules [4-7, 15-16]. To enable comparison with previous work, the proposed approach is illustrated with a simple seawater desalination design example based on Evangelista [6]. This example by has been addressed in numerous published studies [4-7, 15-16]. to illustrate SWRO membrane superstructure network optimization. The membrane model to predict membrane unit performance is based on the Evangelista [6] short-cut method as per Equations (37) through (40). For details about assumptions or limitations associated with equations (37)-(40) it is referred to the original paper by Evangelista [6]. The number of

modules present in an RO synthesis unit (NMj) depends primarily on the flow, and the applied and osmotic pressure difference.

$$NM_j = A\, SM_j\, \gamma(\Delta P_j - \Delta\pi_j) \tag{37}$$

$$\gamma = \frac{\eta}{1+16A\mu r_o l l_s \eta / r_i^4} \tag{38}$$

$$\eta = \frac{\tanh[(16A\mu r_o/r_i^2)^{1/2}(l/r_i)]}{(16A\mu r_o/r_i^2)^{1/2}(l/r_i)} \tag{39}$$

$$X_{i,j}^P = \frac{\mathrm{K_i}\ X_{i,j}^m}{A\ \gamma(\Delta P_j - \Delta\pi_j)} \tag{40}$$

The objective function employed is adopted from Voros et al. [7] and Saif et al. [15,16]. The objective is to minimize the total annualized cost over all RO units, pumps and turbines in the system. The cost of each RO stage/pass is calculated using the number of modules multiplied by a cost parameter (c_{ro}) and the respective cost contribution is represented by (C_{RO}). The fixed cost of pumps and turbines ($C^{P/E}{}_{FIXED}$) are calculated using the number of power produced/recovered throughout all the network raised to a fractional constant (βpu,βtu) multiplied by a cost parameter (a_{pu}, a_{tu}). The variable cost of pumps and turbines (The fixed cost of pumps and turbines ($C^{P/E}{}_{FIXED}$) are calculated using the number of power produced/recovered throughout all the network and multiplied by a cost parameter (a_{pu}, a_{tu}). Parameters for fixed and variable cost coefficients for RO modules, pump and energy recovery turbines are given in table 4.

$$\text{Min} \quad TC = C_{RO} + C^{P/E}{}_{FIXED} + C^{P/E}{}_{OPER} \tag{41}$$

$$C_{RO} = \sum_{j=1}^{Nro} c_{ro} NM_j \tag{42}$$

$$C_{OPER} = \sum_{j=1}^{Nro} a_{pu} z_{j,j}^P PW_{j,j'}^P + \sum_{j=1}^{Nro} a_{tu} z_{j,j}^B PW_{j,j'}^B + \sum_{j=1}^{Nro} a_{pu} z_j^P PW_j^{PP} + \sum_{j=1}^{Nro} a_{tu} z_j^B PW_j^{BB} + \sum_{j'=1}^{Nro} a_{pu}\, z_{j'}^{FEED} PW_{j'}^{FRO} \quad \forall\, j' \in J \tag{43}$$

$$C_{FIXED} = \sum_{j=1}^{Nro} a_{pu}\left(z_{j,j}^{P} PW_{j,j'}^{P}\right)^{\beta pu} + \sum_{j=1}^{Nro} a_{tu}\left(z_{j,j}^{B} PW_{j,j'}^{B}\right)^{\beta tu} + \sum_{j=1}^{Nro} a_{pu}\left(z_{j}^{P} PW_{j}^{PP}\right)^{\beta pu} + \sum_{j=1}^{Nro} a_{tu}\left(z_{j}^{B} PW_{j}^{BB}\right)^{\beta tu} + \sum_{j'=1}^{Nro} a_{pu}\left(z_{j'}^{FEED} PW_{j'}^{FRO}\right)^{\beta pu} \quad \forall j' \in J \tag{44}$$

Table 4. Input data and parameters used for seawater desalination case study [5,15]

Parameter/Variable	**Value**
$\boldsymbol{F^{FEED}}$ total inlet feedwater flowrate into the network (kg/s)	19.29 (high end) 13.052 (low end)
$\boldsymbol{X_i^{FEED}}$ composition of component i in inlet feedwater stream	0.03480
$\boldsymbol{P^{FEED}}$ feedwater pressure into the network (bar)	1
$\boldsymbol{P^{PROD}}$ final permeate pressure (bar)	1
$\boldsymbol{P^{BRINE}}$ final reject pressure (bar)	1
$\boldsymbol{F^{PROD,MIN}}$ minimum permeate flow required in the network (kg/s)	5.79
$\boldsymbol{X_i^{PROD,MAX}}$ maximum allowable concentration of component i in the permeate stream	0.00057
$\boldsymbol{SM_j}$ membrane Area per module in RO unit j (m^2)	152
$\Delta \boldsymbol{P_j}$ pressure drop in RO unit j (bar)	0.22
$\boldsymbol{P_j^{F,MAX}}$ maximum allowable feed pressure in RO unit j (bar)	70
$\Delta\, \boldsymbol{P^{SPEC}}$ maximum allowable pressure difference that would allow the placement of ERDs (bar)	1
$\boldsymbol{A}$ pure water permeability (kg/(s N))	1.22×10^{-10}
$\mathbf{K_i}$ transport parameter of solute i (kg/(s m^2))	4.0×10^{-6}
$\boldsymbol{r_i}$ inner radius of hollow fiber (m)	21×10^{-6}
$\boldsymbol{r_o}$ outer radius of hollow fiber (m)	50×10^{-6}
$\boldsymbol{l}$ fiber length (m)	0.75
$\boldsymbol{l_s}$ fiber seal length (m)	0.075
$\boldsymbol{c_{ro}}$ cost coefficient of an RO module ($/(modue yr))	1450
$\boldsymbol{a_{pu}}$ operating cost coefficient of a pump unit ($/(kg/s) yr))	80
$\boldsymbol{a_{tu}}$ operating cost coefficient of an energy recovery turbine unit ($/(kg/s) yr))	34
$\boldsymbol{b_{pu}}$ fixed cost coefficient of a pump unit cost ($/(kg/s)$^{0.79}$ yr))	139.93
$\boldsymbol{\beta_{pu}}$ fractional constant corresponding to a pump unit fixed cost	0.79
$\boldsymbol{b_{tu}}$ fixed cost coefficient of a turbine unit cost ($/(kg/s)$^{0.47}$ yr))	93.62
$\boldsymbol{\beta_{tu}}$ fractional constant corresponding to a turbine unit fixed cost	0.47

The overall objective aims at minimizing the total cost of the network (TC) consisting of RO units, pumps and ERDs. In the adopted case study, TC is assumed to primarily depend on the cost/number of membrane modules for each RO synthesis units, and the cost of pumps and turbines (fixed and operating) which is in turn related to the power involved. The problem data are presented in Table 4. The results obtained using the presented approach are compared to previous findings for this case study [4-7, 15-16]. Tables 5 and 6 summarize the findings from Stages 1 and 2 of the approach as well as previous work.

4.7.1 ***Stage 1-Targeting***

Targeting is performed using a lean superstructure of a maximum of three membrane units as shown in Figure 7. The reported global solution has a total annualized cost of 2.45×10^5 \$/yr as opposed to 2.7×10^5 \$/yr reported for previous work using a local solver [5, 14]. This result corresponds to a feed water flow rate into the desalination network of 19.29 kg/s.

Saif et al. [15,16] report a design with a cost of 2.3×10^5 \$/yr that exhibits a feed to brine bypass so that only a total of 13.05 kg/s of the 19.29 kg/s of feed water are fed through membrane units. A feedwater-to-brine bypass stream is an eliminated stream connection in our representation. This is because pretreatment of feed water is costly and the bypassing of pretreated feed water to brine (waste) is economically unattractive. However, the objective function used in the case study does not account for pretreatment costs so that such bypasses are not penalized during optimisation. To enable comparison

with Saif et al. [15, 16], we repeat the optimization with a feed flow rate of 13.05 kg/s. An optimum network with a total annualized cost of $2.29x10^5$ $/yr is determined for this case, which is slightly superior to the optimal design reported earlier [15, 16]. The minor discrepancies in optimum cost can be attributed to the absence of pumps which overcome very small pressure differences in our design. Below, we refer to the original case study with a feed flow of 19.29 kg/s as the higher-end input feed case. The case of a 13.05 kg/s feed flow is referred to as the lower-end input feed case.

The optimal designs were extracted from the lean superstructure in under three minutes of CPU time for both input feed cases and a superstructure size of three membrane units using the easy to use implementation of the approach in Microsoft Excel with the LINDO global solver on a standard PC, which compares favorably to CPU times above ten minutes as reported previously for the global optimization of comprehensive superstructures of a size of only two units for this case [15, 16].

4.7.2 ***Stage 2- Development of Alternative Designs***

Next, we explore the distinct design class configurations up to a total of three membrane units. Design Classes (1a, 2b, 3c and 3d) were found to be infeasible options based on the data in Table 4. As for the remaining options, Figures 11 & 12 provide an illustration for optimal solution examples that were obtained utilizing the proposed network synthesis and search strategy (both using a combined lean superstructure covering the various dimensions of all design classes as well as utilizing the individual design classes).

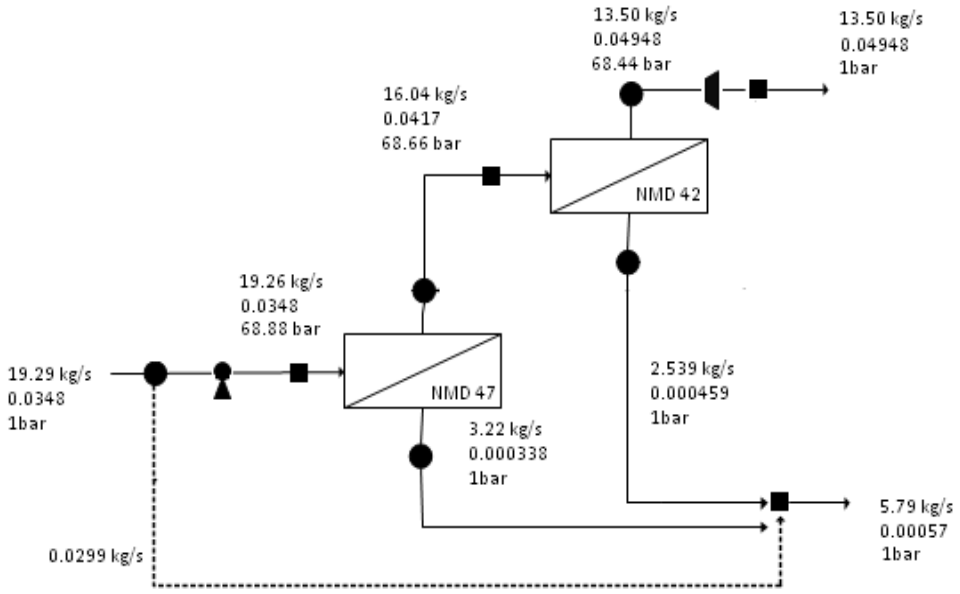

Figure 11. Optimal design for class 2a (high end feed)

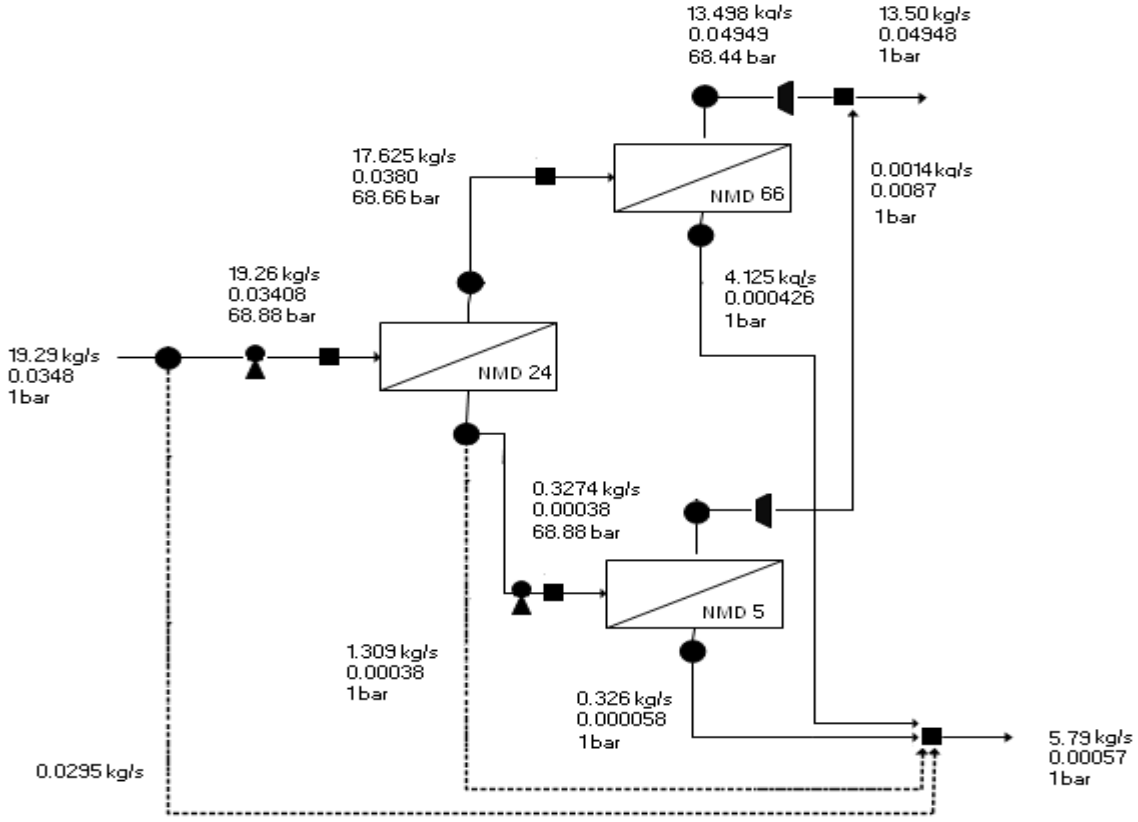

Figure 12. Optimal design and operating conditions, based on class 3e, for RO network seawater desalination case study (high end feed)

For comparison purposes, optimal solutions from previous efforts are shown in Figures 13 and 14 below [5, 15-16].

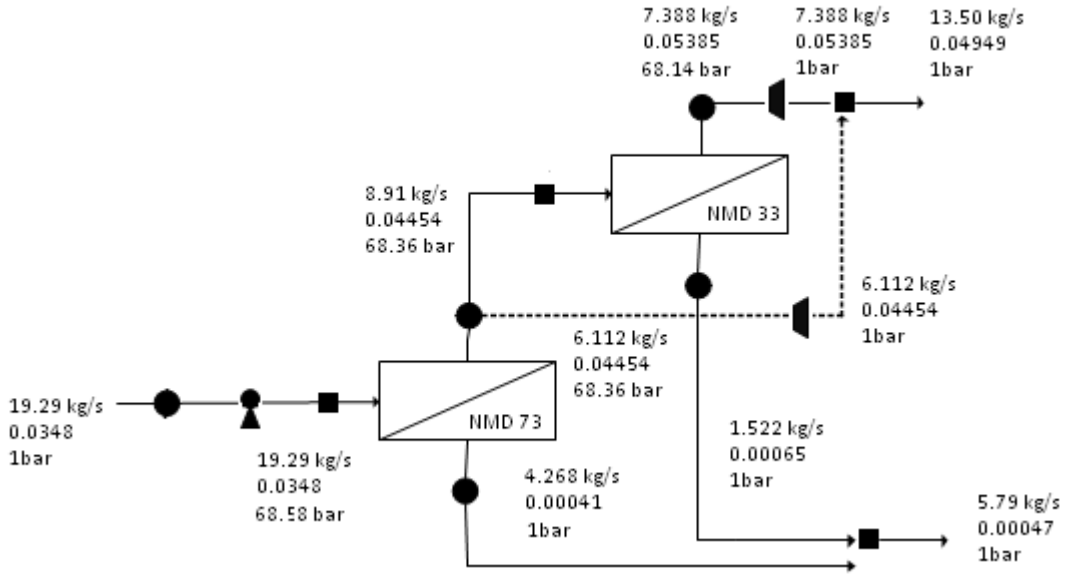

Figure 13. Optimal design and operating conditions for RO network seawater desalination case study obtained by El-Halwagi [5]

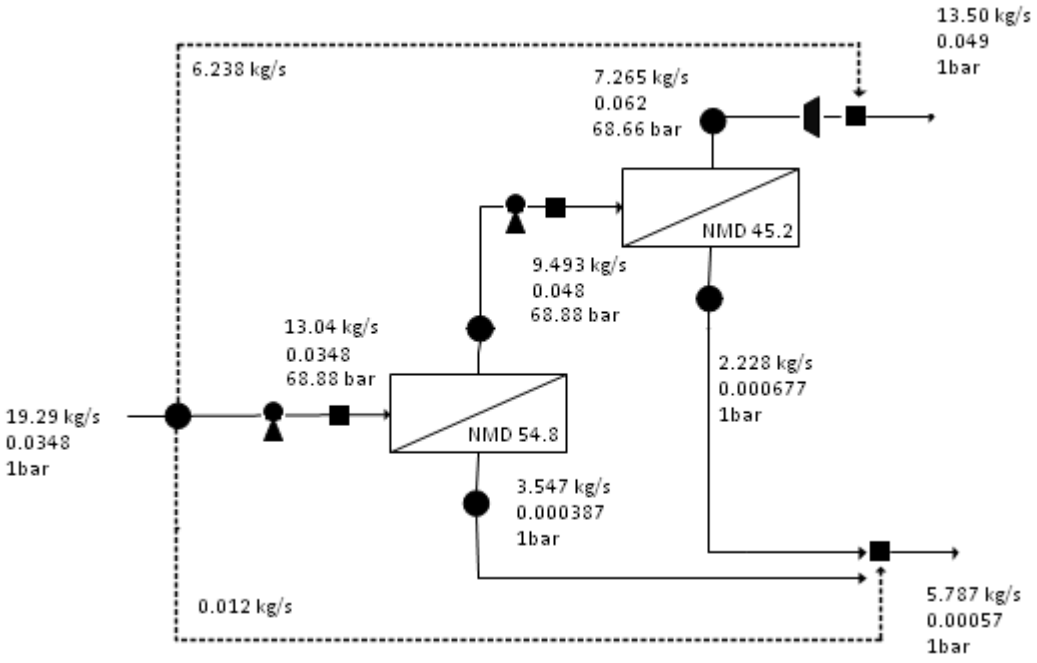

Figure 14. Optimal design and operating conditions for RO network seawater desalination case study obtained by Saif et al. [15]

Table 5 (higher-end input feed) and Table 6 (lower-end input feed) detail the results obtained for all design classes in terms of split fractions, number of membrane modules and the total annual cost within the corresponding feasible design classes.

Table 5. Summary of results for desalination case study, higher-end input feed

	# of Modules	**Total Water Recovery (%)**	**Optional Streams, Split Fractions**	**Eliminated Streams not considered in class representation, Split Fractions**	**Total Cost ($/yr)**	**CPU time (s)**
Previous Work [5][a]	Unit1: 73 Unit2 (stage): 33	Unit1:22.1 Unit2:17.08 Total: 30	Stream3: 0.406	None	$270,868/yr	117 using GINO (local optimization)
Class 1	infeasible	-	-	-	-	-
Class 2a	Unit1: 47 Unit2 (Stage): 42	Unit1:16.72 Unit2:15.83 Total: 30	Stream1: 0.00155	None	$245,428/yr	34 using LINDO, what'sBest!
Class 2b	infeasible	-	-	-	-	-
Class 3a	Unit1: 70 Unit2 (Stage): 10 Unit3 (Stage): 11	Unit1: 24.1 Unit2:18.7 Unit3:8.99 Total: 30	Stream1: 0.00138 Stream4: 0.5163 Stream5: 0.600	None	$252,879/yr	22 using LINDO, what'sBest!
Class 3b	Unit1: 55 Unit2 (Stage): 34 Unit3 (Pass): 5	Unit1:19.36 Unit2:13.1 Unit3:99.5 Total: 30	Stream1: 0.00155 Stream5: 0.864	None	$254,632/yr	22 using LINDO, what'sBest!
Class 3c	infeasible	-	-	-	-	-
Class 3d	infeasible	-	-	-	-	-
Class 3e	Unit1: 25 Unit2 (Pass): 5 Unit3 (Stage): 66	Unit1:8.49 Unit2:99.56 Unit3:23.40 Total: 30	Stream1: 0.00153 Stream3: 0.8	None	$256,452/yr	31 using LINDO, what'sBest!
Lean Superstructure[b]	Unit1: 47 Unit2 (Stage): 42	Unit1:16.72 Unit2:15.83 Total: 30	Stream1: 0.00155	None	$245,428/yr	177 using LINDO, what'sBest!

[a] *Superstructure size: 2 units*
[b] *Superstructure size: 3 units*

Table 6. Summary of results for desalination case study, lower-end input feed

	# of Modules	Water Recovery (%)	Optional Streams, Split Fractions	Eliminated Streams not considered in class representation, Split Fractions	Total Cost ($/yr)	CPU time [s]
Previous Work [15,16]	Unit1:54.8 Unit2 (Stage): 45.2	Unit 1:27.2 Unit 2:23.5 Total: 30	Stream1: 0.000622	Feed-to-brine bypass: 0.323	$230,906/yr	643.3 using CPLEX GAMS22.5
Class 1	infeasible	-	-	-	-	-
Class 2a	Unit1: 52 Unit2 (Stage):47	Unit1:26.2 Unit2:26.6 Total: 44.4	Stream1: 0.00099	None	$229,102/yr	37 using LINDO,what'sBest!
Class 2b	infeasible	-	-	-	-	-
Class 3a	Unit1: 70 Unit2 (Stage):16 Unit3 (Stage):17	Unit1:33.4 Unit2:21.5 Unit3:10.6 Total:44.4	Stream1: 0.00058 Stream 4: 0.107 Stream 5: 0.600	None	$239,721/yr	42 using LINDO, what'sBest!
Class 3b	Unit1: 49 Unit2 (Stage): 50 Unit3 (Pass) : 5	Unit1:24.9 Unit2:25.9 Unit3:99.4 Total:44.4	Stream1: 0.00098 Stream 5: 0.9179	None	$237,917/yr	24 using LINDO, what'sBest!
Class 3c	infeasible	-	-	-	-	-
Class 3d	infeasible	-	-	-	-	-
Class 3e	Unit1: 30 Unit2 (Pass) : 4 Unit3 (Stage):70	Unit1:15.6 Unit2:97.6 Unit3:34.0 Total:44.4	Stream1: 0.00118 Stream3: 0.7	None	$239,342yr	32 using LINDO,what'sBest!
Lean Superstructure	Unit1: 52 Unit2 (Stage):47	Unit1:26.2 Unit2:26.6 Total: 44.4	Stream1: 0.00099	None	$229,102/yr	135 using LINDO,what'sBest!

[a] *Superstructure size: 2 units*
[b] *Superstructure size: 3 units*

Overall, the two-unit staged arrangement (class 2a) is the lowest cost design for the given system parameters and objective. The optimal design class 2a design is shown in Figure 11 for the higher-end input feed case. This design corresponds to the optimal design extracted from the lean superstructure in Stage 1. The total annualized costs of the optimal solutions across all feasible design classes for both higher and lower end input feed cases are within 5% of the best solution, indicating a flat optimum and a multiple choices of high performance designs. Figure 12 shows the optimal solution for design class 3e as an alternative, which employs three membrane units in a stage and pass arrangement. The cost breakdowns of the optimum solutions within each of the feasible design classes is shown in Figure 15, which demonstrates the relatively flat optimum across all classes, indicating slight variation of optimum solutions within the options explored.

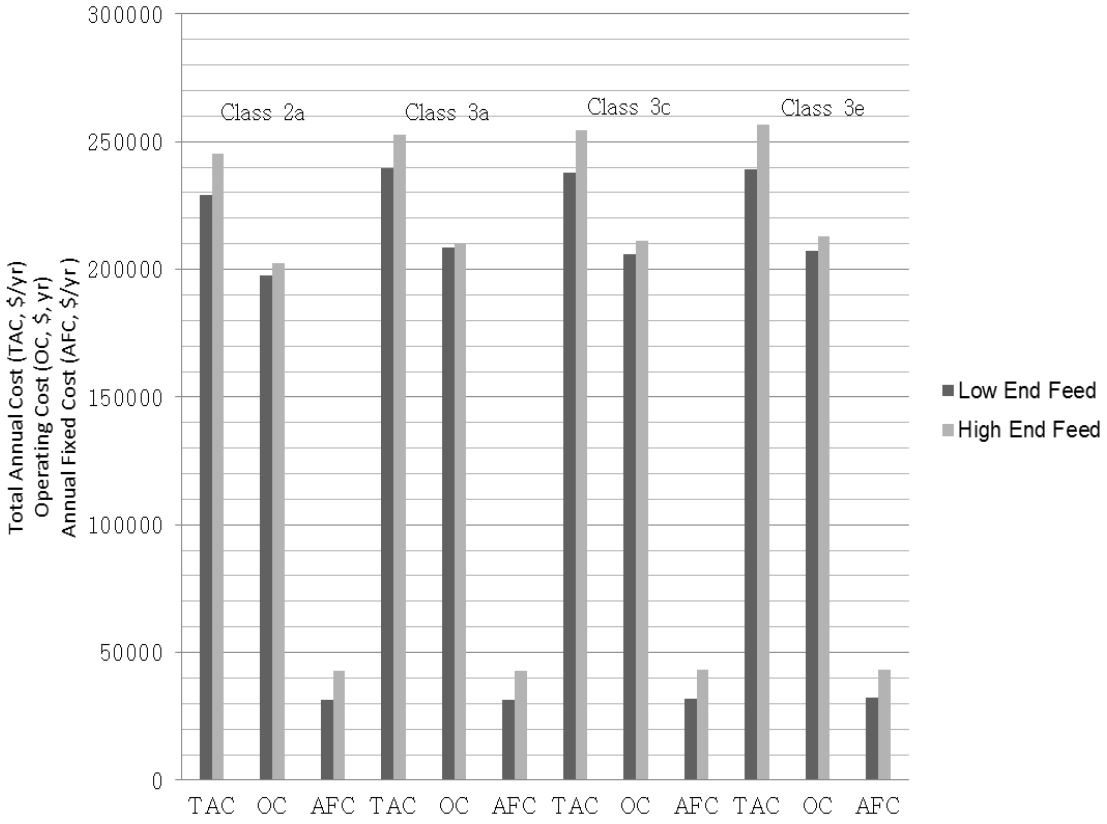

Figure 15. Dependence of total cost functions upon feasible design class

The optimal solution for each design class can be identified very quickly using the corresponding lean superstructures in Stage 2. Tables 5 and 6 presented above show that solutions across all classes were developed in under 45 seconds of CPU time, using Microsoft Excel with the LINDO global solver on a standard PC. Stage 2 of the synthesis approach enables the quick exploration of structurally different design alternatives. This provides the design engineer with a better understanding of the design space and potential high-performance alternatives as compared to full superstructure optimization alone.

The case study has been selected to enable comparison of the proposed approach to previous work in SWRO membrane network synthesis using superstructure optimization. The comparison has shown that the proposed approach enables the reliable and quick identification of designs in Stages 1 and 2 of the method. Larger systems can be handled at significantly reduced CPU times in an easier to use implementation as compared to previous superstructure optimization approaches.

5. SYNTHESIS OF OPTIMAL SEAWATER REVERSE OSMOSIS NETWORKS WITH MULTIPLE WATER QUALITY PARAMETERS

This section makes use of the previously developed SWRO network synthesis approach that has been the subject of Section 4. By mainly utilizing the previously described superstructure optimization approach, considerations for multiple seawater feed water quality parameters, in the form of more detailed composition specifications have been integrated within SWRO network optimization. In other words, in contrast to previous approaches that consider sea water to consist of two components only, i.e. "water" and a total salt content lumped together as "Total Dissolved Solids (TDS)", the developed superstructure models account for detailed water quality information throughout the system. This involves the extraction of models that capture the performance of common membrane elements, as predicted by commercially available membrane simulator tools, and in turn embedding them into the network optimization problem. Moreover, a detailed economic assessment that captures all the significant capital and operating costs associated in SWRO processes is utilized as the objective function, so as to obtain more efficient and reliable cost information related to the economic performance of SWRO systems.

5.1 RO Membrane Modeling

It is well recognized that a reverse osmosis membrane acts as a semi-permeable barrier to feed flow under pressure, resulting in the selective passage of solvent (mainly

water) molecules into a separate permeate stream. Hence, the overall process allows for an efficient separation of product water from unwanted solutes present in the feed. Chemical potential gradients across the membrane not only provide driving forces for solvent transport, but also for various solute ions that could pass across the membrane. Depending on the size of the membrane pores as well as the membrane's solute rejection capabilities, solutes may pass through the membrane up to a certain extent; this is because RO membranes are imperfect barriers to dissolved salts in feedwater, hence causing slight salt quantities to slip through the membrane. Thus, reverse osmosis pore dimensions are designed based on favorable solvent passage conditions as well as salt rejection characteristics that accommodate desirable permeate concentration limits [18].

The type of membranes used in any effective desalination network greatly depends on recommendations from membrane manufacturers according to the specific membrane properties, as well as calculations of projected system performance based on the set of given operating conditions. Even though solvent passage and salt rejection, two of the fundamental membrane performance assessment properties, are classified as intrinsic properties of the individual membranes, they could also be influenced by variable operating parameters, such as different conditions of temperature, pressure etc [18]. Thus, it is necessary to establish consistent membrane prediction capabilities, based on assessing membrane operating criteria that affect both salt and solvent passage through the membranes.

Various RO theoretical models have been established for the purpose of predicting membrane performance ((Kedem-Katchalsky 1958), (Spiegler-Kedem 1966),

(Evangelista 1985) [4, 30-31]. However, many of these models lack a representation of the multiple water quality nature of feedwater into the RO system. Moreover, the non-linearity of existing models may add further complexity in cases that would attempt to modify existing ones so as to incorporate multiple water quality parameters into the model prediction capacity. Thus, the use of enhanced non-linear RO models may hold back any usefulness that need to be extracted within a network optimization problem. The following section presents some analytical relations that could be used to determine an improved technical membrane performance in terms of salt rejection capacities of individual ions so as to capture a simple reflection of the multiple component feedwater nature, based on favorable system operating conditions. Established correlations are developed according to numerical simulation results using specialized membrane design programs such as ROSA (Reverse Osmosis Systems Analysis) Filmtech software [32], and IMSDesign (Hydranautics Membrane Solutions Design Software) [33].

5.2 Factors Affecting Membrane Performance

In general, and due to the complex nature of reverse osmosis membrane properties, membrane performance (both water recovery and salt rejection) can be influenced by various operating parameters within the system: feed pressure and feedwater concentration, temperature, and pH [17]. In practice, there is normally an overlap of effects coming from more than one variable since many of the operating parameters are interrelated. However, the degree to which membrane performance could be affected varies significantly, and this depends on which of the various operating

parameters manifest significant impact on membrane properties, as well as which of the system's operating conditions that are always regarded as favorable.

5.2.1 ***Feed Pressure***

Feed pressure is one of the major operating parameters that affect the economics of the desalination. For given conditions of feed water composition and temperature, feed pressure is directly related to the water recovery rate in the process. Higher recovery rates would require a relatively higher feed pressure at which the system has to operate. Increased feedwater pressure also results in increased salt rejection but, the relationship is less evident than the case of water recovery. As feedwater pressure is increased, salt passage becomes less significant since water molecules move through the membrane at a faster rate than the salt molecules are transported. Hence, as feed pressure increases, both water recovery and salt rejection increase. However, at a certain pressure level, salt rejection no longer increases since salt passage remains coupled with water flowing through the membrane. In other words, there is an upper limit to the amount of salt that can be excluded via increasing feedwater pressure, and thus an increase in water recovery is more significant than an increase in solute rejection under higher pressure conditions.

Reverse osmosis membranes are designed to withstand high feed pressure conditions up to certain levels, above which the membranes could no longer function effectively. The maximum allowable feed pressure conditions are usually specified by the manufacturer; typical maximum feed pressure values for SWRO membranes are

around 70 bars [17], and this could vary slightly depending on the types of membranes used. The tendency to design systems for the highest recovery rates possible is mostly a favorable condition for process design since high water recovery results in a maximum water production rate, and a lower volume of the concentrate. Hence, the maximum seawater desalination water recovery is established as soon as the concentrate osmotic pressure approaches the physical pressure limit of the membranes.

5.2.2 ***Feedwater Concentration***

The maximum achievable water recovery in a reverse osmosis system not only depends on limiting pressure conditions, but also on the concentration of salts present in the feedwater and their tendency to precipitate on the membrane surface, and hence form scaling compounds, as their concentrations increase while permeate is being separated from the feed. Thus, there is a limit to how much frequently-present scale forming compounds, such as calcium carbonate, magnesium carbonate, calcium sulphate, strontium sulphate, could be concentrated without exceeding their respective solubility limits [17]. Scaling symptoms are mostly prominent, but not solely limited, to the very last stages of a SWRO network due to being subjected to the highest concentration of dissolved salts within the system. Hence, controlling scaling within a reverse osmosis plant is critical to enable successful operation of the process by minimizing membrane damage. Many chemical treatment options are available; for instance, the use of sulphuric acid to reduce and control the pH of the system has been the traditional way of preventing calcium carbonate scaling (which occurs at relatively high pH conditions)

[17]. This is because sulfuric acid is relatively easier to handle than other acids and is readily available. However, since sulphuric acid is quite hazardous, and increases the sulphate content of the water other alternatives are generally employed such as the use of scale inhibiting compounds, known as antiscalants. Addition of antiscalants into the system have proven to provide the greatest success in controlling both carbonate and sulfate scaling, two of the most prominent scaling forms that could occur during seawater desalination, It is always necessary to implement the use of a quality scale inhibitor that is specifically devised for reverse osmosis membranes and suitably engineered for appropriately controlling high levels of scale forming compounds. Moreover, it is important to ensure proper dosing procedures based on antiscalant manufacturer recommendations in order to successfully control scaling within the system. Thus, the best way to maintain cost effective production is to operate the system at maximum recovery rates whilst making sure to incorporate preventive membrane scaling procedures.

5.2.3 ***pH***

The pH tolerance of various SWRO membranes, particularly thin-film membranes, show very stable values of both water recovery and membrane salt rejection and hence are slightly affected by changes in the system's pH [17].

5.2.4 ***Temperature***

Water recovery and salt rejection are very sensitive to changes in feedwater temperature. An increase in the feedwater temperature corresponds to a relatively a higher diffusion rate of water molecules through the membrane, and hence an increased water recovery [17]. Similarly, increased feedwater temperature also results in a higher salt diffusion rate through the membrane and thus higher salt passage, and correspondingly lower salt rejection values.

5.3 RO Model Correlations & Validation

Having explained the various effects of operating parameters within a typical reverse osmosis system, simple attempts have been employed to correlate key operating parameters for the purpose of developing an effective multiple water quality parameter prediction capacity for membrane performance based on salt rejection characteristics within a membrane process. The approach involves exploiting numerical simulation data via specialized membrane design software, similar to the approach adopted by Alahmad [26]. ROSA Filmtech and IMSDesign were both utilized to extract useful membrane performance criteria so as to produce predictive relationships for all individual ions/components that could possibly be present within typically described standard seawater. Table 7 outlines feedwater qualities for the various standard seawater feed sources that have been considered [34, 35].

Table 7. Feedwater quality analysis for standard seawater feed sources

Feed Water Quality	**Typical Seawater**	**Eastern Mediterranean**	**Red Sea at Jeddah**	**Arabian Gulf at Kuwait**
Na	10556	11800	14255	15850
Mg	1262	1403	742	1765
Ca	400	423	225	500
K	380	463	210	460
Sr	13	-	-	-
Cl	18980	21200	22219	23000
HCO3	140	-	146	142
SO4	2649	2950	3078	3200
Br	65	155	72	80
BO3	26	72	-	-
F	1	-	-	-
SiO3	1	-	-	1.5
I	<1	2	-	-
Total Dissolved Solids (TDS)	34483	38600	41000	45000

Moreover, the feedwater temperature was varied from 20 – 40 ^{o}C, whilst operating under maximum feed pressure conditions and constant feedwater flowrate. Hence, in order to ensure maximized water recovery within the system, the maximum feed pressure value was always employed. Moreover, effective dosing of antiscalants was always assumed, in order to avoid potential scaling conditions. Effective antiscalant dosing requirements and concentrate salinity limits are outlined in Table 8, based on the estimations provided by Avista Advisor Chemical Calculations Software [36] for all 4 feedwaters investigated.

Table 8. Antiscalant dosing estimation based on system water recovery variation, according to standard seawater feed qualities

Feed water	Typical Seawater		Eastern Mediterranean		Arabian Gulf at Kuwait		Red Sea at Jeddah	
	Antiscalant Dose(ppm) & Salinity Limits (g/L)	Pump Rate (L/h)	Antiscalant Dose (ppm) & Salinity Limits (g/L)	Pump Rate (L/h)	Antiscalant Dose (ppm) & Salinity Limits (g/L)	Pump Rate (L/h)	Antiscalant Dose (ppm) & Salinity Limits (g/L)	Pump Rate (L/h)
0<Y<65	2.5 34.72< S<98.22	0.01	2.5 38.69< S<109.5	0.01	2.5 41.44< S<117.2	0.01	2.5 50.86< S<143.9	0.01
65<Y<76	-	-	-	-	3.0 117.2< S<170.9	0.012	-	-
65<Y<79	-	-	3.0 109.5< S<182.4	0.012	-	-	-	-
65<Y<81	3.0 98.22< S<180.9	0.012	-	-	-	-	-	-
65<Y<84	-	-	-	-	-	-	3.0 143.9< S<314.8	0.012
76<Y<77	-	-	-	-	3.44 170.9< S<178.4	0.014	-	-
77<Y<78	-	-	-	-	4.07 178.4< S<186.5	0.016	-	-
78<Y<79	-	-	-	-	4.95 186.5< S<195.4	0.02	-	-
79<Y<80	-	-	3.19 182.4< S<191.6	0.013	-	-	-	-
80<Y<81	-	-	3.91 191.6< S<201.6	0.016	-	-	-	-
81<Y<82	3.22 180.9< S<191.0	0.013	-	-	-	-	-	-
82<Y<83	4.10 191.0< S<202.2	0.017	-	-	-	-	-	-
83<Y<84	-	-	-	-	-	-	-	-
84<Y<85	-	-	-	-	-	-	3.14 314.8< S<335.7	0.013
>79	-	-	-	-	NE	NE	-	-
>81	-	-	NE	NE	-	-	-	-
>83	NE	NE	-	-	-	-	-	-
>86	-	-	-	-	-	-	NE	NE

It can be noted that higher water recoveries within the system are coupled with increased antiscalant dosing up to a certain limit in which further antiscalant addition is no longer effective (shown as NE conditions). Moreover, it is shown that scaling limits heavily depend on the compositions of hardness ions within the solution since feedwater qualities with respectively higher hardness concentrations yield lower salinity limit ranges for effective antiscalant conditions.

Therefore, the concentrate stream salinity values must always be monitored so as to make sure that operation is maintained within the recommended salinity limits for the respective water solutions, to ensure valid operating conditions whilst carrying out all numerical simulations.

Subsequently, linear regression was employed to model the relationship between salt rejections and temperature variations. Temperature of the system has not been optimized, but rather was used as a simple representative parameter indicating the degree of rejection associated with different ions. These correlative results were employed within the overall network optimization problem. The main motivation behind correlation extraction of individual correlations, which in turn relate membrane rejection performance criteria of various seawater constituents to the system operating conditions, was to keep the optimization problem user friendly by capturing a scale for workable parameters across a range of operating temperature conditions. Moreover, having correlations that relate temperature to membrane rejection performance for different seawater components can subsequently allow for the determination of optimal temperature operating conditions for certain scenarios that would desire the

determination of optimum workable conditions in terms of temperature by specifying it as one of the adjustable variables within the overall network optimization. This accordingly paves the way for other parameters to be introduced and optimized such as pH, which can be one of the favorable parameters to consider when considerations intended for certain boron removal requirements are needed for identifying optimal design configurations.

5.4 Model Correlations & Validation (ROSA)

As mentioned earlier, ROSA Filmtech and IMSDesign were both utilized to extract useful membrane performance criteria so as to produce meaningful predictive relationships for all chief individual seawater constitunets. ROSA data were modeled using linear functions, and unknown model parameters were estimated, the results are outlined in Tables 9 &10.

Table 9. Correlation coefficient values for common seawater ions based on ROSA simulation data

Ions	Typical Seawater	Eastern Mediterranean	Arabian Gulf at Kuwait	Red Sea at Jeddah
Na	y = -0.0597x + 100.63 R^2 = 0.985	y = -0.0608x + 100.63 R^2 = 0.9851	y = -0.0775x + 100.8 R^2 = 0.9846	y = -0.0633x +100.65 R^2 = 0.9849
Mg	y = -0.0138x + 100.15 R^2 = 0.9828	y = -0.0139x + 100.15 R^2 = 0.9841	y = -0.0187x + 100.2 R^2 = 0.9839	y = -0.0074x +100.08 R^2 = 0.9795
Ca	y = -0.0138x + 100.15 R^2 = 0.9828	y = -0.0139x + 100.15 R^2 = 0.9841	y = -0.0187x + 100.2 R^2 = 0.9839	y = -0.0074x +100.08 R^2 = 0.9795
K	y = -0.0678x + 100.71 R^2 = 0.9853	y = -0.0694x + 100.72 R^2 = 0.9852	y = -0.0891x + 100.92 R^2 = 0.9846	y = -0.0726x +100.74 R^2 = 0.9853
Sr	y = -0.0123x + 100.1 R^2 = 0.9361	-	-	-
Cl	y = -0.0548x + 100.57 R^2 = 0.985	y = -0.056x + 100.58 R^2 = 0.985	y = -0.0878x + 100.91 R^2 = 0.9846	y = -0.0632x +100.65 R^2 = 0.9849
HCO3	y = -0.0728x + 100.69 R^2 = 0.9817	-	y = -0.0955x + 100.95 R^2 = 0.9826	y = -0.0776x +100.74 R^2 = 0.9823
SO4	y = -0.0056x + 100.06 R^2 = 0.9844	y = -0.0056x + 100.06 R^2 = 0.9836	y = -0.0071x + 100.08 R^2 = 0.9831	y = -0.0058x +100.06 R^2 = 0.9838

Table 10. Correlation coefficient values for common seawater ions based on ROSA simulation data (multiple segments)

Ions	Typical Seawater	Eastern Mediterranean	Arabian Gulf at Kuwait	Red Sea at Jeddah
Na	$(20\text{-}30)^0$C y = -0.0471x + 100.31 R^2 = 0.9954 $(30\text{-}40)^0$C y = -0.0727x + 101.09 R^2 = 0.9966	$(20\text{-}30)^0$C y = -0.0479x + 100.31 R^2 = 0.9953 $(30\text{-}40)^0$C y = -0.0743x + 101.11 R^2 = 0.9963	$(20\text{-}30)^0$C y = -0.0606x + 100.39 R^2 = 0.9947 $(30\text{-}40)^0$C y = -0.0948x + 101.42 R^2 = 0.9955	$(20\text{-}30)^0$C y = -0.0498x + 100.32 R^2 = 0.9952 $(30\text{-}40)^0$C y = -0.0774x + 101.15 R^2 = 0.9963
Mg	y = -0.0138x + 100.15 R^2 = 0.9828	y = -0.0139x + 100.15 R^2 = 0.9841	y = -0.0187x + 100.2 R^2 = 0.9839	y = -0.0074x +100.08 R^2 = 0.9795
Ca	y = -0.0138x + 100.15 R^2 = 0.9828	y = -0.0139x + 100.15 R^2 = 0.9841	y = -0.0187x + 100.2 R^2 = 0.9839	y = -0.0074x +100.08 R^2 = 0.9795
K	$(20\text{-}30)^0$C y = -0.0537x + 100.36 R^2 = 0.9952 $(30\text{-}40)^0$C y = -0.0824x + 101.22 R^2 = 0.9967	$(20\text{-}30)^0$C y = -0.0548x + 100.35 R^2 = 0.9956 $(30\text{-}40)^0$C y = -0.0848x + 101.26 R^2 = 0.9963	$(20\text{-}30)^0$C y = -0.0697x + 100.44 R^2 = 0.9949 $(30\text{-}40)^0$C y = -0.109x + 101.63 R^2 = 0.9955	$(20\text{-}30)^0$C y = -0.0575x + 100.37 R^2 = 0.9955 $(30\text{-}40)^0$C y = -0.0886x + 101.31 R^2 = 0.996
Sr	y = -0.0123x + 100.1 R^2 = 0.9361	-	-	-
Cl	$(20\text{-}30)^0$C y = -0.0454x + 100.34 R^2 = 0.994 $(30\text{-}40)^0$C y = -0.0695x + 101.1 R^2 = 0.9975	$(20\text{-}30)^0$C y = -0.0441x + 100.29 R^2 = 0.9953 $(30\text{-}40)^0$C y = -0.0684x + 101.02 R^2 = 0.9963	$(20\text{-}30)^0$C y = -0.0687x + 100.44 R^2 = 0.9947 $(30\text{-}40)^0$C y = -0.1074x + 101.61 R^2 = 0.9955	$(20\text{-}30)^0$C y = -0.0498x + 100.32 R^2 = 0.9952 $(30\text{-}40)^0$C y = -0.0774x + 101.15 R^2 = 0.9963
HCO3	$(20\text{-}30)^0$C y = -0.0557x + 100.27 R^2 = 0.9946 $(30\text{-}40)^0$C y = -0.0905x + 101.32 R^2 = 0.9965	-	$(20\text{-}30)^0$C y = -0.0732x + 100.4 R^2 = 0.9939 $(30\text{-}40)^0$C y = -0.1183x + 101.76 R^2 = 0.9953	$(20\text{-}30)^0$C y = -0.0595x + 100.3 R^2 = 0.9945 $(30\text{-}40)^0$C y = -0.0964x + 101.41 R^2 = 0.9961
SO4	y = -0.0056x + 100.06 R^2 = 0.9844	y = -0.0056x + 100.06 R^2 = 0.9836	y = -0.0071x + 100.08 R^2 = 0.9831	y = -0.0058x +100.06 R^2 = 0.9838

Moreover, Figures 16-23 further illustrate that salt rejection indeed can be represented by linear models, according to ROSA predictions based on the specified system temperature variations, and favorable system operating conditions (both maximum recovery and minimum scaling as described earlier). Depending on the desired level of accuracy, some components can yield better correlations using multiple segments (shown in Figures 17, 19, 21 & 23 for all outlined feedwater qualities in Table 7.

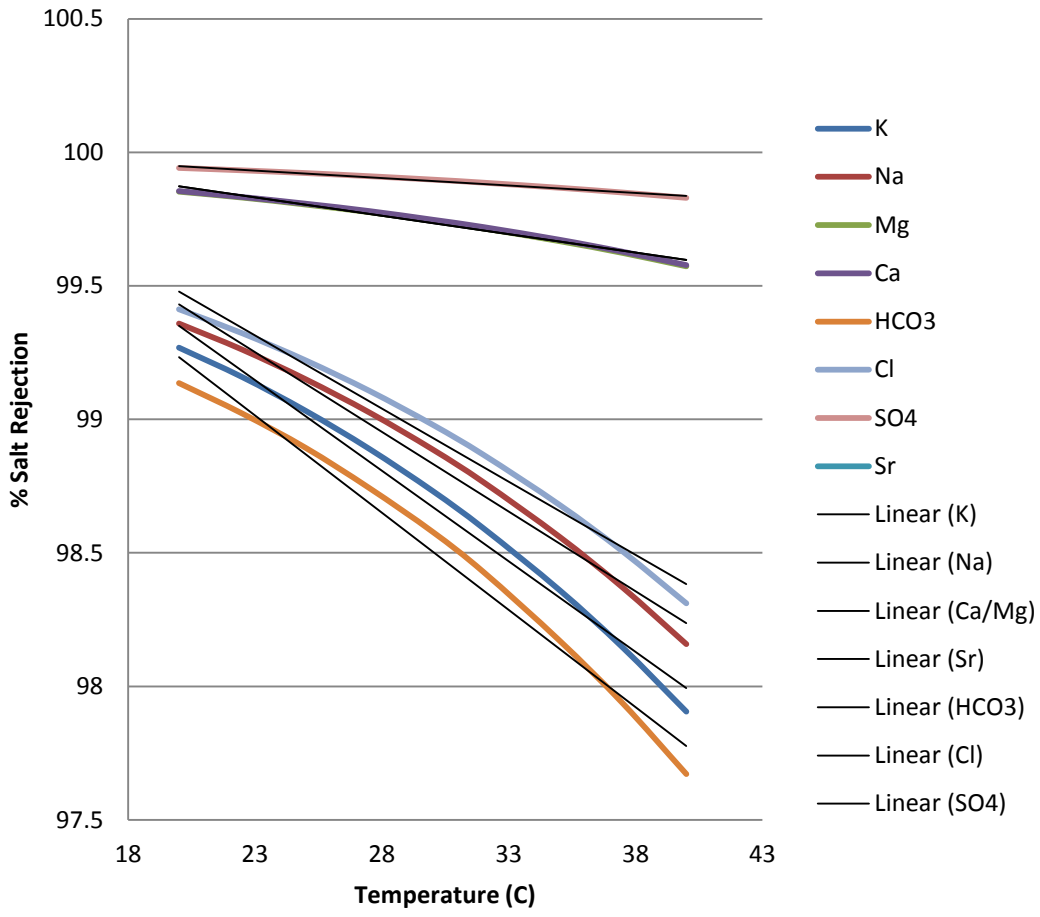

Figure 16. ROSA plots: rejection vs. temperature at maximum feed pressure conditions and constant feed flow for SW30HRLE – 440i elements, typical seawater feed results

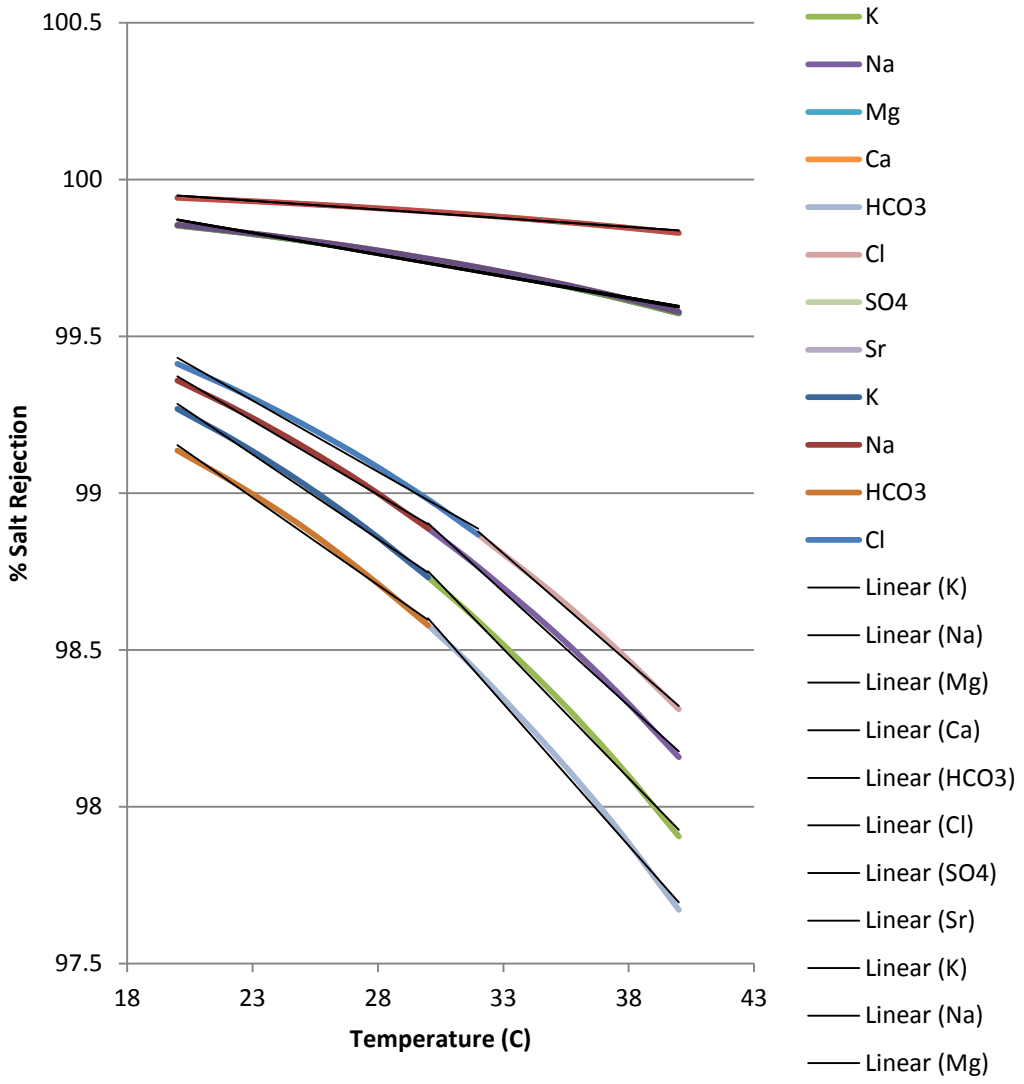

Figure 17. [Multiple segments] ROSA plots: rejection vs. temperature at maximum feed pressure conditions and constant feed flow for SW30HRLE – 440i elements, typical seawater feed results

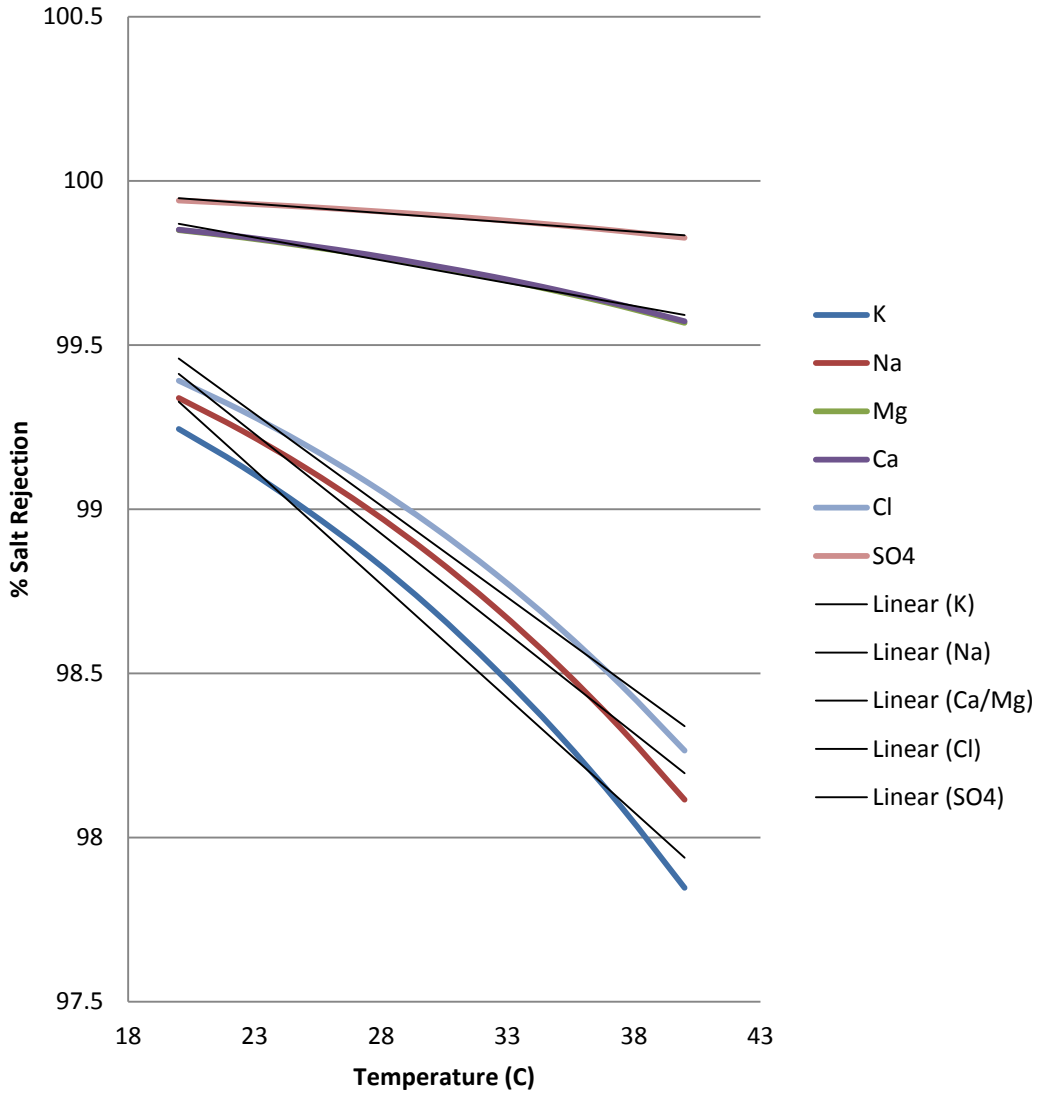

Figure 18. ROSA plots: rejection vs. temperature at maximum feed pressure conditions and constant feed flow for SW30HRLE – 440i elements, Eastern Mediterranean feed results

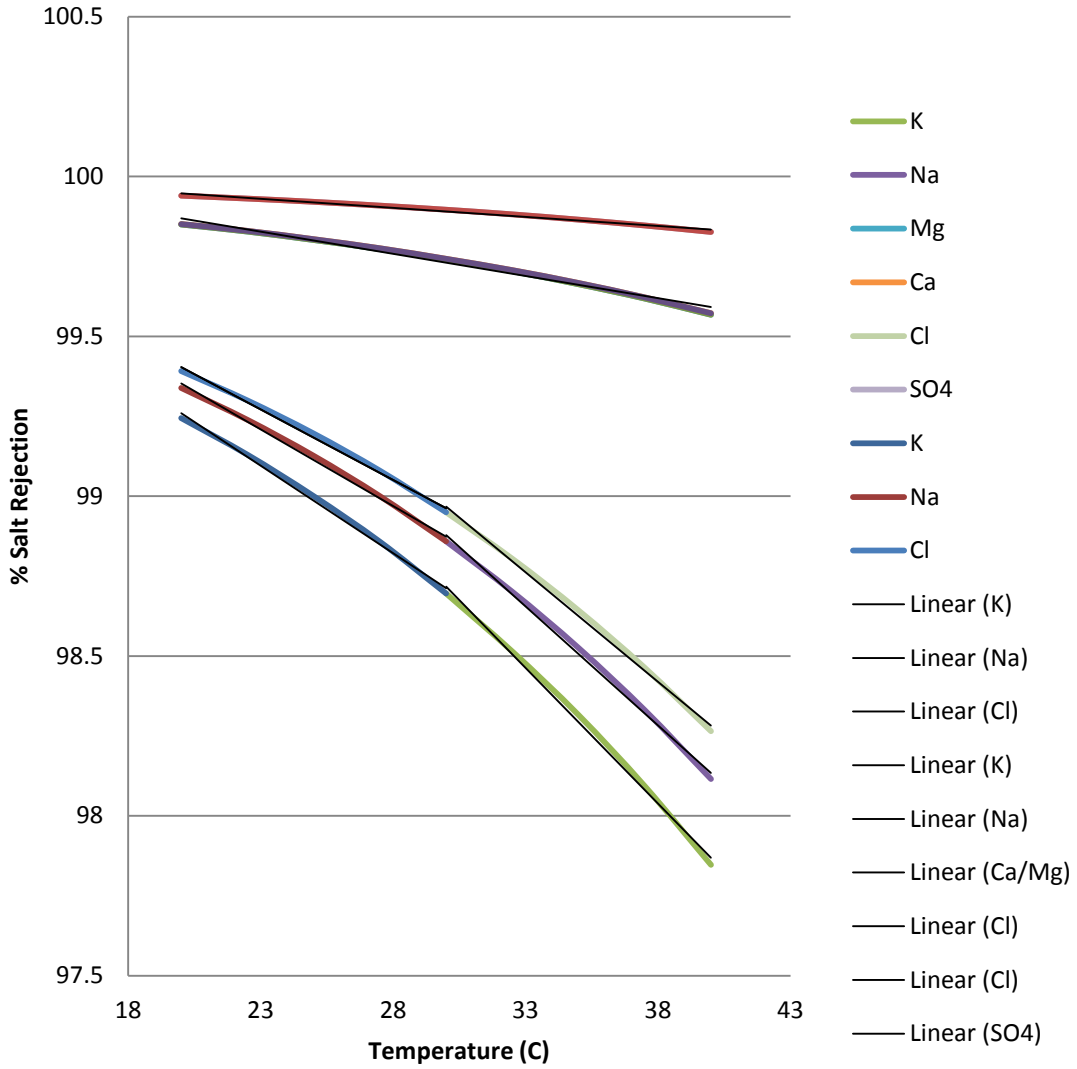

Figure 19. [Multiple segments] ROSA plots: rejection vs. temperature at maximum feed pressure conditions and constant feed flow for SW30HRLE – 440i elements, Eastern Mediterranean feed results

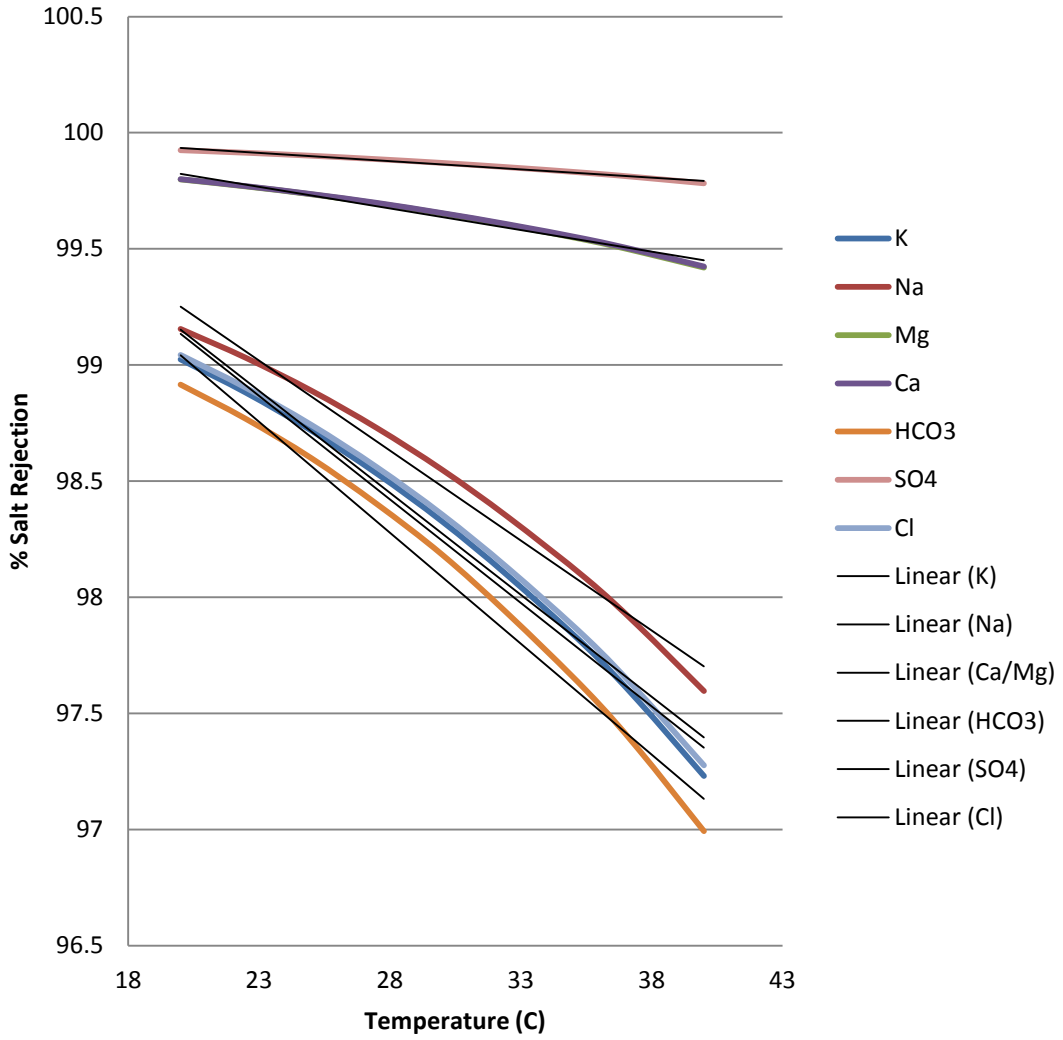

Figure 20. ROSA plots: rejection vs. temperature at maximum feed pressure conditions and constant feed flow for SW30HRLE – 440i elements, Arabian Gulf feed results

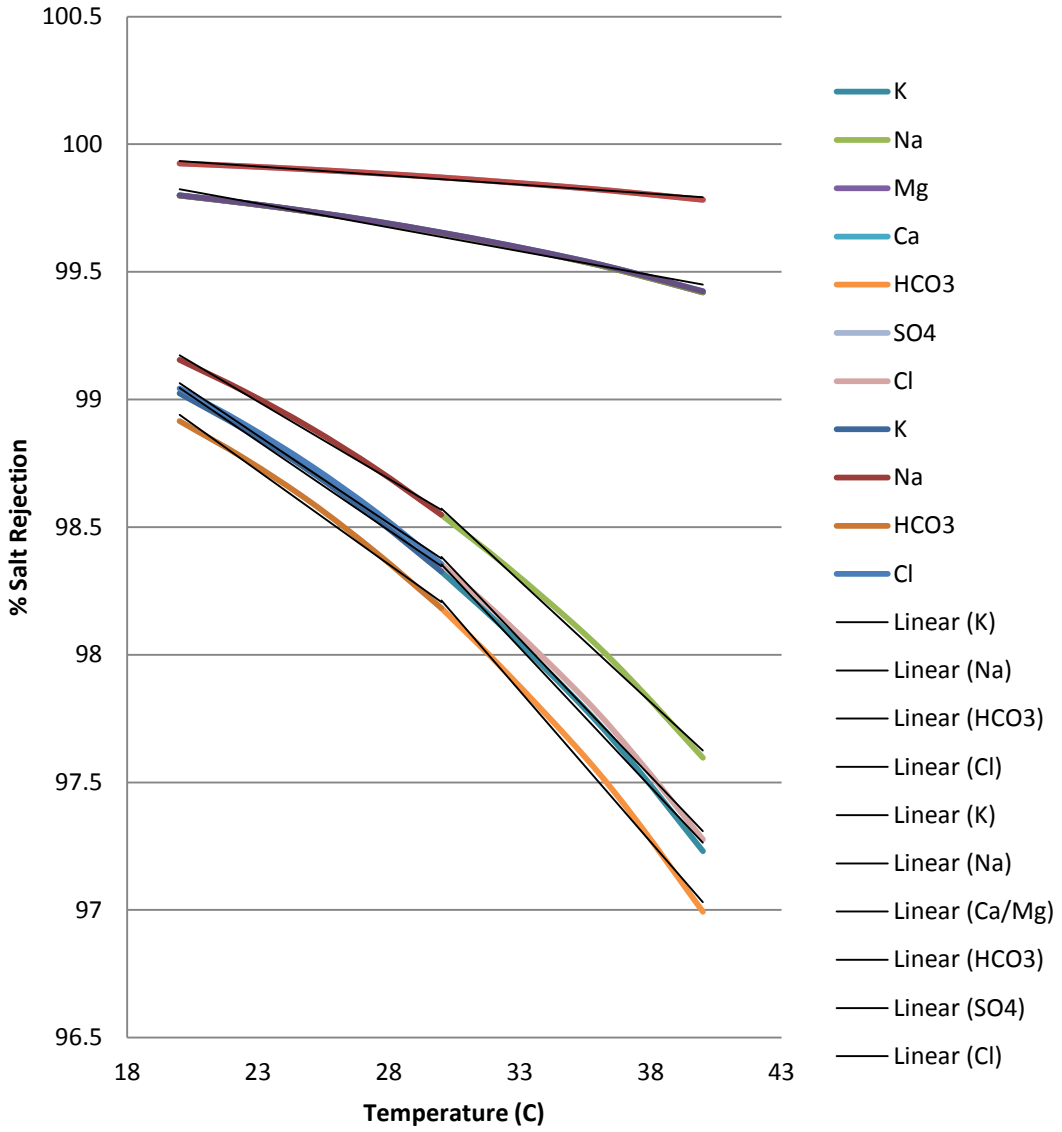

Figure 21. [Multiple segments] ROSA plots: rejection vs. temperature at maximum feed pressure conditions and constant feed flow for SW30HRLE – 440i elements, Arabian Gulf feed results

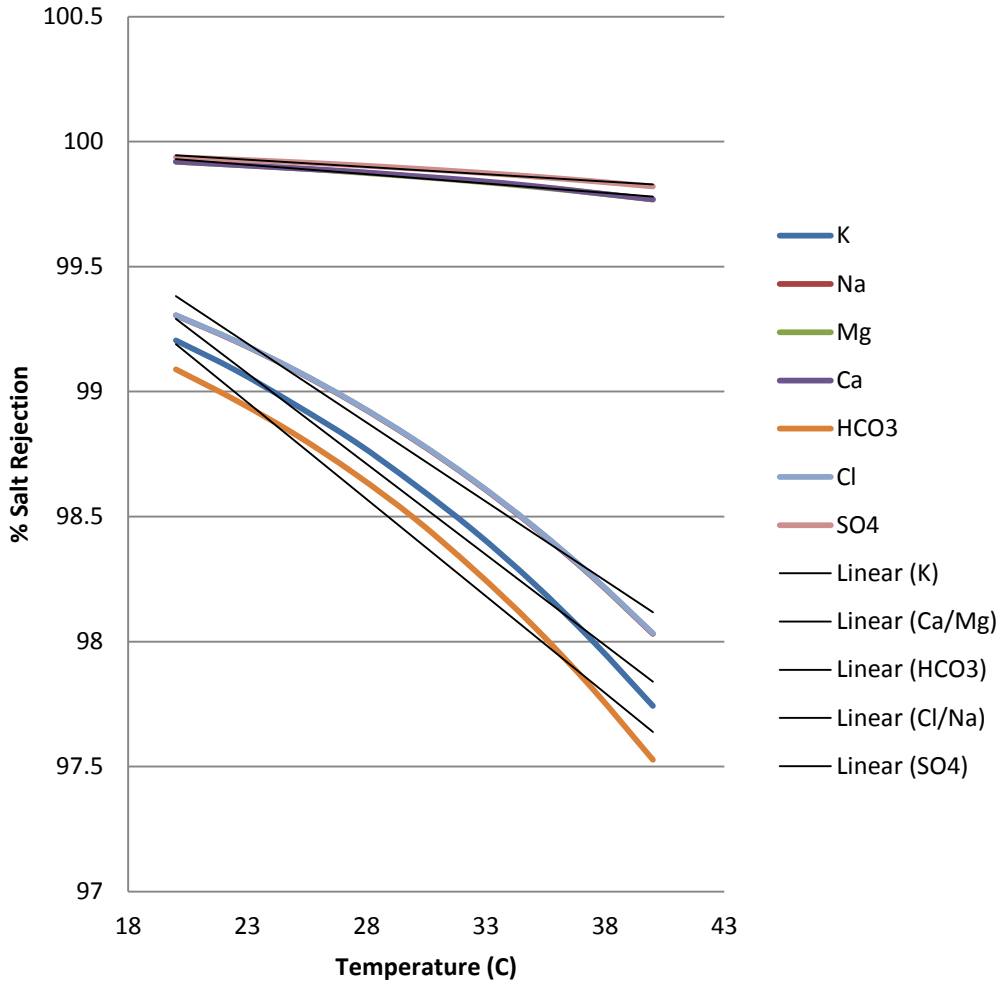

Figure 22. ROSA plots: rejection vs. temperature at maximum feed pressure conditions and constant feed flow for SW30HRLE – 440i elements, Red Sea feed results

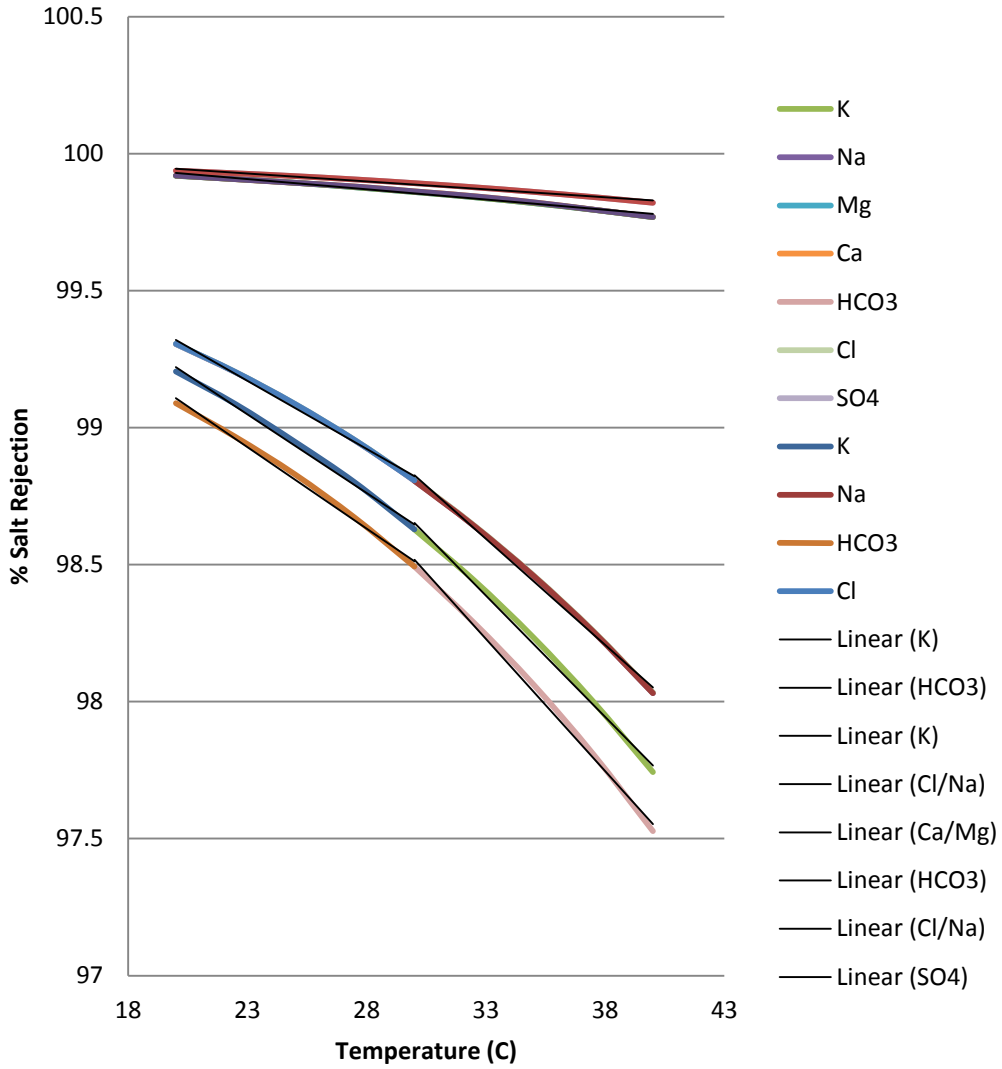

Figure 23. [Multiple segments] ROSA plots: rejection vs. temperature at maximum feed pressure conditions and constant feed flow for SW30HRLE – 440i elements, Red Sea feed results

All different water qualities exhibit a decrease of all ion salt rejection values, but the overall range remains within 97-99.9 %. This reflects an excellent ability of RO membranes to significantly reduce the amount of dissolved salts in the permeate stream. Both sulfate and bicarbonate ions exhibit the highest and lowest salt rejections respectively, regardless of feedwater quality changes. However, the rest of the ions lie

somewhere in between, with slight variations in the rejection rankings, depending on the feedwater quality specified.

5.5 Model Correlations & Validation (IMSDesign)

Figures 24-27 show salt rejection-temperature relations, according to IMSDesign software predictions also based on the specified system temperature variations, and favorable system operating conditions (both maximum recovery and minimum scaling as described earlier).

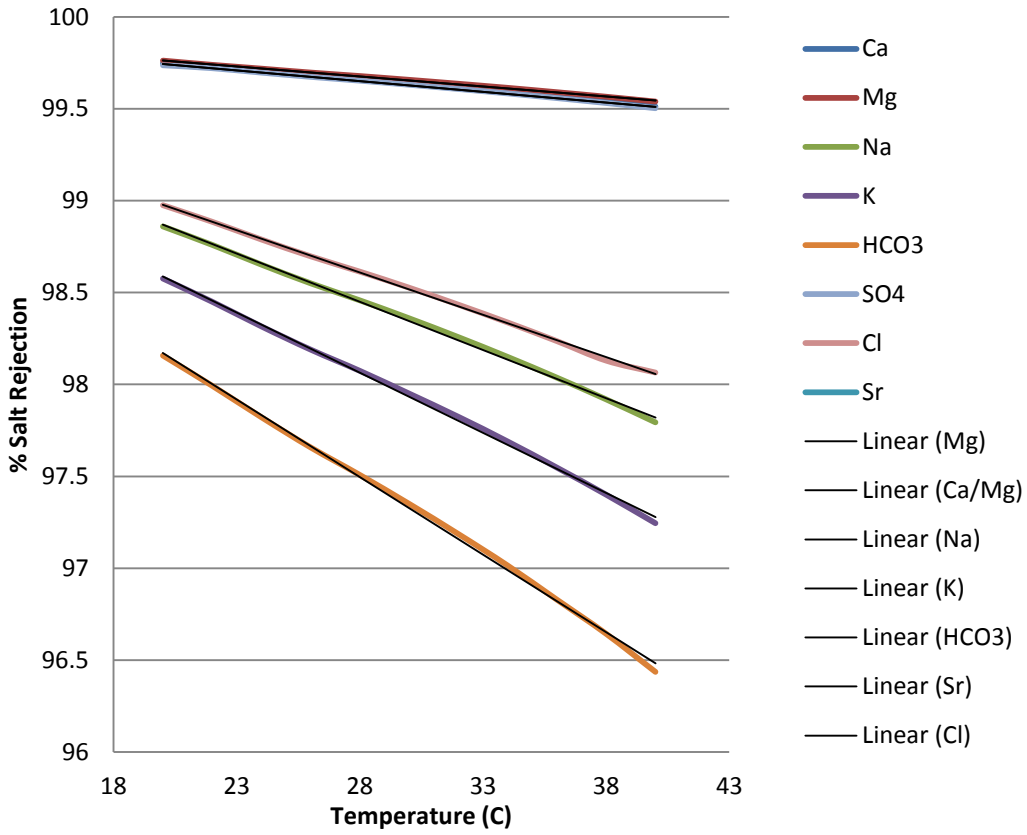

Figure 24. IMSDesign plots: rejection vs. temperature at maximum feed pressure conditions and constant feed flow for SWC5 – 4040 elements, typical seawater feed results

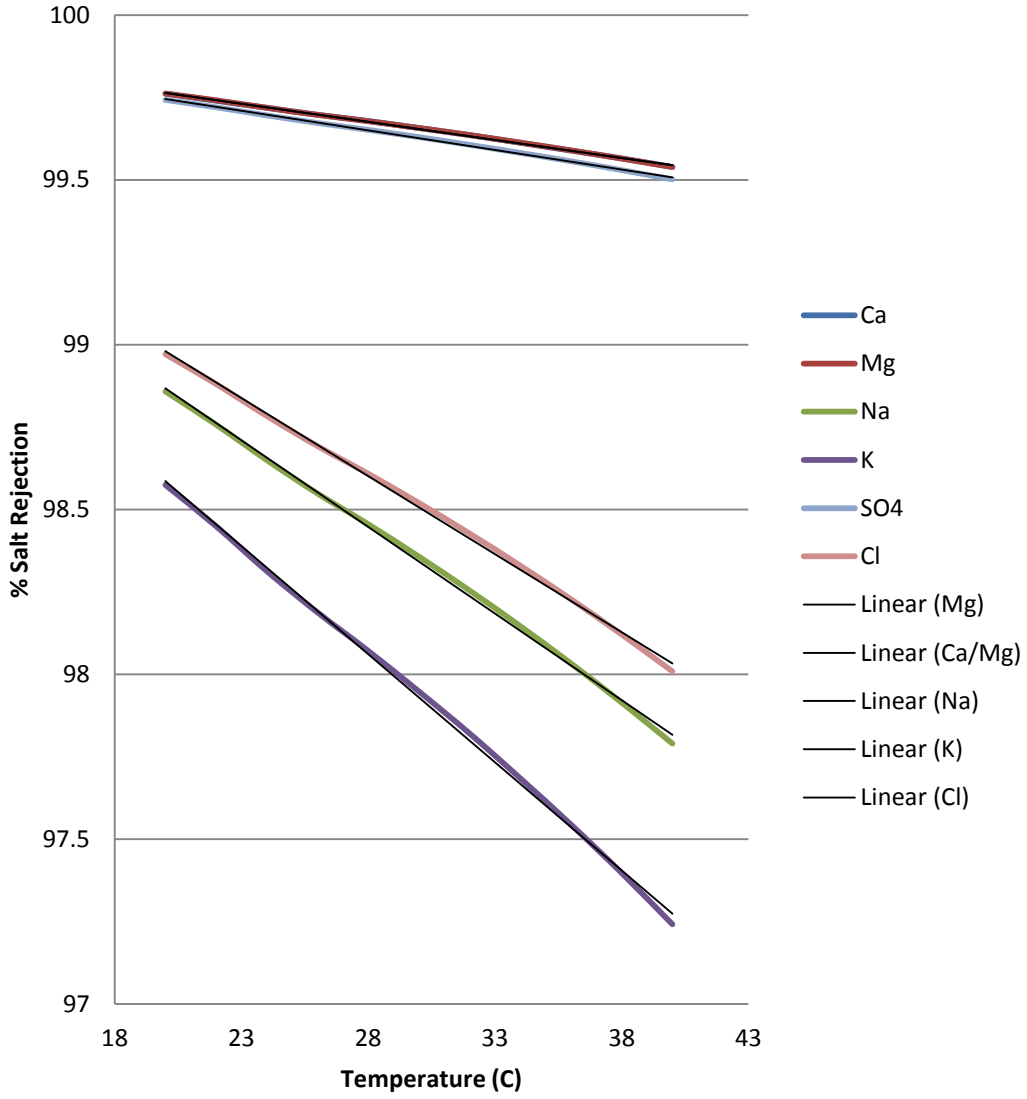

Figure 25. IMSDesign plots: rejection vs. temperature at maximum feed pressure conditions and constant feed flow for SWC5 – 4040 elements, Eastern Mediterranean feed results

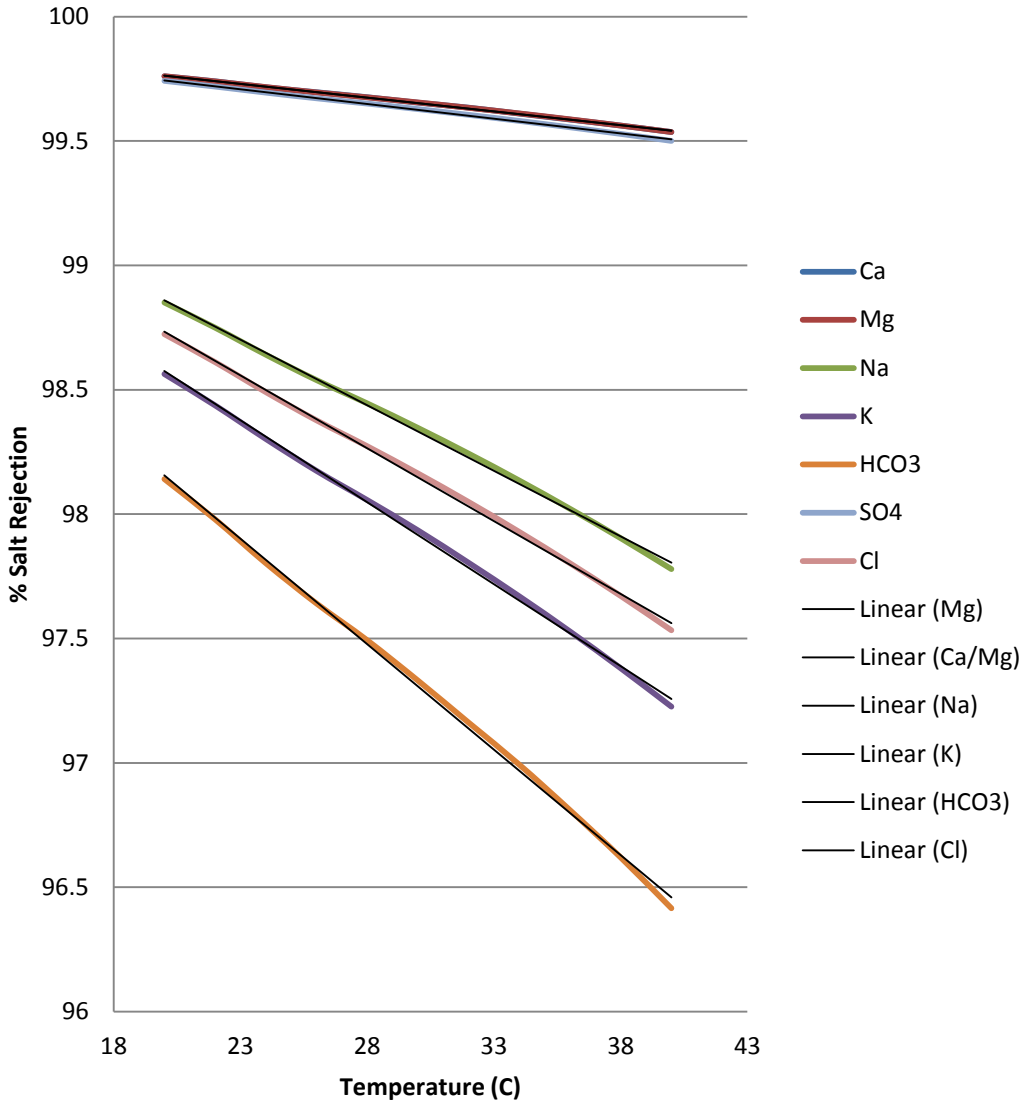

Figure 26. IMSDesign plots: rejection vs. temperature at maximum feed pressure conditions and constant feed flow for SWC5 – 4040 elements, Arabian Gulf feed results

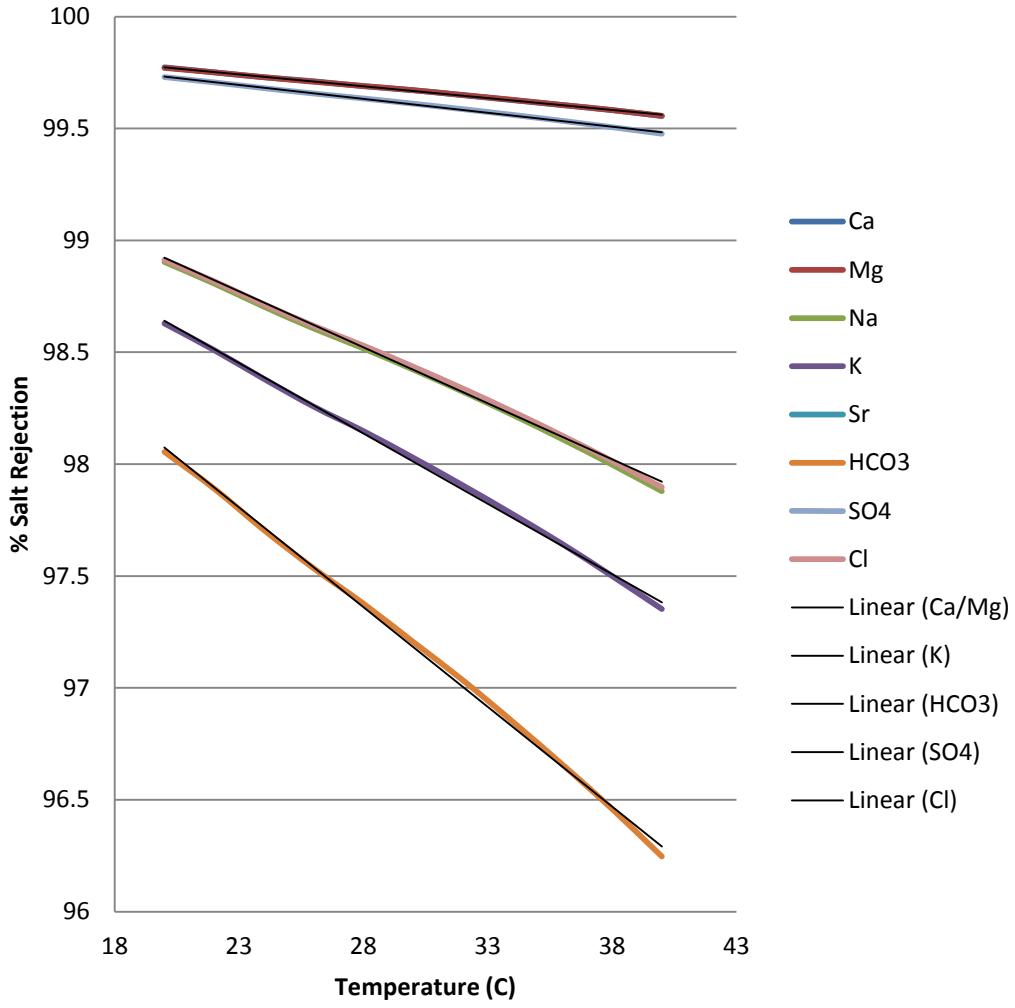

Figure 27. IMSDesign plots: rejection vs. temperature at maximum feed pressure conditions and constant feed flow for SWC5 – 4040 elements, Red Sea feed results

Moreover, all numerical data were modeled using linear functions, and unknown model parameters were estimated. The respective correlations are outlined in Table 11.

Table 11. Correlation coefficient values for common seawater ions based on IMSDesign simulation data

Ions	Typical Seawater	Eastern Mediterranean	Arabian Gulf at Kuwait	Red Sea at Jeddah
Na	y = -0.05x + 99.92 R^2 = 0.9985	y = -0.05x + 99.92 R^2 = 0.9985	y = -0.05x + 99.92 R^2 = 0.9987	y = -0.05x + 99.92 R^2 = 0.9986
Mg	y = -0.01x + 99.98 R^2 = 0.9984	y = -0.01x + 99.98 R^2 = 0.9986	y = -0.01x + 99.98 R^2 = 0.9986	y = -0.01x + 99.98 R^2 = 0.9985
Ca	y = -0.01x + 99.98 R^2 = 0.9982	y = -0.01x + 99.98 R^2 = 0.9985	y = -0.01x + 99.98 R^2 = 0.9986	y = -0.01x + 99.99 R^2 = 0.9987
K	y = -0.07x + 99.9 R^2 = 0.9985	y = -0.07x + 99.9 R^2 = 0.9986	y = -0.07x + 99.89 R^2 = 0.9987	y = -0.06x + 99.9 R^2 = 0.9987
Sr	y = -0.01x + 1 R^2 = 0.9229	-	-	-
Cl	y = -0.05x + 99.9 R^2 = 0.9992	y = -0.05x + 99.93 R^2 = 0.9985	y = -0.06x + 99.91 R^2 = 0.9987	y = -0.05x + 99.92 R^2 = 0.9986
HCO3	y = -0.08x + 99.86 R^2 = 0.9984	-	y = -0.08x + 99.85 R^2 = 0.9985	y = -0.09x + 99.86 R^2 = 0.9986
SO4	y = -0.01x + 99.98 R^2 = 0.9974	y = -2E-03x + 100 R^2 = 0.9986	y = -0.01x + 99.98 R^2 = 0.9986	y = -0.01x + 99.98 R^2 = 0.9986

IMSDesign data show very similar to trends ROSA software predictions, with all ion salt rejection values remaining within 96-99.7%. However, compared to ROSA predictions, data sets obtained via IMSDesign software represent better linear fits using single segments over the entire 20-40 ^{o}C temperature range. Moreover, salt rejection sensitivity caused by a slight change in feedwater quality characteristics can be ignored as the corresponding graphs and correlations exhibit minor differences. Nevertheless, any set of desired parameters, based on numerical software simulations can be used to manifest the multiple water quality aspect, within the overall network design problem, since it would simply correspond to a matter of updating the correlation parameters, depending on the desired level of accuracy.

5.6 Economic Assessment

Estimation of key economic parameters of a SWRO desalination plant involves the use of correlations that account for Capital Costs, as well as Operation and Maintenance Costs within the desalination system facilities. Capital costs are those costs associated with the implementation of a given desalination project from the early beginnings of its development and design, through construction, and commissioning until acceptance for normal operation [18]. Therefore, project construction expenditures constitute the largest entity of capital cost expenditures; due to their direct physical association with the construction of plant, these costs are often referred to as Direct Capital Costs [18]. Remaining Capital Costs, i.e. those costs involved with engineering, administrative and financing phases are indicated as Indirect Capital Costs [18]. Subsequently, estimating the total installation costs for the plant, and equipment associated within can be obtained by using an appropriate Lang factor. The capital cost for the construction of a SWRO desalination plant is then usually remunerated over a repayment term usually 5-30 years, referred to as the useful plant lifetime. Each amortized payment can be expressed as total capital expenditures throughout a one year period ($/yr) or as capital costs per m^3 of desalinated water produced.

Operating and Maintenance Costs, on the other hand, are those costs associated with plant operations, in the form of power requirements, chemical supplies, labor etc., together with maintenance of plant equipment, buildings and utilities. They are often expressed as a total entity of operational expenditures throughout a one year period ($/yr) or as costs per m^3 of desalinated water produced [18]. As in the case of Capital

Costs, Operational and Maintenance Costs (O&M) are classified into two different categories: *(1)* Fixed O&M costs, involving operational costs that are independent of the actual amount of fresh water produced, and *(2)* Variable O&M costs, those costs that are related to the amount of desalinated water produced by the desalination plant. Examples of Fixed O&M expenditures involve costs of equipment maintenance performance monitoring, and other administrative costs within the plant, whereas power costs, chemicals, replacement of consumables are all classified as Variable O&M expenditures.

Therefore, a more comprehensive economic objective function has been embedded into the optimization function, so as to capture the multiple entities of fixed and variable costs associated with a standard SWRO desalination plant. This has been implemented through the use of a more detailed cost breakdown assessment procedure, consisting of computations for the Total Annualized Cost (TAC), as function of an annualized form of Total Capital Investment (TCI) added to the Total Operating Cost (TOC) of the system. The Total Capital Investment (TCI) consists of Direct Capital Costs (DCC), Soft Costs (SC) as well as a Contingency Cost factor. Soft Costs (SC) account for costs of project engineering services, project development, and project financing and contingency is taken to be 5% of both Direct Capital Costs and Soft costs. The Total Operating & Maintenance Cost (TOC) consists of both Variable O&M Costs (VOC), and Fixed O&M Costs (FOC) [18, 37-40]. A Lang Factor (LF) and a Depreciation (D) value were assumed to be associated with the total capital investment term, over the useful plant lifetime (assumed to be 20 years) [18]. Table 12 summarizes all categories involved within the economical assessment.

Table 12. Summary of equations for economical assessment

Total Annual Cost (Objective Function)	$Min \quad TAC = TCI\frac{LF}{D} + TOC$	(45)
Total Capital Investment	$TCI = DCC + SC + CC_{contingency}$	(46)
Direct Capital Costs	$DCC = CC_{Site\ Preparation} + CC_{Intake} + CC_{Pretreatment} + CC_{RO\ System} + CC_{Post\ treatment} + CC_{Waste\ disposal/Cleaning} + CC_{Inst\ \&\ Control} + CC_{Buildings} + CC_{Electrical} + CC_{Startup}$	(47)
Site Preparation	$CC_{Site\ Preparation} = 864 \times F^{FEED}$	(48)
Intake	$CC_{Intake} = 4320 \times F^{FEED}$	(49)
Pretreatment	$CC_{Pretreatment} = 8640 \times F^{FEED}$	(50)
RO System	$CC_{RO\ System} = CC_{RO\ Skids} + CC_{Piping} + CC_{cartridge\ filters} + CC_{RO\ modules} + CC_{RO\ Pumps} + CC_{RO\ ERDs}$	(51)
RO Skids	$CC_{RO\ Skids} = \sum_{j=1}^{Nro} 5000 \times NM_j$	(52)
RO piping	$CC_{Piping} = 1369.61 \times \frac{F^{PROD}}{F^{PROD}/F^{FEED}}$	(53)
RO Cartridge Filters	$CC_{cartridge\ filters} = 112836 \times \left(\frac{F^{FEED} \times 86.4}{3600 \times 24/NS}\right)^{0.831} \times NS \times 1.2$	(54)
RO Modules	$CC_{RO\ modules} = \sum_{j=1}^{Nro} 4000 \times NM_j$	(55)
RO Pumps	$CC_{RO\ pumps} = 58000 \times (PW^{RO,Pumps} \times 0.0134)^{0.65}; if\ PW^{RO,Pumps} < 224\ kW,$ $C_{RO\ pumps} = 50000 + 234.5 \times PW^{RO,Pumps}; if\ PW^{RO,Pumps} > 224\ kW$	(56)
RO Energy Recovery Devices	$CC_{RO\ ERDs} = 85000 \times \left(PW^{RO,ERDs} \times \frac{1.34}{100}\right)^{0.65}; if\ PW^{RO,ERDs} < 373\ \mathrm{hp}$ $CC_{RO\ ERDs} = 0.378 \times (PW^{RO,ERDs} \times 1.34)^{0.81} \times 1000;\ if\ PW^{RO,ERDs} > 373\ \mathrm{hp},$	(57)

Table 12. Continued

Post Treatment	$CC_{Post\ treatment} = 1728 \times F^{FEED}$	(58)
Waste Disposal & Cleaning	$CC_{Waste\ disposal/Cleaning} = CC_{Membrane\ Cleaning} + CC_{Solids} + CC_{concentrate\ stream\ disposal}$	(59)
Membrane Cleaning Chemicals	$CC_{Membrane\ Cleaning} = 864 \times F^{FEED}$	(60)
Solids	$CC_{Solids} = 864 \times F^{FEED}$	(61)
Concentrate Stream Disposal	$CC_{concentrate\ stream\ disposal} = 432 \times F^{FEED}$	(62)
Instrumentation & Control	$CC_{Inst\ \&\ Control} = 300000 + 65000 \times NS$	(63)
Buildings	$CC_{Buildings} = (-10^{-6} \times (86.4 \times F^{PROD})^2 + 0.3668\text{^}(86.4 \times F^{PROD}) + 1887.9 \times 5 + 4320 \times F^{FEED}$	(64)
Electrical	$CC_{Electrical} = 614 \times (F^{PROD} \times 86.4)^{0.65}$	(65)
Auxiliary Service Equipment	$CC_{Aux\ Service\ Eqp} = 1728 \times F^{FEED}$	(66)
Startup, Commission & Acceptance	$CC_{Startup} = 2160 \times F^{FEED}$	(67)
Soft Costs	$SC = CC_{Project\ services} + CC_{Project\ development} + CC_{Project\ financing}$	(68)
	$CC_{Project\ services} = 8640 \times F^{FEED}$	(69)
Project Engineering Services	$CC_{Project\ development} = 7776 \times F^{FEED}$	(70)
Project Development	$CC_{Project\ financing} = 0.04\ DCC$	(71)
Project Financing	$CC_{contingency} = 0.05(DCC + SC)$	(72)
Total Operating Costs	$TOC = VOC + FOC$	(73)
Variable Operating & Maintenance (O&M) Costs	$VOC = OC_{Power} + OC_{chemicals} + OC_{Membrane\ replacement} + OC_{Filter\ replacement} + OC_{Waste\ stream\ disposal}$	(74)
Power Costs	$OC_{Power} = OC_{Intake} + OC_{Pretreatment} + OC_{RO} + OC_{Post\ treamtent} + OC_{Membrane\ cleaning} + OC_{Service\ facilities}$	(75)
Intake	$OC_{Intake} = \frac{0.191 \times (PW^{RO,Pumps} - PW^{RO,ERDs}) \times 24 \times PWC \times 365}{3.38}$	(76)
Pretreatment	$OC_{Pretreatment} = \frac{0.013 \times (PW^{RO,Pumps} - PW^{RO,ERDs}) \times 24 \times PWC \times 365}{3.38}$	(77)
Reverse Osmosis	$OC_{RO} = (PW^{RO,Pumps} - PW^{RO,ERDs}) \times PWC \times 365 \times 24$	(78)

Table 12. Continued

Post Treatment	$OC_{Post\ treamtent} = \frac{0.177\times(PW^{RO,Pumps}-PW^{RO,ERDs})\times 24\times PWC\times 365}{3.38}$	(79)
Membrane Cleaning	$OC_{Membrane\ cleaning} = \frac{0.027\times(PW^{RO,Pumps}-PW^{RO,ERDs})\times 24\times PWC\times 365}{3.38}$	(80)
Service Facilities	$OC_{Service\ facilities} = \frac{0.13\times(PW^{RO,Pumps}-PW^{RO,ERDs})\times 24\times PWC\times 365}{3.38}$	(81)
Chemicals	$OC_{Chemicals} = 473.04 \times F^{FEED}$	(82)
Membrane Replacement	$OC_{Membrane\ replacement} = \sum_{j=1}^{Nro} 613.5 \times NM_j$	(83)
Cartridge Filter Replacement	$OC_{Filter\ replacement} = 23.097 \times F^{FEED} \times NS \times 2.94$	(89)
Waste Stream Disposal	$OC_{Waste\ stream\ disposal} = 315.36 \times F^{FEED}$	(90)
Fixed Operating & Maintenance Costs	$FOC = OC_{Labor} + OC_{Manitenance} + OC_{Env.\ \&\ Monitoring} + OC_{Indirect\ O\&M}$	(91)
Labor	$OC_{Labor} = 473.04 \times F^{FEED}$	(92)
Maintenance	$OC_{Manitenance} = 788.4 \times F^{FEED}$	(93)
Environmental & Performance Monitoring	$OC_{Env.\ \&\ Monitoring} = 63.072 \times F^{FEED}$	(94)
Indirect O&M	$OC_{Indirect\ O\&M} = 946.08 \times F^{FEED}$	(95)
Power Requirements, Pumps	$PW^{RO,Pumps} = \left[\sum_{j=1}^{Nro} z_{j,j'}^{P} PW_{j,j'}^{P} + \sum_{j=1}^{Nro} z_j^{PP} PW_j^{PP} + \sum_{j'=1}^{Nro} z_{j'}^{FRO} PW_{j'}^{FRO}\right]$	(96)
Power Recovery, ERDs	$PW^{RO,ERDs} = 1.34 \times \left[\sum_{j=1}^{Nro} z_{j,j'}^{B} PW_{j,j'}^{B} + \sum_{j=1}^{Nro} z_j^{BB} PW_j^{BB}\right]$	(97)

5.7 Problem Statement & Implementation

Given a feedwater stream, described by a total mass flow rate F^{FEED} , an inlet pressure P^{FEED} , and a set of multiple feedwater components $i, i \in I$ with clearly defined compositions under specified feed temperature conditions, it is required to determine a corresponding cost effective membrane desalination network system according to viable membrane unit set-up options, using pre-specified cost function equations. The overall network considers known treating performances and interconnections that would satisfy minimum product water flow $F^{PROD,Min}$ of the permeate outlet stream, as well as the maximum concentration $X^{PROD,Max}$ of the outlet stream.

The mathematical representation of the problem involves a set of established system constraints involving total and component mass balance calculations around the inlet process splitter, outlet process mixers (both reject and permeate), mixers and splitters associated with individual membrane units in the system; The mathematical Formulation is outlined in Appendix A, and equations (103)-(116) & (130)-(145) were taken from section 4. Component mass balance calculations incorporate correlative predictions outlined in section 5.4 and 5.5, which provide a multiple water quality computational aspect based on reverse osmosis membrane performance. Additional RO membrane modeling equations adopted, for finding the number of modules required per stage, were according to the outlined models provided in the ROSA technical manual [17]. Table 13 summarizes the membrane correlations adopted.

Table 13. Summary of equations for RO membrane model

Total Number of Membrane Modules (per system Stage/Pass)	$NM_j = \frac{19000F_j^F}{3.28^2 SM_j \bar{A}(\bar{\pi})_j (TCF_j)(FF_j)\left(P_j^F - \frac{\Delta P_{fc,j}}{2} - P_j^P - \pi_j^F\left(\left(\frac{C_{fc}}{C_f}\right)_j \times exp^{(0.7\times R_j)} - (1-R_j)\right)\right)}$ j∈J	(98)
Membrane permeability as a function of average concentrate side osmotic pressure	$if\ \pi_j^F < 25, \quad \bar{A}(\bar{\pi})_j = 0.125$ $if\ 25 < \pi_j^F < 200, \quad \bar{A}(\bar{\pi})_j = 0.125 - 0.011\left(\frac{(\pi_j^F - 25)}{35}\right)$ j∈J $if\ \pi_j^F > 200, \quad \bar{A}(\bar{\pi})_j = 0.07 - 0.0001(\pi_j^F - 200)$ j∈J	(99)
Temperature correction factor	$if\ T \geq 25, \quad TCF_j = exp^{2460\times\left(\frac{1}{298} - \frac{1}{273+T}\right)}$ $if\ T \leq 25, \quad TCF_j = exp^{3020\times\left(\frac{1}{298} - \frac{1}{273+T}\right)}$	(100)
Average concentrate side system pressure drop	$\Delta P_{fc,j} = (6.8948 \times 10^{-2})(0.04)\left(13.2\frac{(F_j^F + F_j^B)}{2}\right)^2$ j∈J	(101)
Log mean concentrate-side to feed concentration ratio	$\left(\frac{C_{fc}}{C_f}\right)_j = \frac{-\ln(1-R_j)}{R_j}$ j∈J	(102)
Membrane feed stream osmotic pressure (Total & Component)	$\pi_{i,j}^F = (6.8948 \times 10^{-2})\frac{1.12(273+T)F_j^F X_{i,j}^F}{39102}$ i∈I and j∈J $\pi_j^F = \sum_{i=1}^{Nc}\pi_{i,j}^F$ j∈J	(103)

Moreover, an economic objective function that aims to minimize the Total Annualized Cost (TAC) has been employed, which in turn corresponds to minimizing the summation of an annualized form of Total Capital Investment (TCI) and the Total Operating Cost (TOC) of the system. A mathematical description of the objective function adopted has been discussed in Section 5.6.

The optimization problem constitutes a mixed integer nonlinear program (MINLP), in which the aim is to minimize the total cost described by Equations (45)-(97), subject to process equality constraints of Equations (103)-(129); (134)-(145) and inequality constraints of Equations (130)-(133); (146)-(155). The handling and manipulation of binary terms have been given described in Section 4.2-4.5.

In an effort to make the methodology easy to use, the superstructure optimization schemes have been implemented using Microsoft Excel 2010, on a desktop PC (Intel® Core ™ i7-2620M, 2.7 GHz, 8.00 GB RAM, 64-bit Operating System). The lean superstructure optimization problems are solved using the "*what'sBest 9.0"* LINDO Mixed-Integer Global Solver for Microsoft Excel [29].

5.8 Illustrative Example (Case Study 2)

This case study involves investigating optimum design configurations for 4 different feedwater qualities (Typical Seawater, Eastern Mediterranean, Arabian Gulf and Red Sea) outlined in Table 1. A partitioned search approach based on the principle of lean multiple superstructure design classes for determining an optimal design given certain membrane network performance criteria was applied in the following SWRO desalination case study example. Input data and parameters are summarized below in Table 14.

Table 14. Input data and parameters used for seawater desalination case study

Parameter/Variable	Value
F^{FEED} total inlet feedwater flowrate into the network (m^3/day)	40,000
P^{FEED} feedwater pressure into the network (bar)	1
P^{PROD} final permeate pressure (bar)	1
P^{BRINE} final reject pressure (bar)	1
$F^{PROD,MIN}$ minimum permeate flow required in the network (m^3/day)	12,000
$X^{PROD,MAX}$ maximum allowable concentration of dissolved solids in the permeate stream	0.0005
SM_j membrane Area per module in RO unit j (m^2)	245.4
ΔP_j pressure drop in RO unit j (bar)	1.3
$P_j^{F,MAX}$ maximum allowable feed pressure in RO unit j (bar)	70
ΔP^{SPEC} lower end allowable pressure difference that would allow the placement of ERDs (bar)	1
NMD_j^{MAX} maximum number of modules in one stage/pass	300
NMD_j^{MAX} maximum number of modules in one pass	300
NMD_j^{MIN} minimum number of modules in one stage	10
NMD_j^{MIN} minimum number of modules in one pass	4
T Temperature (^oC)	25
NS Number of Skids	1
LF Lang Factor	5
D Depreciation (yr)	20
PWC Power Cost ($/kWh)	0.05

Exploring distinct design class configurations up to a total of 3 membrane units were considered. Design Classes (1a, 2a, 2b, 3a, and 3d) were always found to be infeasible options based on the provided input data in Table 4, for all the different feedwater quality conditions investigated. Table 15 provides a summary of capital and

operating cost expenses of optimal solutions for all feasible design classes. Moreover, Table 15 shows that all solutions require less than one minute of CPU time for searching individual design classes and yielding an optimal solution when searching individual design classes, on a desktop PC (Intel Centrino) using the LINDO Mixed-Integer Global Solver for Microsoft Excel [29].

Table 15. Summary of capital, operating and total cost expenses & CPU computational timings for feasible design classes

Feedwater Quality	**Typical Seawater**	**Eastern Mediterranean**	**Red Sea**	**Arabian Gulf**
Class 1a	infeasible	infeasible	infeasible	infeasible
Class 2a	infeasible	infeasible	infeasible	infeasible
Class 2b	infeasible	infeasible	infeasible	infeasible
Class 3a	infeasible	infeasible	infeasible	infeasible
Class 3b	Capital ($/m3)	Capital ($/m3)	Capital ($/m3)	infeasible
	0.102	0.103	0.104	
	Operating ($/m3)	Operating ($/m3)	Operating ($/m3)	
	0.455	0.466	0.476	
	Total ($/m3)	Total ($/m3)	Total ($/m3)	
	0.557	0.569	0.580	
	CPU: 21s	CPU: 19s	CPU: 21s	
Class 3c	**Capital ($/m3)**	**Capital ($/m3)**	Capital ($/m3)	Capital ($/m3)
	0.102	**0.1029**	0.1046	0.107
	Operating ($/m3)	**Operating ($/m3)**	Operating ($/m3)	Operating ($/m3)
	0.452	**0.4629**	0.489	0.503
	Total ($/m3)	**Total ($/m3)**	Total ($/m3)	Total ($/m3)
	0.554	**0.5658**	0.594	0.611
	CPU: 42s	**CPU: 46s**	CPU: 32s	CPU: 39s
Class 3d	infeasible	infeasible	infeasible	infeasible
Class 3e	Capital ($/m3)	Capital ($/m3)	**Capital ($/m3)**	**Capital ($/m3)**
	0.102	0.103	**0.104**	**0.105**
	Operating ($/m3)	Operating ($/m3)	**Operating ($/m3)**	**Operating ($/m3)**
	0.455	0.467	**0.477**	**0.493**
	Total ($/m3)	Total ($/m3)	**Total ($/m3)**	**Total ($/m3)**
	0.558	0.5703	**0.581**	**0.598**
	CPU: 39s	CPU: 40s	**CPU: 40s**	**CPU: 37s**

Tables 16 and 17 summarize results highlighting water recoveries, number of modules required, concentrations of exit streams within the network, as well as optimized values of split fractions for optional connections within each design class category.

Table 16. Summary of stage/pass parameters and network exit concentrations for feasible design classes

Feedwater Quality	Typical Seawater Recovery #Modules Exit Concentrations		Eastern Mediterranean Recovery #Modules Exit Concentrations		Red Sea Recovery #Modules Exit Concentrations		Arabian Gulf Recovery #Modules Exit Concentrations	
Class 1a	infeasible		infeasible		infeasible		infeasible	
	-		-		-		-	
Class 2a	infeasible		infeasible		infeasible		infeasible	
	-		-		-		-	
Class 2b	infeasible		infeasible		infeasible		infeasible	
	-		-		-		-	
Class 3a	infeasible		infeasible		infeasible		infeasible	
	-		-		-		-	
Class 3b	Stage1: 30.23% Stage2: 29.18% Pass1: 98.83%	Stage1: 300 Stage2: 94 Pass1: 5	Stage1: 39.35% Stage2: 26.03% Pass1: 98.57%	Stage1: 109 Stage2: 300 Pass1: 17	Stage1: 31.09% Stage2: 22.51% Pass1: 98.57%	Stage1: 300 Stage2: 123 Pass1: 28	infeasible	
	Permeate TDS:0.4047 g/L Concentrate TDS:48.94 g/L		Permeate TDS: 0.4043 g/L Concentrate TDS: 54.57 g/L		Permeate TDS: 0.396 g/L Concentrate TDS: 58.45 g/L		-	
Class 3c	Stage1: 20.30% Pass1: 81.19% Stage2: 51.55%	Stage1: 264 Pass1: 6 Stage2: 135	Stage1: 26.76% Pass1: 99.17% Stage2: 40.38%	Stage1: 300 Pass1: 17 Stage2: 101	Stage1: 28.41% Pass1: 98.98% Stage2: 35.09%	Stage1: 300 Pass1: 28 Stage2: 104	Stage1: 28.56% Pass1: 98.23% Stage2: 34.54%	Stage1: 299 Pass1: 43 Stage2: 116
	Permeate TDS: 0.4047 g/L Concentrate TDS:48.94 g/L		Permeate TDS: 0.4043 g/L Concentrate TDS: 54.57 g/L		Permeate TDS: 0.3969 g/L Concentrate TDS: 58.45 g/L		Permeate TDS: 0.4032 g/L Concentrate TDS: 71.78 g/L	
Class 3d	infeasible		infeasible		infeasible		infeasible	
	-		-		-		-	
Class 3e	Stage1: 21.18% Stage2: 32.33% Pass1: 99.63%	Stage1: 106 Stage2: 300 Pass1: 10	Stage1: 44.59% Stage2: 23.92% Pass1: 98.71%	Stage1: 114 Stage2: 295 Pass1: 17	Stage1: 49.43% Stage2: 16.28% Pass1: 98.45%	Stage1: 170 Stage2: 246 Pass1: 28	Stage1: 40.71% Stage2: 13.25% Pass1: 98.09%	Stage1: 253 Stage2: 178 Pass1: 43
	Permeate TDS: 0.4044 g/L Concentrate TDS:48.94 g/L		Permeate TDS: 0.4043 g/L Concentrate TDS: 54.57 g/L		Permeate TDS: 0.3969 g/L Concentrate TDS: 58.45 g/L		Permeate TDS: 0.4032 g/L Concentrate TDS: 71.78 g/L	

Table 17. Summary of spilt fractions for respective optional streams within feasible design classes

FeedWater Quality	Typical Seawater	Eastern Mediterranean	Red Sea	Arabian Gulf
Class 1a	infeasible	infeasible	infeasible	infeasible
Class 2a	infeasible	infeasible	infeasible	infeasible
Class 2b	infeasible	infeasible	infeasible	infeasible
Class 3a	infeasible	infeasible	infeasible	infeasible
Class 3b	S1:0 S2:0.7313 S3:0.9427 S4:0.9 S5:0 S6:0	S1:0 S2:0.7296 S3:0.7792 S4:0.9 S5:0 S6:0	S1:0 S2:0.2517 S3:0 S4:0.9 S5:0 S6:0	infeasible
Class 3c	S1:0 S2:0.9 S3:0.3182 S4:0 S5:0 S6:0 S7:0.9	S1:0 S2:0.8011 S3:0.2401 S4:0 S5:0 S6:0 S7:0.9	S1:0 S2:0.6822 S3:0.2479 S4:0.00049 S5:0 S6:0 S7:0.8995	S1:0 S2:0.4796 S3:0.2697 S4:0 S5:0 S6:0.00026 S7:0.9
Class 3d	infeasible	infeasible	infeasible	infeasible
Class 3e	S1:0 S2:0.7271 S3:0.9 S4:0.0258 S5:0.9 S6:0 S7:0	S1:0 S2:0.7209 S3:0.7532 S4:0.0721 S5:0.9 S6:0 S7:0	S1:0 S2:0.5930 S3:0.6958 S4:0.1008 S5:0.9 S6:0 S7:0	S1:0 S2:0.3997 S3:0.7660 S4:0.9 S5:0.9 S6:0 S7:0

Figures 28-31 illustrate optimal design class solution examples for each water quality. It can be noted that both classes 3c (stage followed by pass design), and 3e (simultaneous stage& pass configuration) provide optimal design solutions for the feed waters.

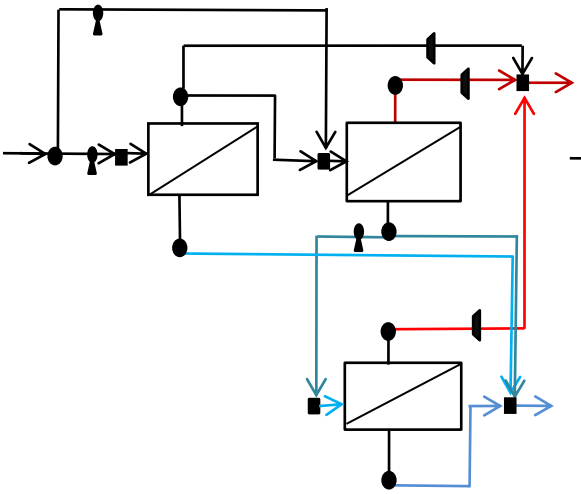

(a) Class 3b Optimal Configuration (CPU=21s)

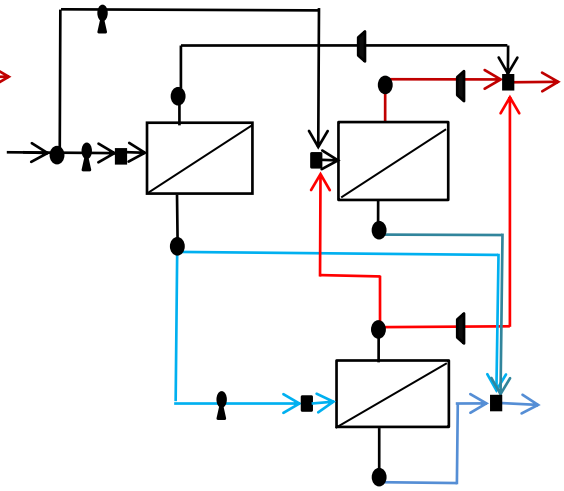

(b) Class 3c Optimal Configuration (CPU=42s)

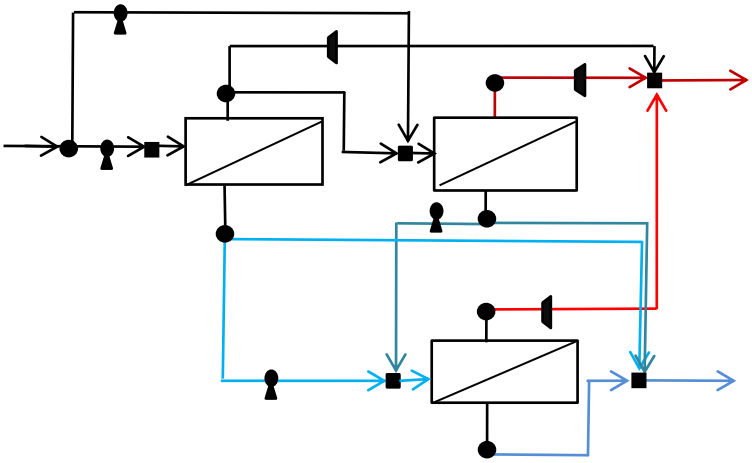

(c) Class 3e Optimal Configuration (CPU=39s)

Figure 28. Typical seawater feed, optimal solutions extracted

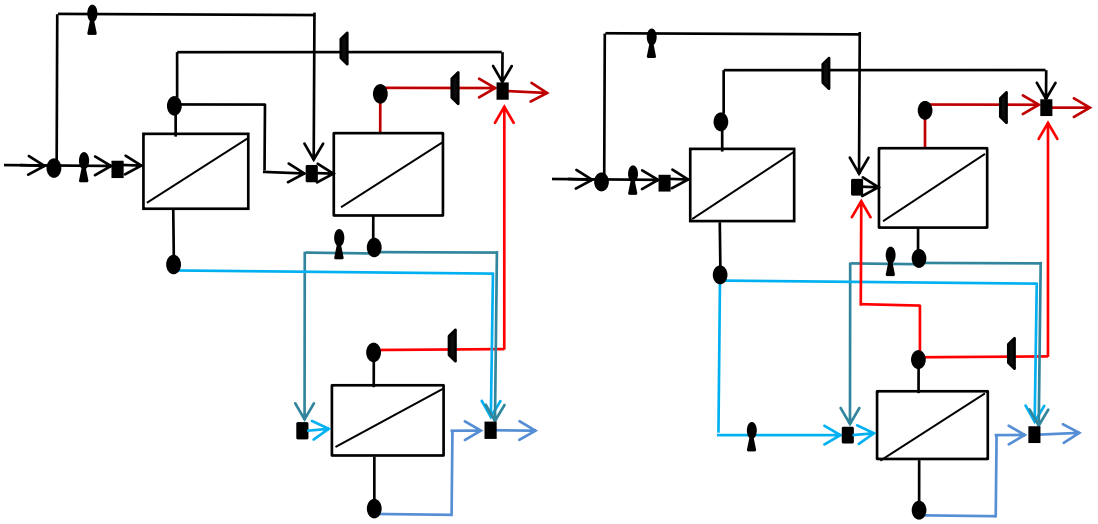

(a) Class 3b Optimal Configuration (CPU=19s)

(b) Class 3c Optimal Configuration (CPU=46s)

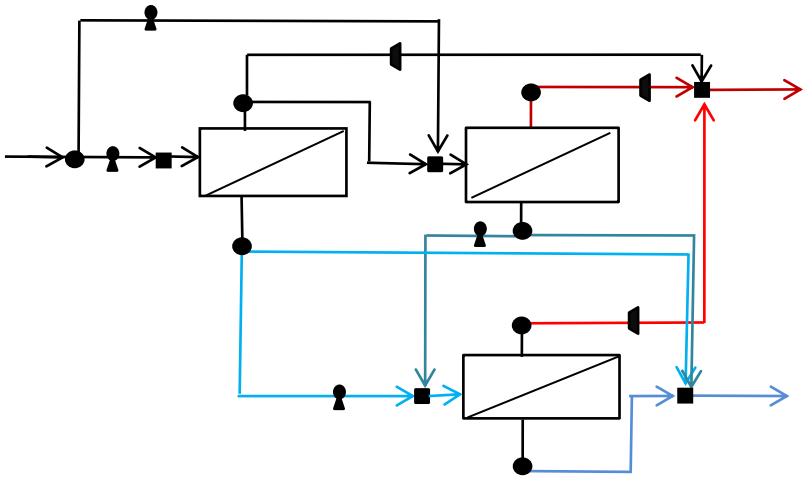

(c) Class 3e Optimal Configuration (CPU=40s)

Figure 29. Eastern Mediterranean feed, optimal solutions extracted

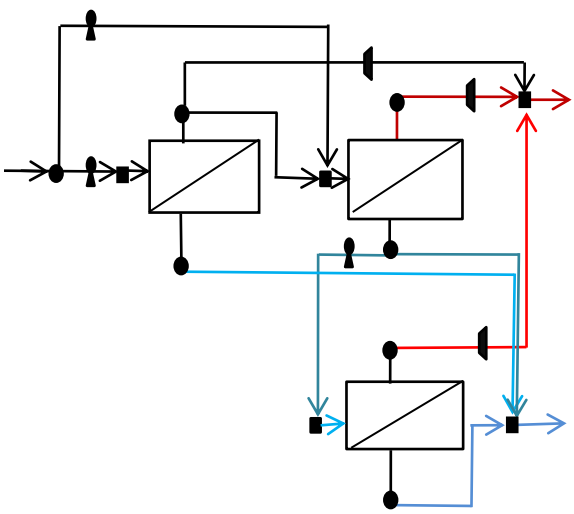

(a) Class 3b Optimal Configuration (CPU=21s)

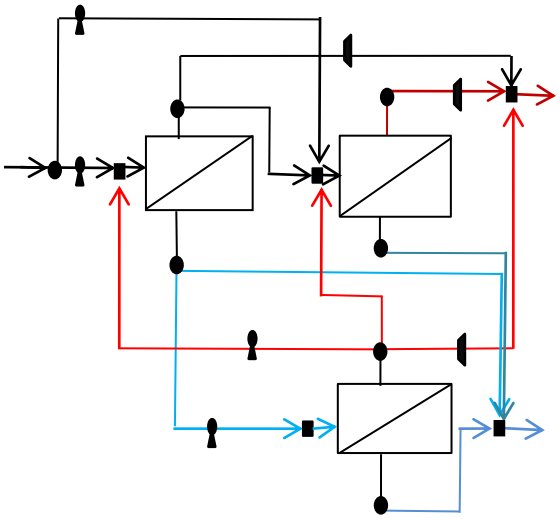

(b) Class 3c Optimal Configuration (CPU=32s)

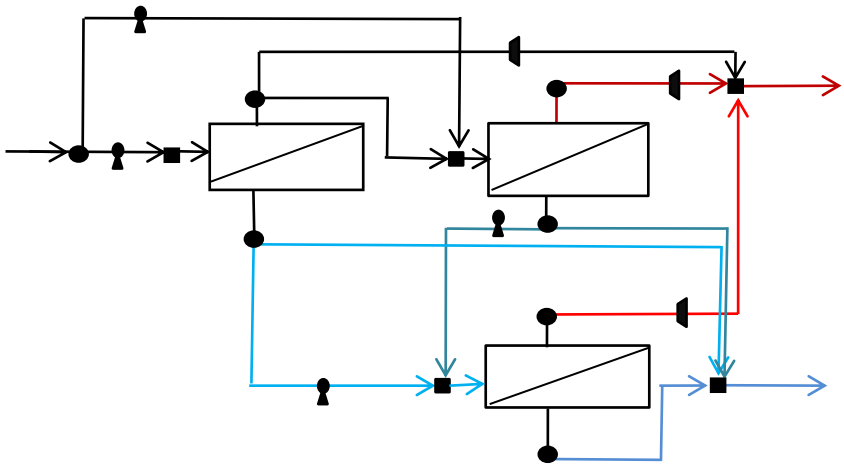

(c) Class 3e Optimal Configuration (CPU=40s)

Figure 30. Red Sea feed, optimal solutions extracted

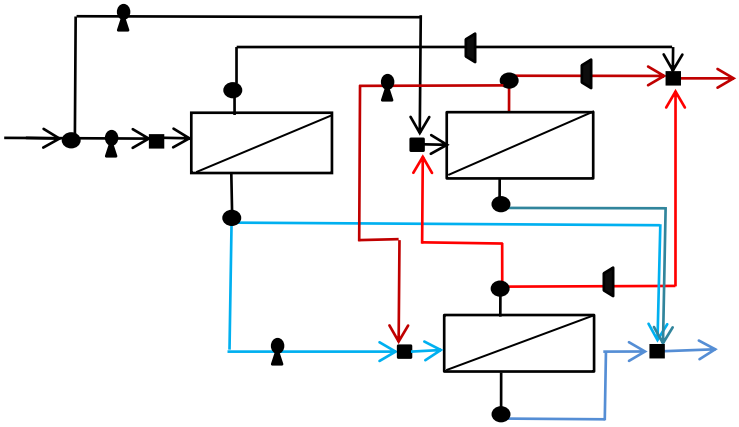

(a) Class 3c Optimal Configuration
(CPU=39s)

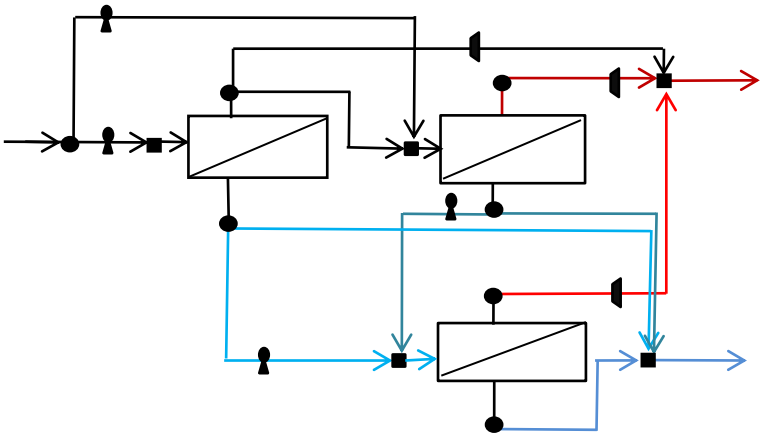

(b) Class 3e Optimal Configuration
(CPU=37s)

Figure 31. Arabian Gulf feed, optimal solutions extracted

Figures 32-35 below provide more detailed configuration solution examples for each feedwater quality that has been investigated. For instance, flowrates, power requirements, respective number of modules, total stream concentration are presented.

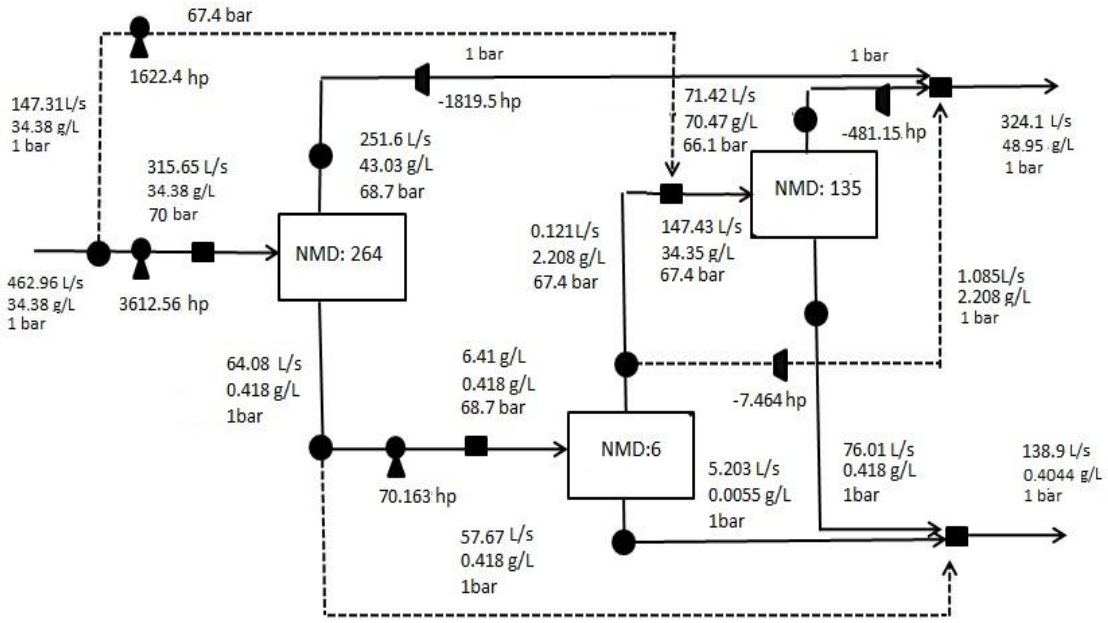

Figure 32. Typical seawater feed detailed solution example (class 3c)

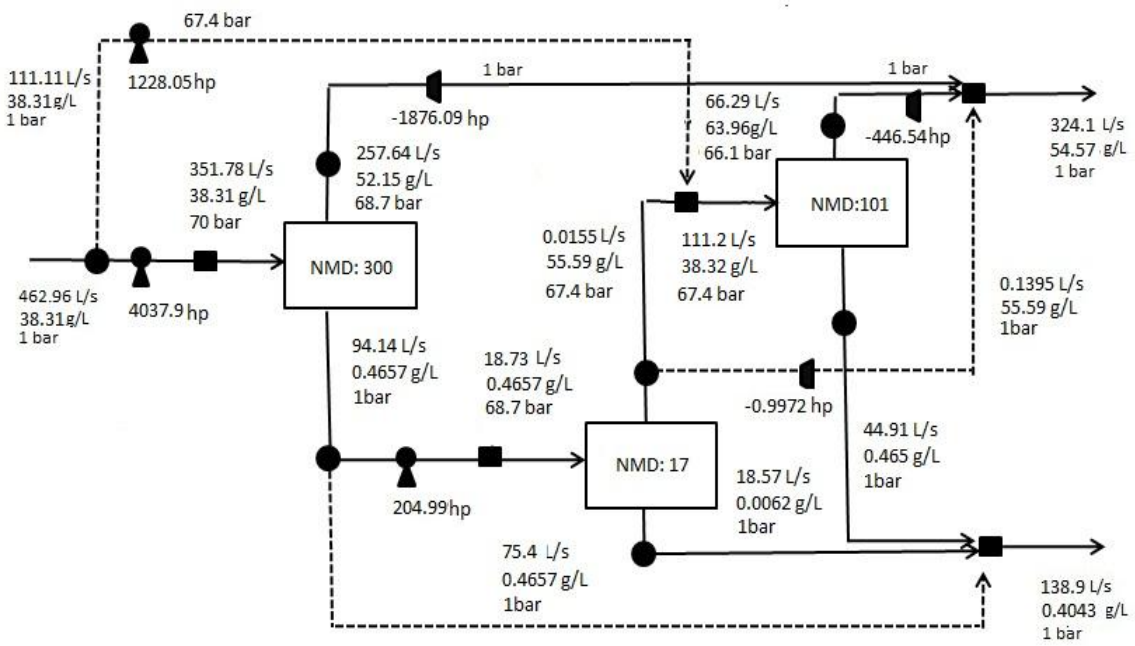

Figure 33. Eastern Mediterranean feed detailed solution example (class 3c)

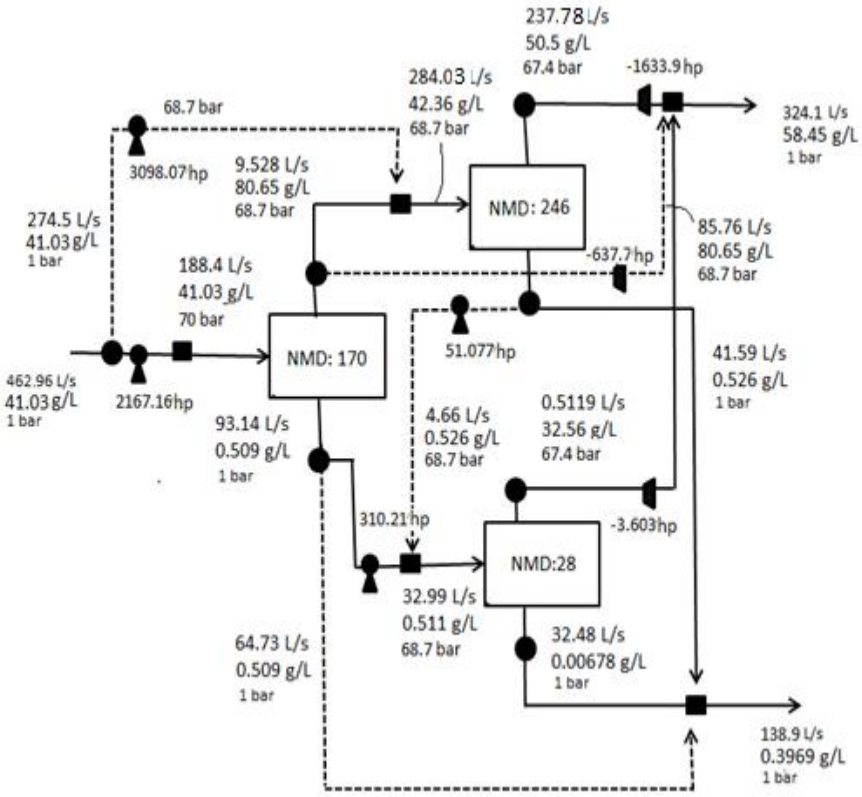

Figure 34. Red Sea feed detailed solution example (class 3e)

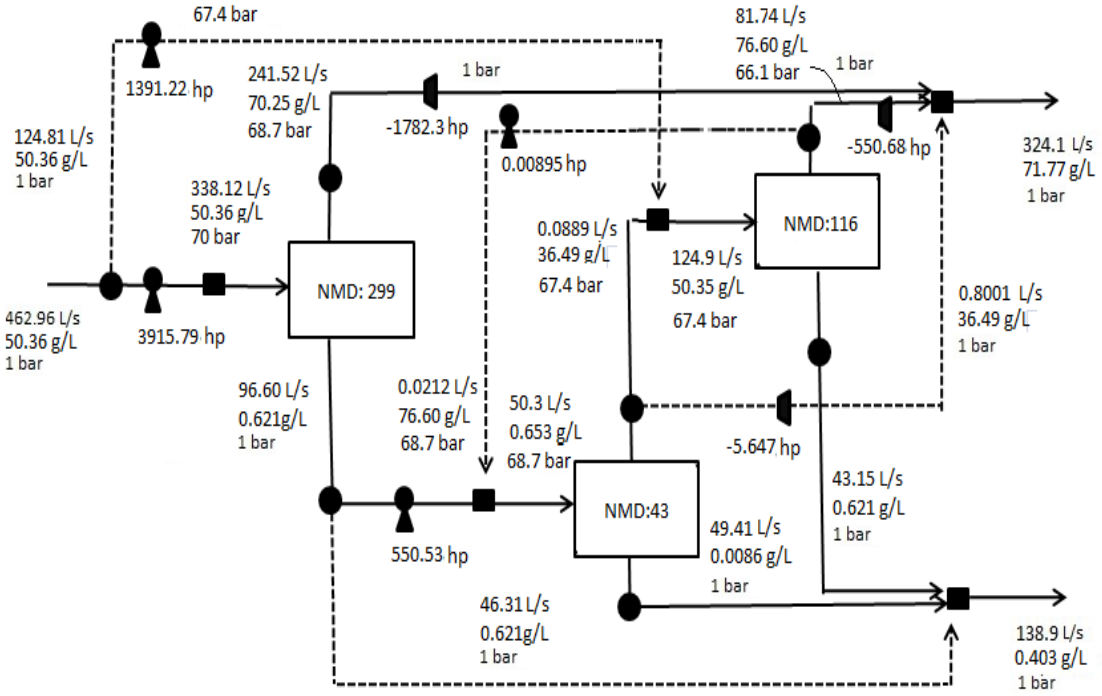

Figure 35. Arabian Gulf feed detailed solution example (class 3c)

Quoted capital cost values for SWRO plants are around US $0.1 to 0.2 per m^3. The average operating expenses are within a range of US $0.4-0.6 per m^3. These estimates includes the replacement of parts and membranes, chemicals for pretreatment of the intake water, plant cleaning and post-treatment of the product water, labour costs etc [37-40]. The optimal capital and operating costs for this case study were found to be between 0.102-0.107 $/ m^3 and 0.455-0.611 $/ m^3 respectively, based on a feedwater flowrate of 40,000 m^3/day into the SWRO desalination network and a 30% water recovery. It was observed that increased feedwater salinity conditions would eventually trigger higher capital and operating expenses. Figure 36 below illustrates the distribution of both capital and operating expenses of all optimal designs.

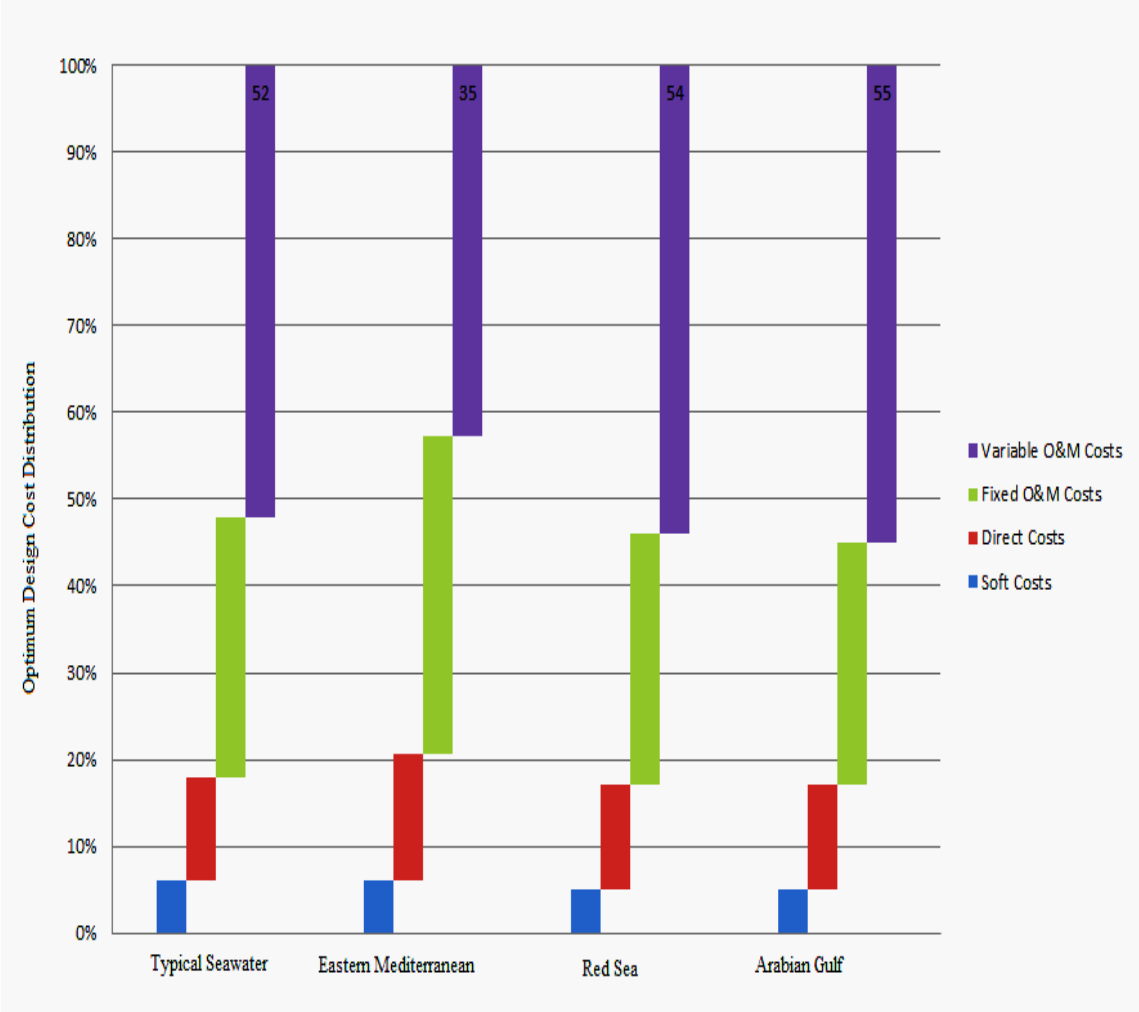

Figure 36. Cost distribution figures of capital and O&M costs for optimal design solutions

It can be noted that very minor differences in cost distributions exist, as a result of differences in inlet feedwater salinity conditions. For instance, Typical seawater (the lowest salinity feed case) results in a total of 18% capital expenses and a total of 82 % costs on O&M expenditures, with a Variable O&M (52%) constituting the highest

proportion of total expenditures. Relatively similar distributions were obtained for other seawater quality cases. The highest salinity case, Arabian Gulf seawater feed, yielded a total of 17% on capital expenditures and a total of 83 % of payments for O&M payments, with a slightly higher distribution for Variable O&M expenses (55%) compared to the typical feedwater case; this category still constitutes the highest proportion of total expenditures.

It was also observed that increased feedwater salinity conditions would eventually trigger higher capital and operating expenses. Tables 18 and 19 summarize both capital and maintenance cost breakdown for respective optimal designs. It has been observed that the Typical Seawater feed (lowest salinity case) requires a 0.1023 $/m^3 of annualized capital expenses as opposed to 0.1052 $/m^3 achieved for Arabian Gulf feed (highest salinity case). Moreover, a total of 0.4526 $/m^3 of annual operating expenses were reported for Typical Seawater feed, against 0.4934 $/m^3 for Arabian Gulf feed. In other words, both capital and operating expenses were found to increase as a result of an increase in the feedwater salinity into the network.

Table 18. Capital cost breakdown for respective optimal designs

Capital Cost Breakdown	Typical Seawater Optimum Design ($/m3/day)	Eastern Mediterranean Optimum Design ($/m3/day)	Red Sea Optimum Design ($/m3/day)	Arabian Gulf Optimum Design ($/m3/day)
Direct Capital (construction costs)				
Site Preparation	0.00147	0.00147	0.00147	0.00147
Intake	0.00735	0.00735	0.00735	0.00735
Pretreatment	0.0147	0.0147	0.0147	0.0147
RO system Equipment				
RO Skids	0.00744	0.00769	0.00816	0.00871
Piping	0.002338	0.002338	0.002338	0.002331
Cartridge Filters	0.000265	0.000265	0.000265	0.000268
RO modules	0.00595	0.00614	0.00652	0.00697
RO Pumps	0.00360	0.00370	0.00380	0.00396
RO ERDs	0.000735	0.000735	0.000735	0.000738
Total RO system Eq	0.02033	0.02086	0.02182	0.02298
Post treatment	0.00294	0.00294	0.00294	0.00294
Waste Disposal				
Membrane cleaning Chemicals	0.00147	0.00147	0.00147	0.00147
Solids	0.00147	0.00147	0.00147	0.00147
Concentrate stream Disposal (Co-location, desal+Power Plant Discharge)	0.00073	0.00073	0.00073	0.00073
Instrumentation and Control	0.00133	0.00133	0.00133	0.00134
Buildings	0.00738	0.00738	0.00738	0.00738
Electrical	0.00101	0.00101	0.00101	0.00101
Auxiliary and Service Equipment	0.00294	0.00294	0.00294	0.00294
Startup, Commissioning & Acceptance	0.00367	0.00367	0.00367	0.00367
Subtotal	0.06683	0.06738	0.06832	0.06948
Soft Costs				
Project Engineering Services	0.01323	0.01323	0.01323	0.01323
Project Development	0.01470	0.01470	0.01470	0.01470
Project Financing	0.00267	0.00269	0.00273	0.0027
Subtotal	0.03061	0.03063	0.03067	0.03072
Contingency	0.00486	0.00489	0.00495	0.00501
Total	0.10232	0.10291	0.10395	0.10521

Table 19. Operating and maintenance cost breakdown for respective optimal designs

Operating and Maintenance Cost Breakdown	Typical Seawater Optimum Design ($/m3)	Eastern Mediterranean Optimum Design ($/m3)	Red Sea Optimum Design ($/m3)	Arabian Gulf Optimum Design ($/m3)
Variable O&M				
Power				
Intake	0.0088	0.0093	0.0099	0.0105
Pretreatment	0.0006	0.0006	0.0007	0.0007
Reverse Osmosis	0.1566	0.1644	0.1751	0.1860
Product Water	0.0082	0.0086	0.0092	0.0097
Membrane Cleaning	0.0013	0.0013	0.0014	0.0015
Service Facilities	0.0060	0.0063	0.0067	0.0072
Total Power Cost	0.1815	0.1906	0.2029	0.2156
Chemicals	0.0350	0.0350	0.0350	0.0350
Membrane Replacement (replaced every 5 yrs)	0.0397	0.0410	0.0435	0.0465
Cartridge Filter Replacement	0.0050	0.0050	0.0050	0.0050
Waste stream Disposal	0.0233	0.0233	0.0233	0.0233
Subtotal	0.2846	0.2949	0.3098	0.3254
Fixed O&M				
Labor	0.0350	0.0350	0.0350	0.0350
Maintenance	0.0583	0.0583	0.0583	0.0583
Environmental & Performance Monitoring	0.0047	0.0047	0.0047	0.0047
Indirect O&M	0.0700	0.0700	0.0700	0.0700
Subtotal	0.1680	0.1680	0.1680	0.1680
Total O&M	0.4526	0.4629	0.4778	0.4934

Since computations involving the extraction of multiple water quality features have been implemented, Tables 20 and 21 provide exit permeate (network and post treatment) as well as concentrate stream compositions for all optimal design solutions.

Table 20. Summary of exit permeate & concentrate stream compositions for optimal design solutions of typical seawater and Eastern Mediterranean feed

	Typical Seawater			Eastern Mediterranean		
Ions	**Network Permeate g/L**	**Post Treatment Permeate g/L**	**Concentrate g/L**	**Network Permeate g/L**	**Post Treatment Permeate g/L**	**Concentrate g/L**
K	0.00679	0.00679	0.540	0.00744	0.00744	0.658
Na	0.13573	0.13573	15.022	0.13624	0.13624	16.799
Mg	0.00335	0.01000	1.801	0.00328	0.01000	2.003
Ca	0.00106	0.03000	0.571	0.00099	0.03000	0.604
Sr	0.00003	0.00003	0.019			
CO3		0.05974			0.06002	
HCO3	0.00289	0.00289	0.199			
SO4	0.00703	0.00703	3.781	0.00690	0.00690	4.211
Cl	0.24778	0.24778	27.016	0.24940	0.24940	30.292
TDS	0.40467	0.5	48.948	0.40426	0.5	54.567
Flow (L/s)	138.9	138.9	324.1	138.9	138.9	324.1

Table 21. Summary of exit permeate & concentrate stream compositions for optimal design solutions of Red Sea and Arabian Gulf feed

	Red Sea			Arabian Gulf		
Ions	**Network Permeate g/L**	**Post Treatment Permeate g/L**	**Concentrate g/L**	**Network Permeate g/L**	**Post Treatment Permeate g/L**	**Concentrate g/L**
K	0.00303	0.00303	0.299	0.00554	0.00554	0.655
Na	0.14768	0.14768	20.301	0.13685	0.13685	22.584
Mg	0.00156	0.01000	1.059	0.00308	0.01000	2.520
Ca	0.00047	0.03000	0.321	0.00087	0.03000	0.714
Sr						
CO3		0.06506			0.06071	
HCO3	0.00244	0.00244	0.208	0.00198	0.00198	0.202
SO4	0.00645	0.00645	4.394	0.00558	0.00558	4.569
Cl	0.23534	0.23534	31.869	0.24934	0.24934	40.532
TDS	0.39697	0.5	58.451	0.40324	0.5	71.776
Flow (L/s)	138.9	138.9	324.1	138.9	138.9	324.1

The multiple quality parameters embedded into the network optimization gives way for tracing down individual feedwater constituents within all feasible design configurations. In other words, the respective concentrations of all ions present in the feedwater can be subsequently determined, after passing through the membrane network and being separated to brine and permeate streams. This enables more relevant information to be extracted from the regarding scaling tendencies of sparingly soluble ions within the feed. Since all feedwaters contain relatively considerable amounts of hardness ions, the addition of precipitation inhibitors or antiscalants is important in all cases, in order to prevent potential scaling problems within the network. All concentrations were carefully monitored so as not to exceed the recommended concentration ranges that were provided in Table 8. This ensures that severely concentrated levels up to which the antiscalant becomes ineffective are prevented.

6. SUMMARY AND CONCLUSIONS

The developed systematic approach to optimal membrane network synthesis for seawater desalination consists of two steps. Step 1 targets the optimal performance of the systems whilst Step 2 yields optimal solutions structurally distinct design classes to guide the design decision maker. In each step compact superstructures are optimized. The proposed approach is observed to identify solutions significantly faster as compared to previously presented superstructure optimization approaches. Moreover, the results offer broader insights into the design problem by providing alternative solutions across the different possible design classes. In line with previous efforts, the superstructure models employed in this work simplify the design problem by considering only the two constituents water and total dissolved solids. In addition, the previously reported case study employed simplified process economics. Given the efficiency of the approach in handling the optimization problems, the consideration of more detailed design information, such as scaling and boron removal, were attempted.

The extension of the approach addresses detailed water quality issues by modeling multiple constituents and accounting for commercially available SWRO membrane units as well as incorporating more realistic economic assessment procedures as synthesis objectives. For the purpose of exploring additional multiple water quality computations within a SWRO network optimization problem, the developed representation was utilized, which involved a partitioned search space. The multicomponent nature of the feedwater stream has been embedded as an additional feature into the network optimization problem, and thus solutions extracted easily track

down the corresponding amounts of individual components constituting the feedwater stream within the network. The methodology has been illustrated using a case study involving four different feedwater qualities, having different corresponding compositions of various seawater components, and it has been demonstrated that the solutions are extracted within reasonable computational timings for feasible design classes.

Boron handling was not considered in this work, since specific treatment measures involving pH adjustment, as well as appropriate selection of membrane elements are necessary for boron-rich water. This issue however, will be one of the main subjects that future work will address later on. Further research efforts directed towards expanding additional aspects such as handling boron-rich waters would eventually call for the integration of a diverse mix of viable RO membrane treatment options within a single design rather than strictly relying on a single membrane type.

REFERENCES

[1] P. Linke, A.C. Kokossis. Advanced Process Design Technology for Pollution Prevention and Waste Treatment. Advances in Environmental Research 8(2) (2004) 229-245.

[2] C. Tsoka , W.R. Johns, P. Linke, and A. Kokossis. Towards Sustainability and Green Chemical Engineering: Tools and Technology Requirements. Green Chemistry 8 (2004) 401-406.

[3] R.V.S. Uppaluri, R. Smith, P. Linke, and A.C. Kokossis. On the Simultaneous Optimization of Pressure and Layout for Gas Permeation Membrane Systems. Journal of Membrane Science 280(1-2) (2006) 832-848.

[4] N. Voros, Z.B. Maroulis, D. Marinos-Kouris, Short-cut Structural Design of Reverse Osmosois Desalination Plants, Journal of Membrane Science 127 (1) (1997) 47-68.

[5] M. El-Halwagi, Synthesis of Reverse Osmosis Networks for Waste Reduction, AIChE Journal 38 (8) (1992) 1185-1198.

[6] F. Evangelista, A Short-cut Method for the Design of Reverse-Osmosis Desalination Plants, Ind. Eng. Chem. Process Des. 24 (1) (1985) 211.

[7] N. Voros, Z.B. Maroulis, D. Marinos-Kouris, Optimization of Reverse Osmosis Networks for Seawater Desalination, Computers Chem. Engng 20 (1) (1996) 345-350.

[8] F. Maskan, D.E. Wiley, P.M Johnston, Optimal design of Reverse Osmosis Module Networks, AIChE Journal 46 (5) (2000) 946-954.

[9] M. Zhu, M. El-Halwagi, M. Al-Ahmad, Optimal Design and Scheduling of Flexible Reverse Osmosis Networks, Journal of Membrane Science 129 (1) (1997) 161-174.

[10] Y. Lu, Y.D. Hua, X.L. Zhang, L.Y. Wu, Q.Z. Liu, Optimum Design of Reverse Osmosis System under Different Feed Concentration and Product Specification, Journal of Membrane Science 287 (1) (2007) 219–229.

[11] F. Vince, F. Marechal, E. Aoustin, P. Bréant, Multi-Objective Optimization of RO Desalination Plant, Desalination 222 (1) (2008) 96–118.

[12] M.G. Marcovecchio, P.A Aguirre, N.J. Scenna, Global Optimal Design of Reverse Osmosis Networks for Seawater Desalination: Modeling and Algorithm, Desalination 184 (1) (2005) 259–271.

[13] J. Marriott, E. Sorensen, The Optimal Design of Membrane Systems, Chemical Engineering Science 58 (1) (2003) 4991 – 5004.

[14] C. Guria, K. Prashant . S. Bhattachary, S. K. Gupta. Multi-objective Optimization of Reverse Osmosis Desalination Units using Different Adaptations of the Non-dominated Sorting Genetic Algorithm (NSGA), Computers and Chemical Engineering 29 (2005) 1977–1995.

[15] Y. Saif, A. Elkamel, M. Pritzker, Global Optimization of Reverse Osmosis Network for Wastewater Treatment and Minimization, Ind. Eng. Chem. Res. 47 (1) (2008) 3060-3070.

[16] Y. Saif, A. Elkamel, M. Pritzker, Optimal Design of Reverse Osmosis Networks for Wastewater Treatment, Chemical Engineering and Processing 47 (2008) 2163–2174.

[17] Dow Water & Process Solutions, Midland MI, USA, FILMTEC Reverse Osmosis Membranes: Technical Manual Form No. 609-00071-1009.

[18] M. Wilf, The Guidebook to Membrane Desalination Technology: Reverse Osmosis, Nanofiltrartion and Hybrid Systems: Process Design, Application and Economics.Balban Desalination Publications, L'Aquila, Italy 2007

[19] H. Ohya, S. Sourirajan, Some General Equations for Reverse Osmosis Process Design, AIChE Journal 15 (6) (1969) 829-36.

[20] M.L. Costa, and J.M. Dickson, Modelling of Modules and Systems in Reverse Osmosis. Part I: Theoretical System Design Model Development, Desalination, 80 (1) (1991) 251-274.

[21] M. Sekino, Precise Analytical Model of Hollow Fiber Reverse Osmosis Modules, Journal of Membrane Science 85 (1) (1993) 241-252.

[22] V.S. Polyakov, S.V. Polyakov, On the calculation of Reverse Osmosis Plants with Spiral-Wound Membrane Elements, Desalination 104 (1) (1996) 215-226.

[23] M. Bastaki, A. Abbas, Predicting the performance of RO membranes, Desalination 132 (1) (2000) 181-187.

[24] S. Kim, M.V. Hoek, Modeling Concentration Polarization in Reverse Osmosis Processes, Desalination 186 (1) (2005) 111–128.

[25] V.K. Gupta, S.T. Hwang, W.B. Krantz, A.R. Greenberg, Characterization of Nanofiltration and Reverse Osmosis Membrane Performance for Aqueous Salt Solutions using Irreversible Thermodynamics, Desalination 208 (1) (2007) 1–18.

[26] M. Alahmad, Prediction of Performance of Sea Water Reverse Osmosis Units, Desalination 261 (1) (2010) 131–137.

[27] A. M. Ghobeity, Optimal Time Dependent Operation of Seawater Reverse Osmosis, Desalination 263 (1) (2010) 76-88.

[28] D.M. Rodriguez, P. Linke, D. Linke, M.Z. Stijepovic, (2010). Optimal Conceptual Design of Processes with Heterogeneous Catalytic Reactors. Chemical Engineering Journal 163(3), 438-449.

[29] Lindo Systems, What'sBest! 9.0 - Excel Add-In for Linear, Nonlinear, and Integer Modeling and Optimization, http://www.lindo.com/index.php?option=com_content&view=article&id=3&Itemid=11 O.

[30] A. K. Kedem, Thermodynamic Analysis of the Permeability of Biological Membranes to Non-electrolytes, Biochimica et Biophysica Acta. 27 (1) (1958) 229-246.

[31] K.S, Speigler, O. Kedem, Thermodynamics of Hyperfiltration (Reverse Osmosis): Criteria for Efficient Membranes Desalination. 1(4) (1966) 311-326.

[32] Dow Water & Process Solutions, Reverse Osmosis Systems Analysis ROSA 7.0.1, System design software using DOW FILMTEC™ elements, http://www.dowwaterandprocess.com/support_training/design_tools/rosa.htm

[33] Nitto Denko Hydranautics, Integrated Membrane Solutions Design Software v.2011, http://www.membranes.com/index.php?pagename=imsdesign

[34] A. Cipollina, G. Micale, L. Rizzuti, Seawater Desalination Conventional and Renewable Energy Processes. Springer-Verlag Berlin Heidelberg, Berlin, Germany 2008

[35] Lenntech water treatment and Purification holding, Water Condition and Purifiation. January 2005

[36] Avista Technologies, Avista Advisor Chemical Calculations Software v.3, http://www.avistatech.com/Ancillary/Avista%20Advisor.htm

[37] GWI (2007) Desalination markets 2007, a global industry forecast (CD rom), Global Water Intelligence, Media Analytics Ltd., The Jam Factory, Park End St, Oxford OX1 1HU, UK, www.globalwaterintel.com/index.php

[38] S. Frioui, R. Oumeddour, Investment and Production Costs of Desalination Plants by Semi-empirical Method, Desalination 223(1) (2008) 457–463

[39] I.C. Karagiannis, P.G Soldatos, Water Desalination Cost Literature: Review and Assessment, Desalination 223(1) (2008) 448–456

[40] R.T.Vicente, G.R, Lourdes, Thermoeconomic Analysis of a Seawater Reverse Osmosis Plant, Desalination 181(1) (2005) 43-59

APPENDIX A

MATHEMATICAL FORMULATION (SECTION 5.7)

$$Minimize \;\; TAC \tag{1}$$

TAC is determined as per Equations (45) through (97) of Table 12.

$Subject.to$:

$$\sum_{j'=1}^{Nro} f_{j'}^{FEED} y_{j'}^{FEED} + f^{FEED} y^{FEED} = 1 \tag{103}$$

$$y_{j'}^{FEED} \in \{0,1\} \;\; \forall\, j' \in J$$

$$y^{FEED} \in \{0,1\}$$

$$\sum_{j'=1}^{Nro} f_{j,j'}^{P}\, y_{j,j'}^{P} + f_j^P y_j^P = 1 \quad \text{j}\in\text{J} \tag{104}$$

$$y_{j,j'}^{P}\,,\; y_j^P \,, \in \{0,1\} \;\; \forall\, j, j' \in J$$

$$\sum_{j'=1}^{Nro} f_{j,j'}^{B}\, y_{j,j'}^{B} + f_j^B y_j^B = 1 \quad \text{j}\in\text{J} \tag{105}$$

$$y_{j,j'}^{P}\,,\; y_j^B \in \{0,1\} \;\; \forall\, j, j' \in J$$

$$F^{PROD} = F^{FEED} f^{FEED} y^{FEED} + \sum_{j=1}^{Nro} f_j^P y_j^P\, F_j^P \qquad \text{j}\in\text{J} \tag{106}$$

$$F^{PROD} X^{PROD} = F^{FEED} f^{FEED} y^{FEED} X^{FEED} + \sum_{j=1}^{Nro} f_j^P\, F_j^P y_j^P\, X_j^P \qquad \text{j}\in\text{J} \tag{107}$$

$$y_j^P \in \{0,1\} \;\; \forall\, j \in J$$

$$y^{FEED} \in \{0,1\}$$

$$F^{BRINE} = \sum_{j=1}^{Nro} f_j^B y_j^B\, F_j^B \qquad \text{j}\in\text{J} \tag{108}$$

$$F^{BRINE} X^{BRINE} = \sum_{j=1}^{Nro} f_j^B\, y_j^B\, F_j^B\, X_j^B \qquad \text{j}\in\text{J} \tag{109}$$

$$y_j^B \in \{0,1\} \;\; \forall\, j \in J$$

$$F_j^F y_j = F^{FEED} f_{j'}^{FEED} y_{j'}^{FEED} + \sum_{j=1}^{Nro} F_j^F f_{j,j'}^{P}\, y_{j,j'}^{P} + \sum_{j=1}^{Nro} F_j^F f_{j,j'}^{B}\, y_{j,j'}^{B} \tag{110}$$

j,j'∈,J

$$F_j^F\, X_j^F y_j = F^{FEED} f_{j'}^{FEED} X^{FEED} y_{j'}^{FEED} + \sum_{j=1}^{Nro} F_j^F f_{j,j'}^{P}\, X_{j,j'}^{P} y_{j,j'}^{P} + \sum_{j=1}^{Nro} F_j^F f_{j,j'}^{B}\, X_{j,j'}^{B} y_{j,j'}^{B},$$

j,j'∈,J (111)

$$y_{j'}^{FEED},\; y_{j,j'}^{B},\; y_{j,j'}^{P} \in \{0,1\} \;\; \forall\, j, j' \in J$$

$$F_j^F = F_j^B + F_j^P \qquad \text{j}\in\text{J} \tag{112}$$

$$F_j^P = R_j \times F_j^F \qquad j\in J \tag{113}$$

$$F_j^F \times X_j^F = F_j^B \times X_j^B + F_j^P \times X_j^P \qquad j\in J \tag{114}$$

$$F^{FEED} = F^{BRINE} + F^{PROD} \tag{115}$$

$$F^{FEED} X^{FEED} = F^{BRINE} X^{BRINE} + F^{PROD} X^{PROD} \tag{116}$$

$$F^{PROD} X_i^{PROD} = F^{FEED} f^{FEED} y^{FEED} X_i^{FEED} + {}^{Nro}_{j=1}\sum f_j^P \; F_j^P y_j^P \; X_{i,j}^P \tag{117}$$

$i\in I,\ j\in J$

$$F^{BRINE} X_i^{BRINE} = {}^{Nro}_{j=1}\sum f_j^B \; y_j^B \; F_j^B \; X_{i,j}^B \quad i\in I,\ j\in J \tag{118}$$

$$F_j^F \; X_{i,j}^F y_j = F^{FEED} f_{j'}^{FEED} X_i^{FEED} y_{j'}^{FEED} \; + {}^{Nro}_{j=1}\sum F_j^F f_{j,j'}^P \, X_{i,j,j'}^P y_{j,j'}^P \; + {}^{Nro}_{j=1}\sum F_j^F f_{j,j'}^B \, X_{i,j,j'}^B y_{j,j'}^B$$

$i\in I \quad j,j'\in J$ (119)

$$F_j^F \times X_{i,j}^F = F_j^B \times X_{i,j}^B + F_j^P \times X_{i,j}^P \qquad i\in I \text{ and } j\in J \tag{120}$$

$$X_{i,j}^P = X_{i,j}^F \times (1 - \gamma_{i,j}) \qquad i\in I \text{ and } j\in J \tag{121}$$

$$F^{FEED} X_i^{FEED} = F^{BRINE} X_i^{BRINE} + F^{PROD} X_i^{PROD} \qquad i\in I \tag{122}$$

$$X^{FEED} = {}^{Nc}_{i=1}\sum X_i^{FEED} \tag{123}$$

$$X^{PROD} = {}^{Nc}_{i=1}\sum X_i^{PROD} \tag{124}$$

$$X^{BRINE} = {}^{Nc}_{i=1}\sum X_i^{BRINE} \tag{125}$$

$$X_j^P = {}^{Nc}_{i=1}\sum X_{i,j}^P \qquad j\in J \tag{126}$$

$$X_j^B = {}^{Nc}_{i=1}\sum X_{i,j}^B \qquad j\in J \tag{127}$$

$$X_{j,j'}^P = {}^{Nc}_{i=1}\sum X_{i,j,j'}^P \qquad j\in J \tag{128}$$

$$X_{j,j'}^B = {}^{Nc}_{i=1}\sum X_{i,j,j'}^B \qquad j\in J \tag{129}$$

$$X^{PROD} \le X^{PROD,MAX} \; i\in I \tag{130}$$

$$F^{PROD} \ge F^{PROD,MIN} \tag{131}$$

$$P_j^F \le P_j^{F,MAX} \qquad j\in J \tag{132}$$

$$NM_j^{MIN} \le NM_j \le NM_j^{MAX} \; j\in J \tag{133}$$

$$P_j^P = P^{PROD} \qquad j\in J \tag{134}$$

$$P_j^B = P_j^F - \Delta P_j \qquad j\in J \tag{135}$$

$$PI_{j'}^{FRO} = P^{FEED} \qquad j'\in J \tag{136}$$

$$PI_j^{PP} = P_j^P \qquad j\in J \tag{137}$$

$$PI_{j,j'}^{P} = P_j^P \qquad j,j' \in J \tag{138}$$

$$PI_j^{BB} = P_j^B \qquad j \in J \tag{139}$$

$$PI_{j,j'}^{B} = P_j^B \qquad j,j' \in J \tag{140}$$

$$PF_{j'}^{FRO} = P_j^F \qquad j,j' \in J \tag{141}$$

$$PF_{j,j'}^{P} = P_j^F \qquad j,j' \in J \tag{142}$$

$$PF_{j,j'}^{B} = P_j^F \qquad j,j' \in J \tag{143}$$

$$PF_j^{BB} = P^{BRINE} \qquad j \in J \tag{144}$$

$$PF_j^{PP} = P^{PROD} \qquad j \in J \tag{145}$$

$$H_{j'}^{FRO} = \begin{Bmatrix} \frac{10.197}{SG}\left(PF_{j'}^{FRO} - PI_{j'}^{FRO}\right)\ if\left(PF_{j'}^{FRO} - PI_{j'}^{FRO} > 0\right) \forall j' \in J \\ 0\ if\left(PF_{j'}^{FRO} - PI_{j'}^{FRO} = 0\right) \forall j' \in J \\ \frac{10.197}{SG}\left(PF_{j'}^{FRO} - PI_{j'}^{FRO}\right)\ if\ \left(PF_{j'}^{FRO} - PI_{j'}^{FRO}\right) < 0 \wedge \left|PF_{j'}^{FRO} - PI_{j'}^{FRO}\right| > \Delta P^{SPEC} \forall j' \in J \\ 0\ if\ \left(PF_{j'}^{FRO} - PI_{j'}^{FRO}\right) < 0 \wedge \left|PF_{j'}^{FRO} - PI_{j'}^{FRO}\right| < \Delta P^{SPEC}\ \forall j' \in J \end{Bmatrix} \tag{146}$$

$$H_{j,j'}^{P} = \begin{Bmatrix} \frac{10.197}{SG}\left(PF_{j,j'}^{P} - PI_{j,j'}^{P}\right)\ if\left(PF_{j,j'}^{P} - PI_{j,j'}^{P} > 0\right) \forall j' \in J \\ 0\ if\left(PF_{j,j'}^{P} - PI_{j,j'}^{P} = 0\right) \forall j' \in J \\ \frac{10.197}{SG}\left(PF_{j,j'}^{P} - PI_{j,j'}^{P}\right)\ if\ \left(PF_{j,j'}^{P} - PI_{j,j'}^{P}\right) < 0 \wedge \left|PF_{j,j'}^{P} - PI_{j,j'}^{P}\right| > \Delta P^{SPEC} \forall j' \in J \\ 0\ if\ \left(PF_{j,j'}^{P} - PI_{j,j'}^{P}\right) < 0 \wedge \left|PF_{j,j'}^{P} - PI_{j,j'}^{P}\right| < \Delta P^{SPEC}\ \forall j' \in J \end{Bmatrix} \tag{147}$$

$$H_{j,j'}^{B} = \begin{Bmatrix} \frac{10.197}{SG}\left(PF_{j,j'}^{B} - PI_{j,j'}^{B}\right)\ if\left(PF_{j,j'}^{B} - PI_{j,j'}^{B} > 0\right) \forall j' \in J \\ 0\ if\left(PF_{j,j'}^{B} - PI_{j,j'}^{B} = 0\right) \forall j' \in J \\ \frac{10.197}{SG}\left(PF_{j,j'}^{B} - PI_{j,j'}^{B}\right)\ if\ \left(PF_{j,j'}^{B} - PI_{j,j'}^{B}\right) < 0 \wedge \left|PF_{j,j'}^{B} - PI_{j,j'}^{B}\right| > \Delta P^{SPEC} \forall j' \in J \\ 0\ if\ \left(PF_{j,j'}^{B} - PI_{j,j'}^{B}\right) < 0 \wedge \left|PF_{j,j'}^{B} - PI_{j,j'}^{B}\right| < \Delta P^{SPEC}\ \forall j' \in J \end{Bmatrix} \tag{148}$$

$$H_j^{PP} = \begin{Bmatrix} \frac{10.197}{SG}\left(PF_j^{PP} - PI_j^{PP}\right)\ if(\ PF_j^{PP} - PI_j^{PP}\ > 0)\ \forall j' \in J \\ 0\ \ if\left(\ PF_{j,j'}^{B} - PI_{j,j'}^{B}\ = 0\right)\forall j' \in J \\ \frac{10.197}{SG}\left(PF_j^{PP} - PI_j^{PP}\right)\ if\ (PF_j^{PP} - PI_j^{PP}\ ) < 0 \wedge \left|\ PF_j^{PP} - PI_j^{PP}\ \right| > \Delta P^{SPEC} \forall j' \in J \\ 0\ \ if\ (PF_j^{PP} - PI_j^{PP}\ ) < 0 \wedge \left|\ PF_j^{PP} - PI_j^{PP}\ \right| < \Delta P^{SPEC}\ \forall j' \in J \end{Bmatrix} \quad (149)$$

$$H_j^{BB} = \begin{Bmatrix} \frac{10.197}{SG}\left(PF_j^{BB} - PI_j^{BB}\right)\ if(\ PF_j^{BB} - PI_j^{BB}\ > 0)\ \forall j' \in J \\ 0\ \ if\left(\ PF_j^{BB} - PI_j^{BB}\ = 0\right)\forall j' \in J \\ \frac{10.197}{SG}\left(PF_j^{BB} - PI_j^{BB}\right)\ if\ (PF_j^{BB} - PI_j^{BB}\ ) < 0 \wedge \left|\ PF_j^{BB} - PI_j^{BB}\ \right| > \Delta P^{SPEC} \forall j' \in J \\ 0\ \ if\ (PF_j^{BB} - PI_j^{BB}\ ) < 0 \wedge \left|\ PF_j^{BB} - PI_j^{BB}\ \right| < \Delta P^{SPEC}\ \forall j' \in J \end{Bmatrix} \quad (150)$$

$$PW_{j'}^{FRO} = \begin{Bmatrix} if\ H_{j'}^{FRO} > 0\ \frac{H_{j'}^{FRO} F^{FEED} f_{j'}^{FRO}\left[997.075 + 0.7592305 X^{FEED} - 0.004201\left(X^{FEED}\right)^{1.5} + 0.00048314\left(X^{FEED}\right)^{2}\right]\eta^{pump}}{3.67\times10^{5}} \forall j' \in J \\ H_{j'}^{FRO} < 0\ \frac{H_{j'}^{FRO} F^{FEED} f_{j'}^{FRO}\left[997.075 + 0.7592305 X^{FEED} - 0.004201\left(X^{FEED}\right)^{1.5} + 0.00048314\left(X^{FEED}\right)^{2}\right]}{3.67\times10^{5}\ \eta^{turb}} \forall j' \in J \end{Bmatrix} \quad (151)$$

$$PW_{j,j'}^{P} = \begin{Bmatrix} if\ H_{j,j'}^{P} > 0\ \frac{H_{j,j'}^{P} F_j^F f_{j,j'}^{P}\left[997.075 + 0.7592305 X_{j,j'}^{P} - 0.004201\left(X_{j,j'}^{P}\right)^{1.5} + 0.00048314\left(X_{j,j'}^{P}\right)^{2}\right]\eta^{pump}}{3.67\times10^{5}} \forall j, j' \in J \\ H_{j,j'}^{P} < 0\ \ \frac{H_{j,j'}^{P} F_j^F f_{j,j'}^{P}\left[997.075 + 0.7592305 X_{j,j'}^{P} - 0.004201\left(X_{j,j'}^{P}\right)^{1.5} + 0.00048314\left(X_{j,j'}^{P}\right)^{2}\right]}{3.67\times10^{5}\ \eta^{turb}} \forall j, j' \in J \end{Bmatrix} \quad (152)$$

$$PW_{j,j'}^{B} = \begin{Bmatrix} if\ H_{j,j'}^{B} > 0\ \frac{H_{j,j'}^{B} F_j^F f_{j,j'}^{B}\left[997.075 + 0.7592305 X_{j,j'}^{B} - 0.004201\left(X_{j,j'}^{B}\right)^{1.5} + 0.00048314\left(X_{j,j'}^{B}\right)^{2}\right]\eta^{pump}}{3.67\times10^{5}} \forall j, j' \in J \\ H_{j,j'}^{B} < 0\ \ \frac{H_{j,j'}^{B} F_j^F f_{j,j'}^{B}\left[997.075 + 0.7592305 X_{j,j'}^{B} - 0.004201\left(X_{j,j'}^{B}\right)^{1.5} + 0.00048314\left(X_{j,j'}^{B}\right)^{2}\right]}{3.67\times10^{5}\ \eta^{turb}} \forall j, j' \in J \end{Bmatrix} \quad (153)$$

$$PW_j^{PP} = \begin{Bmatrix} if\ H_j^{PP} > 0\ \frac{H_j^P F_j^P f_j^{PP}\left[997.075 + 0.7592305 X_j^P - 0.004201\left(X_j^P\right)^{1.5} + 0.00048314\left(X_j^P\right)^{2}\right]\eta^{pump}}{3.67\times10^{5}}\ \forall j \in J \\ H_j^{PP} < 0\ \ \frac{H_j^P F_j^P f_j^{PP}\left[997.075 + 0.7592305 X_j^P - 0.004201\left(X_j^P\right)^{1.5} + 0.00048314\left(X_j^P\right)^{2}\right]}{3.67\times10^{5}\ \eta^{turb}}\ \forall j \in J \end{Bmatrix} \quad (154)$$

$$PW_j^{BB} = \begin{Bmatrix} if\ H_{j'}^{BB} > 0 \dfrac{H_j^B F_j^B f_j^{BB}\left[997.075+0.7592305X_j^B-0.004201\left(X_j^B\right)^{1.5}+0.00048314\left(X_j^B\right)^2\right]\eta^{pump}}{3.67\times10^5} \ \forall j \in J \\ H_j^{BB} < 0 \ \dfrac{H_j^B F_j^B f_j^{BB}\left[997.075+0.7592305X_j^B-0.004201\left(X_j^B\right)^{1.5}+0.00048314\left(X_j^B\right)^2\right]}{3.67\times10^5\,\eta^{turb}} \ \forall j \in J \end{Bmatrix} \quad (155)$$

VITA

Name: Sabla Alnouri

Address: Texas A & M University at Qatar,
Education City – Doha, Qatar
P.O. Box 23874

Email Address: sabla.alnouri@gmail.com

Education: B.S., Chemical Engineering, Texas A & M University at Qatar, 2008
M.S., Chemical Engineering, Texas A&M University at Qatar, 2012